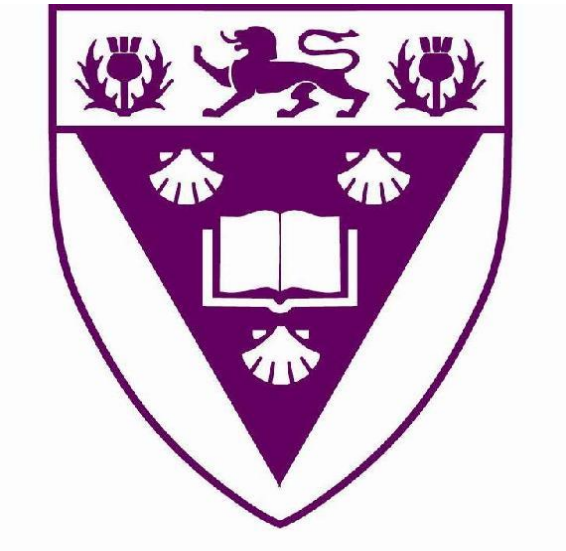

Investigating assay formats for screening malaria Hsp90-Hop interaction inhibitors

Thesis submitted in fulfilment of the requirements for the degree of

MASTER OF SCIENCE IN BIOCHEMISTRY

Department of Biochemistry and Microbiology

Rhodes University

Grahamstown

South Africa

By

Leigh-anne Derry

January 2018

Supervisor: H.C. Hoppe

ABSTRACT

Although significant gains have been made in the combat against malaria in the last decade, the persistent threat of drug and insecticide resistance continues to motivate the search for new classes of antimalarial drug compounds and targets. Due to their predominance in cellular reactions, protein-protein interactions (P-PIs) are emerging as a promising general target class for therapeutic development. The P-PI which is the focus of this project is the interaction between the chaperone heat shock protein 90 (Hsp90) and its co-chaperone Hsp70/Hsp90 organising protein (Hop). Hop binds to Hsp70 and Hsp90 and facilitates the transfer of client proteins (proteins undergoing folding) from the former to the latter and also regulates nucleotide exchange on Hsp90. Due to its role in correcting protein misfolding during cell stress, Hsp90 is being pursued as a cancer drug target and compounds that inhibit its ATPase activity have entered clinical trials. However, it has been proposed that inhibiting the interaction between Hsp90 and Hop may be alternative approach for inhibiting Hsp90 function for cancer therapy. The malaria parasite *Plasmodium falciparum* experiences temperature fluctuations during vector-host transitions and febrile episodes and cell stress due to rapid growth and immune responses. Hence, it also depends on chaperones, including *Pf*Hsp90, to maintain protein functionality and pathogenesis, demonstrated *inter alia* by the sensitivity of parasites to Hsp90 inhibitors. In addition, *Pf*Hsp90 exists as a complex with the malarial Hop homologue, *Pf*Hop, in parasite lysates. Consequently, the purpose of this study was to explore P-PI assay formats that can confirm the interaction of *Pf*Hsp90 and *Pf*Hop and can be used to identify inhibitors of the interaction, preferably in a medium- to high-throughput screening mode.

As a first approach, cell-based bioluminescence and fluorescence resonance energy transfer (BRET and FRET) assays were performed in HeLa cells. To facilitate this, expression plasmid

constructs containing coding sequences of *P. falciparum* and mammalian Hsp90 and Hop and their interacting domains (Hsp90 C-domain and Hop TPR2A domain) fused to the BRET and FRET reporter proteins – yellow fluorescent protein (YFP), cyan fluorescent protein (CFP) and *Renilla* luciferase (Rluc) - were prepared and used for HeLa cell transient transfections. The FRET assay produced positive interaction signals for the full-length *P. falciparum* and mammalian Hsp90-Hop interactions. However, C-domain-TPR2A domain interactions were not detected, no interactions could be demonstrated with the BRET assay and western blotting experiments failed to detect expression of all the interaction partners in transiently transfected HeLa cells. Consequently, an alternative *in vitro* FRET assay format using recombinant proteins was investigated. Expression constructs for the *P. falciparum* and mammalian C-domains and TPR2A domains fused respectively to YFP and CFP were prepared and the corresponding fusion proteins expressed and purified from *E. coli*. No interaction was found with the mammalian interaction partners, but interaction of the *P. falciparum* C-domain and TPR2A domain was consistently detected with a robust Z' factor value of 0.54. A peptide corresponding to the *Pf*TPR2A domain sequence primarily responsible for Hsp90 binding (based on a human TPR2A peptide described by Horibe *et al.*, 2011) was designed and showed dose-dependent inhibition of the interaction, with 53.7% inhibition at 100 µM. The components of the assay are limited to the purified recombinant proteins, requires minimal liquid steps and may thus be a useful primary screening format for identifying inhibitors of *P. falciparum* Hsp90-Hop interaction.

TABLE OF CONTENTS

LIST OF FIGURES

LIST OF TABLES

SYMBOLS AND ABBREVIATIONS

Å: Ångström

AD: activation domain

Antp: Antennapedia homeodomain protein

APS: ammonium persulfate

Arg: arginine

Asp: aspartic acid

BRET: bioluminescence resonance energy transfer

BSA: bovine serum albumin

CFP: cyan fluorescent protein

CHO: Chinese hamster ovary

COS-7 cells: African green monkey fibroblasts

DBD: DNA binding domain

DMEM: Dulbecco's modified Eagle's medium

DMSO: dimethyl sulfoxide

DNA: deoxyribonucleic acid

EDTA: ethylenediaminetetraacetic acid

EGTA: ethylene glycol-bis(β-aminoethyl ether)-N,N,N',N'-tetraacetic acid

ER: endoplasmic reticulum

FBS: fetal bovine serum

FP: fluorescent proteins

FRET: Förster resonance energy transfer

GFP: green fluorescent protein

Glu: glutamic Acid

GST: glutathione *S*-transferase

hCdom: human Hsp90 C-domain

HEK: human embryonic kidney

HEPES: 4-(2-hydroxyethyl)-1-piperazineethanesulfonic acid

hHsp90: human heat shock protein 90

HOP: Hsp90/Hsp70 organising protein

HRP: horseradish peroxidase

HSE: heat shock element

HSF: heat shock transcription factor

Hsp: heat shock protein

Hsp90: heat shock protein 90

IPTG: isopropyl β-D-1-thiogalactopyranoside

LB: lysogeny broth

Lys: lysine

mTPR2A: murine TPR2A domain

PBS: phosphate-buffered Saline

PCR: polymerase chain reaction

*Pf*Cdom: *P. falciparum* Hsp90 C-domain

*Pf*Hsp90: *P. falciparum* heat shock protein 90

*Pf*TPR2A: *P. falciparum* TPR2A domain

P-PI: protein-protein interaction

Rluc: *Renilla* luciferase

ROS: reactive oxygen species

SDS-PAGE: sodium dodecyl sulfate polyacrylamide gel electrophoresis

SDS: sodium dodecyl sulfate

sHsps: small heat shock proteins

SPF: streptomycin, penicillin, Fungizone

TBS: Tris-buffered saline

TE: Tris-EDTA

TEMED: tetramethylethylenediamine

YFP: yellow fluorescent protein

α: Alpha

β: Beta

ACKNOWLEDGEMENTS

This work was funded by a Deutsche Forschungsgemeinschaft (DFG) German-African co-operation in Infectiology grant: "Molecular Interactions of PfHop as a target for anti-malarial drug development". Additional support was provided by a Medical Research Council SA University Flagship Project award: “Integration of bioassay capacity, target identification and multidisciplinary research for the discovery of drug lead compounds (CCBR-RU)”.

Professor Heinrich Hoppe, for being supportive, patient, for helping me at all costs and for coming to all my parties. I really will miss you.

Further Acknowledgements:

My parents, Alan and Jennifer Derry, for your constant support and encouragement, and for reading through my drafts.

Emma Mostert, for being my rock, my constant companion, the person who can relieve my stress, and make me laugh.

Werner Buchner, for never failing to comfort me, even when you weren’t sure what you were comforting me about.

Michelle Isaacs: for being my role model and giving me hope for a future in academia.

Dumisani Mnklandla: for being my very sassy protein purification teacher.

Lynn Wambua, thank you for being the chocolate in the Neapolitan ice cream that is our multicultural friendship. Your knowledge of Trizma base and T.V series is something to aspire to and I can’t wait to play you in the re-enactment of your murder on crime and investigation.

Farrah Khan: Against the assault of laughter, nothing can stand - not even the disappointment of a failed experiment. Thank you for being part of the ‘healing through humour’ support system that our friendship provided and carried through the tough times of postgraduate. It is through my friendship with you that I have discovered new realms of ecstasy.

CHAPTER 1

INTRODUCTION

1.1 MALARIA

1.1.1 Malaria: the perpetual problem

Deaths directly attributed to malaria have decreased by 60% in between the years 2000 and 2015 as a result of new drugs and preventative measures being implemented (WHO, 2015). However, at the end of 2015, there were still 214 million new cases of malaria reported and 438 000 deaths caused worldwide, with the most deaths being of children under the age of five in sub-Saharan Africa (WHO, 2015). Therefore, it is important to continue the ongoing battle against malaria as the recent plateauing of international funding and emerging drug and insecticide resistance threaten to reverse recent gains (WHO, 2013).

Malaria is caused by a parasitic protozoan belonging to the genus *Plasmodium,* which is spread to humans by the bite of the female *Anopheles* mosquito. There are five species of *Plasmodium* that can infect humans; *P.falciparum, P.vivax, P.ovale, P. malariae* and *P.knowlesi*. However, most deaths are caused by *P.falciparum*, since most of the other species cause only a milder form of malaria and *P.knowlesi* rarely causes disease in humans (WHO, 2014).

1.1.2 Current methods of combating malaria

The principal possibilities of combating malaria are currently: eradicating the mosquito vector, preventing the mosquito from biting humans, taking prophylactic drugs before heading to a malaria area or killing the parasites with antimalarial drugs once they have reached the blood stage in their life cycle. These blood stages of the parasites can be imitated and maintained through *in vitro* cultures and can therefore be used to test effects of genetic manipulation to identify drug targets or to screen compounds for potential antimalarials in a laboratory environment (Balu and Adams, 2007; Gamo *et al.* 2010).

However, malaria is proving difficult to combat due to ineffective insecticide spraying programs, the growing resistance of the mosquito to current insecticides and the lack of an effective licensed vaccine (Hill, 2011). The vaccine currently in phase three trials (RTS, S) targets only one life-cycle stage of the parasite, the sporozoite, and not all stages, leading to a low efficacy (Hill, 2011). Therefore, to treat malaria, there is still a heavy reliance on anti-malarial drugs and the current treatment for people diagnosed with malaria is to use artemisinin-based combination treatments (Nosten and White, 2007). The exact mode of action of artemisinin is still unclear, but it is thought to react with iron or heme (which is found in the parasite due to digestion of the host red blood cell haemoglobin) to produce reactive oxygen species (ROS). An abundance of ROS kills the parasites by depolarization of the parasite mitochondria, disrupting their function (Wang *et al.,* 2010). However, there is an alarming increase in artemisinin resistance in South-East Asia linked to mutations in the K13 propeller region of the parasite *(*Tun *et al.,* 2015*),* leading to an increased need for new drug targets and new drug molecules.

1.1.3 Life cycle of the malarial parasite

The malaria parasite under goes a very complex life cycle and understanding it can potentially lead to discovering new drug targets. The life cycle consists of three stages: the pre-erythrocytic cycle, the erythrocytic cycle and the sporogonic cycle. The pre-erythrocytic cycle starts when sporozoites are passed from the salivary gland of a female *Anopheles* mosquito into the blood stream of a human where they invade the hepatocytes in the liver and multiply. The sporozoites subsequently undergo asexual reproduction and develop into schizonts, structures that can contain thousands of merozoites (Campbell, 1997). The schizonts rupture, releasing merozoites into the bloodstream. Each merozoite invades an erythrocyte where it multiplies asexually over a 48-hour development period to form new merozoites that rupture the erythrocyte and reinitiate infection. This cycle of destroying and re-infecting erythrocytes is known as the

erythrocytic cycle and is responsible for the symptoms of malaria. After invading an erythrocyte, some of the merozoites develop into male or female gametocytes. These gametocytes are taken up by a mosquito, mature into gametes and fertilize in the mosquito gut, starting the sporogonic cycle. The zygote, resulting from fusion of the gametes, develops into an ookinete that penetrates the gut wall, forming an oocyst in which the parasite multiplies asexually to produce sporozoites that migrate to the salivary glands and can infect a human when the mosquito takes its next bloodmeal (Cowman *et al.*, 2012). The constant temperature fluctuations experienced by the parasite as it moves from cold-blooded mosquito to warm-blooded human host, the rapid growth of the parasite and the action of the body's immune system against the parasite causes the parasite to be under constant cell stress. To survive and maintain protein homeostasis, there is a high possibility that the parasite depends on a network of heat shock proteins (Acharya *et al.*, 2007). Targeting parasite heat shock protein function with drugs may thus be a novel mode of anti-malarial therapy. This will be discussed in subsequent sections.

1.2 POTENTIAL NEW DRUG TARGETS – PROTEIN-PROTEIN INTERACTIONS.

1.2.1 Importance of Protein-Protein Interactions

Most drug targets currently exploited for therapy are enzymes or receptors that have ligand, substrate, cofactor or allosteric binding sites which can be easily occupied and manipulated by small drug-like molecules (Wells and McClendon, 2007). However, besides enzymes and receptor-ligand interactions, there is a large and mostly overlooked component of cells which constitutes the large majority of reactions in the cell. These are protein-protein interactions (P-PIs) (Bonetta, 2010). According to Bonetta (2010) and updated statistics from the Biological General Repository for Interaction Datasets (BioGRID – a public database of protein interaction data from model organisms and humans), there are currently 367210 known protein

interactions in human cells with more being discovered in both human cells and malarial parasites using 2-hybrid yeast assays (La Count *et al.,* 2005).

Proteins were traditionally identified by their actions as signalling molecules, catalysts or building blocks. Currently, the protein is witnessed as an element in a network of proteins with its function linked to other proteins by protein-protein interactions, known as the interactome. This dependence of proteins on other proteins was for example demonstrated in experiments performed by Jeong *et al.,* (2001) and Hartwell *et al.,* (1999) where a single gene deletion had drastic phenotypic consequences depending on the position of its protein product in the complex of molecular interactions. Protein-protein interactions occur when proteins bind to each other with electrostatic forces, van der Waals forces, hydrogen bonds, hydrophobic interactions and/or disulphide bridges. They can be stable and long-lived or brief and transient and homo-oligomeric (identical protein subunits binding to each other) or hetero-oligomeric (Lo Conte *et al.,* 2000). More stable interactions are often used to form large multimeric complexes in cells, *e.g.* ribosomal subunits (49 and 33 proteins are found in the large and small subunits, respectively), nuclear pores that consist of complexes of up to 30 different proteins, nucleosomes responsible for chromatin formation and the actin and microtubule cytoskeletons. Other more stable interactions include cell-cell and cell-matrix adhesion (Damsky, 2002). In addition, many enzymes in cells exist as multimeric complexes, *e.g.* pyruvate dehydrogenase and glutamate synthase, that consist of up to 30 and 12 subunits, respectively (Stoops *et al.,* 1997, Suzuki and Knaff, 2005). More transient protein-protein interactions are particularly prevalent in signal transduction pathways that link signalling receptor activation to a cellular response and gene transcription, or in protein trafficking pathways, including transport vesicle formation and fusion and protein translocation into organelles (Lo Conte *et al.,* 2000). Protein-protein interactions are thus ubiquitous and crucial for all biological processes, (Couturier and

Deprez, 2012) and the more that is known about them, the more can be understood about the function and organisation of the cell (Waugh, 1954).

1.2.2 Inhibiting protein-protein interactions

From a drug development point of view, protein-protein interactions have been overlooked in the past due to difficulties in finding small drug-like molecules that can interrupt the interaction (Wells and McClendon, 2007). This is due to the fact that the contact surfaces involved in protein-protein interactions are very large (1500-3000 $Å^2$) and would require correspondingly large molecules to competitively bind to the surfaces and disrupt the interaction. By contrast, Lipinsky's rule of five of bioavailable drug-like molecules dictates that drug candidates need to have a molecular weight <500 Da. Protein interaction surfaces may also lack distinctive binding grooves/pockets that could allow multiple interactions between the drug and the protein polypeptide chain and improve drug-protein binding affinity (Cheng *et al.,* 2007). There is also difficulty in distinguishing real binding from artefactual binding as well as the small size of potential protein-protein interaction inhibitor molecule libraries (Arkin and Wells, 2004).

An approach for developing a protein-protein interaction inhibitor from a small molecule starting point has been to synthesize a short peptide that corresponds to the amino acid sequence of the interaction surface of a protein. This approach has been successful for small continuous peptide sequences such as those of the integrins GPIIbIIa, αVβ3 and α4β1 (Sulyok *et al.,* 2001, Gibson *et al.,* 2002, Jackson *et al.,* 2002). Random screening of drugs has shown that certain drugs can inhibit an interaction due to the recruitment of other protein-protein complexes. For example, the binding of cyclosporins to immunophilins causes the formation of novel protein-protein complexes which then bind to the phosphatase calcineurin to exert the

immunosuppressive effect (Schreiber and Crabtree 1992). In addition, compounds may inhibit the function of a transient protein-protein interaction by actually stabilising it. An example is Brefeldin A which has been explored for cancer therapy (Anadu *et al.,* 2006). It stabilises the interaction of Arf 1 GTPase and nucleotide exchange factors, thus preventing the GTPase from completing its function - mediating protein trafficking in the Golgi apparatus (Robineau *et al.,* 2000).

Using site-directed mutagenesis in combination with X-ray crystallography is an effective way in which protein-protein interfaces can be analysed. Scanning mutagenesis methods in which subsets of the protein surfaces are systematically mutated indicate that many protein-protein interaction interfaces contain compact, centralized regions of residues that are crucial for the affinity of the interaction. These regions are called "hot spots". These hot spots are found on both sides of the protein interface and they are complementary to each other, with buried charged residues forming salt bridges and hydrophobic residues from one surface fitting into small nooks on the opposite surface (Arkin and Wells, 2004). Drug-like compounds can now be sought which bind to hot spots, binding deeper and with higher efficiencies (Wells & McClendon, 2007). To find these compounds, effective, sensitive and cheap assays to measure the targeted P-PIs need to be implemented (Wells and McClendon, 2007).

1.3 MOLECULAR CHAPERONES

1.3.1 Molecular chaperones as important Protein-Protein Interaction partners

One of the cell's most important protein-protein interactions is the interaction between molecular chaperones and their client proteins and regulatory proteins (co-chaperones). Molecular chaperones are proteins that primarily assist in protein folding and one of their major functions is to prevent both newly synthesised polypeptide chains and assembled subunits from aggregating into non-functional structures (Ellis, 2006). This is why most chaperones are also known as heat shock proteins, since proteins tend to aggregate and unfold as they are denatured

by stress, including elevated temperatures. Chaperones are consequently upregulated during cell stress and are required to prevent the aggregation or degradation of denatured proteins and assist them to re-fold, thus maintaining a functional proteome in the face of cell stress. Chaperones can act as foldases or holdases. Foldases support the folding of proteins in an ATP dependant manner, *e.g.* GroEL, and holdases bind the protein in its folding intermediate stage *e.g*. DnaJ (Hoffman *et al.,* 2003). Other types of chaperones have been found to be involved in membrane crossing, notably the translocation of proteins into organelles (*e.g*. endoplasmic reticulum and mitochondria) in an unfolded state and responding to diseases linked to protein aggregation such as prion disease and Alzheimer's disease (Sadigh-Eteghad *et al.*,2015). Chaperones have also been linked to cancer maintenance and are often upregulated in cancer cells (Calderwood *et al.,* 2006). This is thought to be due to stresses cancer cells experience during tumour formation, *e.g*. rapid cell growth, nutrient depletion, hypoxia and acidosis and the chaperones are required to counteract protein misfolding/denaturation caused by these conditions.

There are several families of chaperones in cells, notably small heat shock proteins (sHsps), heat shock protein (Hsp) 40, Hsp70, Hsp90 and Hsp110. Hsp90 is the focus of this study.

1.3.2 Heat Shock Protein 90 (Hsp90)

One of the most important chaperones is heat shock protein 90 (Hsp90). As with other chaperones, the main function of Hsp90 is to facilitate protein folding to maintain regular development and growth of an organism (Shonhai, 2010). There are two main isoforms of HSp90; Hsp90α, the major isoform and Hsp90β the minor isoform (Csermely *et al.,* 1998). These isoforms are highly conserved but there are differences in the amino acid sequences of the two isoforms, raising the possibility of that the two isoforms have isoform specific functions

such as binding to different client proteins (proteins that require Hsp90 for folding; Pepin *et al.*,2001). The biochemical separation of these two isoforms is difficult, so therefore experiments are often performed with both isoforms.

1.3.3 Transcription of Hsp90

Increased transcription of Hsp90 occurs when cells have been exposed to proteotoxic stress. Heat shock transcription factors (HSF-1) are activated which are capable of specifically binding to heat shock element (HSE) sequences present in Hsp90 promoters. These HSEs are thus involved in the inducible gene expression of Hsp90.

In an unstressed cellular environment, HSF-1 is present as a monomeric polypeptide, unable to bind to DNA. However, in a stressed environment, HSF homotrimerises, acquires DNA binding ability and translocates from the cytoplasm to the nucleus where is it hyper-phosphorylated and becomes transcriptionally competent (Morimoto *et al.*, 1996). There are two possible ways in which HSF becomes active. One of the possibilities is that in a stressed environment, proteins in the cell start to unfold and therefore the concentration of non-native protein increases and this increase in concentration induces the activation of HSF. It could also be that Hsp90 is attached to HSF in the cytosol under normal conditions. When the concentration of non-native protein builds up, the non-native client proteins will compete for Hsp90 binding, leaving the HSF unbound and able to trimerise. (Zou *et al.*, 1998)

1.3.4 Structure and ATPase cycle of Hsp90

Hsp90 consists of three domains, the N-terminal, central and C-terminal domains (Prodromou and Pearl, 2003). The N-terminal domain has ATPase activity: it binds and hydrolyses ATP in the process of protein folding. The central domain is where client proteins bind and the C-terminal domain is responsible for homodimerisation, modulating ATP activity and binding of

co-chaperones (Prodromou and Pearl, 2003). The C-terminus contains an EEVD motif which is essential for binding to co-chaperones (Prodromou and Pearl, 2003).

The mechanism by which Hsp90 folds client proteins has not been entirely elucidated. As indicated above, Hsp90 exists as a homodimer due to mutual binding of the C-terminal domains of two individual proteins. When the N-terminal domains have no nucleotide bound or are bound to ADP, the dimer assumes a V-shaped "open" conformation. Binding of a client protein and of ATP causes the N-terminal domains to interact, resulting in a "closed" conformation. After hydrolysis of ATP to ADP, the dimer returns to the open conformation and the folded client protein is released. Co-chaperones are also involved in this cycle, *e.g.* Cdc37, hsp70/hsp90 organising protein (Hop), p23 and Aha1 assist with client protein loading, stabilize client binding, modulate ATP binding or stimulate ATP hydrolysis (Li *et al.* 2012).

1.3.5. Hsp90 and cancer

As mentioned previously, cancer cells are exposed to cell stress and contain upregulated chaperones to counter the effects of cell stress on the proteome. Hsp90 has attracted particular attention – it accounts for up to 1-2% of the protein content of cancer cells and is key to stabilising many essential cancer proteins such as signalling kinases, hormone receptors and transcription factors, *e.g.* BCR-ABL, ERB-B2, Polo-1 kinase, epidermal growth factor receptor (EGFR), CRAF, BRAF, AKT/PKB, MET, VECFR, FLT3, CDK4, hTERT, androgen and estrogen receptors, hypoxia inducible factor and telomerase (Calderwood and Gong, 2016). These proteins are directly involved in the malignancy of cancer and they influence growth factor independence, resistance to antigrowth signals, unlimited replicative potential, tissue invasion and metastasis, avoidance of apoptosis, drug resistance and sustained angiogenesis.

Consequently, Hsp90 is currently being pursued as a drug target for cancer, the rationale being that inhibition of Hsp90 function would lead to destabilisation and degradation of the oncogenic client proteins described above. Compared to normal cells, cancer cells may be said to be addicted to oncoproteins. Oncoproteins in cancer cells are usually expressed as mutants and therefore rely more heavily on the Hsp90 machinery to keep them folded and stable. Additionally, cancer cells are also more exposed to hypoxia, acidosis and the deprivation of nutrients compared to normal cells which puts them under constant stress and reinforces their need for heat shock proteins (Sharma and Settleman, 2007).

1.3.6. Inhibiting Hsp90

One of the main Hsp90 inhibitors that has been discovered is the natural product geldanamycin. Geldanamycin's mode of action is to preferentially bind to the N-terminus of Hsp90 and prevent the binding of ATP. With the ATPase activity inhibited, client proteins in several transduction pathways are not tended to by Hsp90 and therefore become unstable and unable to maintain the viability of cancerous cells. Geldanamycin has also been shown to preferentially bind to Hsp90 in cancer cells compared to normal cells, leading to the greater depletion of cancer cells (Kamal *et al.,* 2003). However, *in vivo* geldanamycin displays limited stability and bioavailability, as well as hepatotoxicity. Subsequently, numerous geldanamycin derivatives have been developed and have entered clinical trials, *e.g.* 17-allyamino-17-demethoxy geldanamycin (17-AAG) which has shown promising results in breast cancer patients (Modi *et al.,* 2001).

Another potential inhibitor of Hsp90 is the peptide designed by Plescia *et al.,* (2005), named "shepherdin", which binds to the ATP pocket of Hsp90, destabilising client proteins such as

survivin. Survivin is involved in the control of mitosis and the suppression of apoptosis and when it is in a denatured state the cell ultimately dies from apoptosis (Garg *et al.,* 2016). An additional Hsp90 inhibitor that is widely used in *in vitro* studies is the antibiotic novobiocin. It was the first inhibitor discovered to bind to the C-terminal domain of Hsp90, resulting in disruption of the homodimer and release of client proteins. However, *in vivo* activity of novobiocin is disappointing and additional derivatives are being pursued (Donnelly and Blagg, 2008).

All the Hsp90 inhibitors in clinical trials affect the ATPase activity of Hsp90 N-terminal domain. However, the inhibition of Hsp90 in this way has been shown to upregulate other heat shock proteins which can compensate for the loss of Hsp90 function. Furthermore, these types of drugs have also been shown to cause hepatotoxicity in human and animal subjects (Neckers and Workman, 2012). This has led to the proposal that a more fruitful approach to disrupting Hsp90 function for cancer therapy is to target its interactions with co-chaperones (Brandt & Blagg, 2009; Edkins, 2016). Pertinent in this regard is Hsp70/Hsp90 organising protein (Hop).

1.3.7. Functions of Hop

Hop (Hsp70/Hsp90 organising protein) is the most widely studied co-chaperone with a TPR domain (Odunga *et al.,* 2004). One of the main functions of Hop is simultaneous binding to Hsp90 and Hsp70 and enabling their collaboration in protein folding (Odunga *et al.,* 2004). Hsp70 is thought to initiate the folding of the substrate protein and then passes it on to Hsp90 which completes the folding of the substrate. In this way, Hop acts as a scaffold or adaptor protein that facilitates the transfer of client substrate proteins from Hsp70 to Hsp90. It can further modulate these proteins by controlling their ability to bind to ATP or inhibiting their ability to dissociate from ADP (Johnson *et al.,* 1997). In the ATPase cycle of Hsp90 described earlier (section 1.3.4), Hop binds to Hsp90 in the absence of nucleotides or the presence of

ADP. This allows Hsp90 to remain in the open conformation for longer, facilitating client protein binding.

1.3.8 Structure of Hop

Hop consists of nine tetratricopeptide (TPR) repeats clustered into three domains containing three tetratricopeptide repeats each; TPR1, TPR2A and TPR2B. In between these repeats there are DP1 and DP2 domains. These DP domains are composed of 5 helices forming a V shape and have been found to be crucial in the folding of Hop and their disruption can impair Hop function (Nelson *et al.,* 2013). TPR domains consist of loosely conserved 34 amino acid sequence motifs that are repeated between once and sixteen times per domain. Each 34 amino acid sequence motif forms a pair of antiparallel alpha-helices. These helices are arranged into a super helical structure that encloses a central groove and it is in this groove that the TPR domains can attach to the C-terminus of Hsp90 and Hsp70 containing the sequence motif EEVD (Young *et al.,* 1998). The TPR1 and TPR2B domains interact with the PTIEEVD sequence at the Hsp70 C-terminus while the TPR2A domain specifically interacts with the MEEVD residues at the C-terminus of Hsp90 (Scheufler *et al.,* 2000). Lys (301) and Arg (305) in helix A3 of the TPR2A domain donate hydrogen bonds to the side chains of Asp and Glu of the Hsp90 C-terminal sequence, drawing the two proteins together.

1.3.9 Inhibiting the Hsp90-Hop interaction

To determine whether the disruption of this interaction is able to incapacitate cells, a TPR peptide was created, modelled on the binding interface between Hop and Hsp90. This peptide was designed by Horibe *et al.* (2011) and named hybrid antp-TPR peptide. The structure of this peptide included the highly conserved Lys (301) and Arg (305) residues of the TPR2A domain to enable it to compete for the interaction with Hsp90. In addition, it was attached to a membrane permeable peptide sequence derived from the membrane penetrating Antennapedia homeodomain protein (Antp) to facilitate its entry into cells. It was found that it inhibited the

Hsp90 and Hop interaction specifically, as the peptide did not inhibit the Hsp70/Hop interaction. Inhibition of the binding of Hsp90 to Hop in turn prevented Hsp90 from being able to bind to its client proteins such as survivin, CDK4 and Akt. This prevented them from being able to fold properly and ultimately lead to cell death via apoptosis (Horibe *et al.*, 2011). The use of this peptide furthermore did not increase the concentration of Hsp70 in the cell, which potentially means the cell is not compensating for the loss of Hsp90's heat shock ability. This peptide is also cheap to manufacture and does not seem to have any toxic side effects (Horibe *et al.*, 2011). Importantly, the peptide inhibited the growth of a panel of different cancer cell lines with IC_{50} values in the range 19 – 66 μM, but not non-cancerous cell lines, and also reduced tumour growth in a mouse model of pancreatic cancer.

It has also been shown that the C-terminus of Hsp90 can be allosterically altered using sansalvamide derivatives, hindering Hsp90 interaction with cochaperones including Hop, FKBP38 and FKBP 52 and producing toxicity against HeLa and HCT-116 cancer cell lines in a 5 – 50 μM concentration range (Kunicki *et al.*, 2011; Ardi *et al.*, 2011; Vasko *et al.*,2010). An additional small molecule capable of disrupting Hsp90-Hop interaction is 1,6-dimethyl-3-propylpyrimido[5,4-e][1,2,4]triazine-5,7-dione (C9) which binds to the TPR2A domain of Hop. It was found to be toxic to breast cancer cell lines with IC_{50} values of 1 – 2 μM, but not to non-cancerous fibroblasts (Pimienta *et al.*, 2011). Unlike compounds that inhibit the N-domain ATPase activity of Hsp90, the Hsp90-Hop inhibitors do not appear to cause an upregulation of compensatory heat shock proteins to the same extent. Therefore, novel compounds that block the Hsp90 and Hop interaction could optimistically produce cancer therapeutics.

1.4 MOLECULAR CHAPERONES IN MALARIA

1.4.1 Heat shock proteins in malaria

The *P. falciparum* parasite cycles between a poikilothermic mosquito vector and a homoeothermic human host during its life cycle, experiencing up to a 10°C difference in temperature. The parasite also experiences heat shock stress when the patient suffering from malaria undergoes febrile episodes. The parasite undergoes repeated cycles of rapid cell growth in all its life-cycle stages, generates large amounts of lactic acid which could contribute to acidosis and is thought to experience extensive oxidative stress due to the host immune defences and the generation of reactive oxygen species by haem liberated during haemoglobin digestion (Shonhai, 2010; Maitland and Newton, 2005; Bozdech and Ginsburg, 2004). Moreover, the parasites exports hundreds of proteins (the secretome) across its cell membrane into the host erythrocytes and this trafficking likely involves chaperones, similar to the requirement for chaperones in translocation into other organelles (*e.g.* ER and mitochondria) (Przyborski *et al.*, 2016). Therefore, like cancer cells, *Plasmodium falciparum* is thought to depend on a network of heat shock proteins to protect its proteome against these cell stresses, in order to survive and to sustain the resulting pathogenesis. It may therefore not be surprising that as much as much as 2% of the parasite genome encodes chaperones and abundant representatives of all the main chaperone classes are present (Acharya *et al.*, 2007).

1.4.2 *Pf*Hsp90

There are two genes in the *P.falciparum* genome that are able to express *Pf*Hsp90, however only one gene expresses Hsp90 with an EEVD motif which is capable of binding to co-chaperones (Pavithra *et al.*, 1993). *Pf*hsp90 shares a 64% sequence identity with human Hsp90 (hHsp90), with the most highly conserved domain (75% sequence identity) being the ATP binding N terminus. The main difference between *Pf*hsp90 and hHsp90 is the charged linker region adjacent to the N-terminal ATP binding pocket. This region is thought to regulate ATP

binding (Vaughan *et al.,* 2006). *Pf*Hsp90 has been shown to be present in the ring, trophozoite and the schizont blood stages and has been found to be essential to the survival of the parasite. It furthermore plays a role in the invasion of the red blood cell and once inside the erythrocyte, the parasite also appropriates the erythrocyte's endogenous Hsp90 machinery for its own use (Banumathy *et al.,* 2002). It begins to synthesize and deploy proteins to the erythrocyte cytosol and plasma membrane in order to establish nutrient import mechanisms and secretory apparatus leading to the resulting pathogenesis of the parasite (Banumathy *et al.,* 2002). It has been shown using mass spectrometry that *Pf*Hsp90 is found in complexes with *Pf*Hsp70 and the TPR-rich protein *Pf*PP5 (Dobson *et al.,* 2001), supporting the probability that *Pf*Hsp90 acts in the same way as hHsp90. This is supported by additional studies reporting the interaction of *Pf*Hsp90 with malaria homologues of human Hsp90 co-chaperones – *Pf*Aha1, *Pf*p23, *Pf*FKBP35 and *Pf*Hop (Alag *et al.,* 2009; Chua *et al.*, 2012; Chua *et al.* 2010; Gitau *et al.*, 2012). When inhibition studies were performed with geldanamycin, a well-known Hsp90 inhibitor, the survival rates of parasites were severely compromised, presenting *Pf*Hsp90 as a potential novel drug target for new antimalarials (Banumathy *et al.,* 2002). Geldanamycin and the geldanamycin derivative 17AAG inhibited parasite growth with very good potencies (IC_{50} values of 25 nM and 160 nM, respectively) and 17AAG also significantly inhibited parasite growth at 50 mg/kg in a *P. berghei* mouse model of malaria (Pallavi *et al.,* 2010).

1.4.3 *Pf*Hop

Due to the fact that *Pf*hsp90 and *PfHsp70* play essential roles in the development and function of the parasite, it is thought that they are likely to interact with each other and that they bind to a co-chaperone to aid in this interaction. Like human cells, there is a Hop homologue (*Pf*Hop) present in *Plasmodium falciparum,* with well conserved Hsp-binding amino acids in its TPR1 and TPR2A domains (Acharya *et al.,* 2007). The less well conserved segments on either side of the TPR domains can influence the overall conformations of the helical turns of the TPR

domains, therefore giving each Hop from different species unique structural features (D'Andrea and Regan, 2003). *Pf*Hop is predominately found in the cytosol during the trophozoite stage of the malarial life cycle (Gitau *et al.,* 2011). It was shown using co-immunoprecipitation assays, size exclusion chromatography and immunofluorescence co-localisation microscopy that the homologues *Pf*Hsp90, *Pf*Hsp70 and *Pf*Hop all interacted in complexes in the cytosol (Gitau *et al.,* 2011). Blocking chaperone-co-chaperone interaction has been shown to be effective when pyrimidinones exhibited anti-malarial activity by inhibiting Hsp70/Hop interaction (Shonhai, 2010). Therefore, drugs that can block this P-PI can be considered for alternative anti-malarial therapies.

1.5 PROBLEM STATMENT

The interaction between the chaperones Hsp90 and its co-chaperone Hop has the potential to be a drug target in both mammalian cells and parasites. Therefore, to be able to find small drug molecules that can potentially inhibit the interaction between these two proteins, the protein-protein interaction needs to be reproduced in an *in vitro* assay format that involves as few steps as possible and produces a robust signal that can be read by a plate reader. There is an existing high throughput assay that has been developed for Hsp90 and Hop using AlphaScreen technology (Yi *et al.,* 2009). The assay uses specific acceptor and donor beads attached respectively to a peptide corresponding to the C-terminal 20 amino acids of Hsp90 and to the TPR2A domain of Hop. Excitation of oxygen using a high-energy laser results in light emission by the donor beads which in turn stimulates fluorescence in the acceptor beads when the beads are in close proximity due to Hsp90-Hop interaction. Since the assay uses purified protein fragments it doesn't account for the ability of compounds to transverse cell membranes and inhibit the interaction in a cellular context. Besides the necessity of attaching the protein interaction partners to the reporter beads, another disadvantage of AlphaScreen Technology is

that it requires a high energy laser source. This is not adaptable to all plate readers which makes this technology more limited than other luminescent technologies (Yasgar *et al.,* 2016). Therefore, the aim of this project was to explore alternative protein-protein interaction assay formats that could potentially be implemented to screen compounds for Hsp90-Hop inhibitors, with a particular emphasis on the *P. falciparum* proteins.

1.6 TYPES OF PROTEIN-PROTEIN INTERACTION ASSAYS

As protein protein-interactions have to been shown to be crucial to normal cell function and potential drug targets for a variety of diseases including cancer and malaria, it is important to be able to perform experiments that can detect these interactions. Up to date there have been many successful ways to detect protein-protein interactions, some of which are discussed here.

Protein affinity chromatography is a procedure in which one protein is covalently bound to a resin or beads and allowed to bind to other proteins. Bound proteins can be eluted with high salt concentration solutions or denaturants (Ratner, 1974). Bound proteins can subsequently be identified by mass spectrometry or western blotting (if antibodies to anticipated interaction partners are available). An alternative to covalently coupling the "bait" protein to a resin is to use a bait protein fused to an affinity tag (*e.g.* glutathione-S-transferase) to allow it to non-covalently attach to affinity resins (*e.g.* glutathione-agarose). The advantage of this method is that it is highly sensitive and can detect weak interactions, each protein in the extract has equal opportunity to bind to the resin and, using this method, one is able to determine specific domains or residues responsible for protein binding by introducing mutations in the bait protein attached to the resin (Phizicky and Fields, 1995). However, for this procedure to work, the protein purity and concentration of the bait protein and concentration of lysate proteins need to be high. The interaction assay often needs to be repeated *in vitro* or *in vivo* with alternative interaction assay formats to confirm that the proteins are actually interacting.

Affinity blotting is similar to western blotting, however, instead of binding to an antibody, the bait protein immobilised on the nitro-cellulose membrane binds to other labelled proteins, peptides or ligands. As with affinity chromatography, the membrane-immobilised protein can also be incubated with cell lysates in an attempt to identify interaction partners. However, the procedure requires the re-folding of the bait protein immobilised on the blot which may not always be successful, preventing the detection of interactions.

Co-immunoprecipitation is one of the most widely used methods to detect protein-protein interactions. It uses bait protein specific antibodies immobilised on beads to indirectly purify proteins that bind to the bait protein in a cell lysate. However, all protein-protein interaction assays may yield 'false positives'. To ensure that the identified interaction is accurate and that any resulting protein interaction is actually taking place in the cell and not an artefact of cell lysis or non-specific binding, further experiments need to be performed.

The above-mentioned assay formats are some of the useful *in vitro* methods for identifying the interaction partners of a particular bait protein in cell lysates. Cell-based methods for detecting or confirming the interaction of two particular proteins include fragment complementation assays in which the one interaction partner is fused to one half of a reporter protein and co-expressed in cells with the second interaction partner fused to the other half of the reporter. Interaction of the proteins restores the function of the reporter. An example of a reporter used in this fashion is green fluorescent protein (GFP) – interaction partners are fused to the N- and C-terminal domains of GFP respectively and expressed in cells (usually *E. coli*). Protein interaction re-constitutes GFP fluorescence (the "split-GFP" assay; Wilson *et al.,* 2004). This assay format was recently used to explore the interactions of the C-terminal domains of *Pf*Hsp70 and *Pf*Hsp90 and the TPR domains of *Pf*Hop (Zininga *et al.,* 2015).

A celebrated cell-based protein-protein interaction assay is the 2-hybrid assay, typically performed in yeast. In a classical 2-hybrid approach, one of the proteins of interest is attached to the DNA binding domain (BD) of a transcription factor and the other protein is attached to a transcription activation domain (AD) (Fields and Song, 1989). Upon expression of the respective fusion constructs in yeast cells, the DNA binding domain attaches to an activation sequence which is upstream from a promoter controlling the expression of a reporter gene. The interaction of the two proteins of interest recruits the activation domain, forming a functional transcriptional factor. RNA polymerase can then be recruited and the reporter gene downstream of the promoter will be transcribed and expressed (Fields and Song, 1989). The reporter gene encodes a protein whose function provides a simple readout, *e.g.* firefly luciferase, β-galactosidase or URA3 (Orotidine 5'-phosphate decarboxylase). The 2-hybrid assay is widely used as it is easy to employ, relatively inexpensive, it can detect protein-protein interactions *in vivo* and can be adapted for high-throughput assays (Fields and Song, 1989). One of the main disadvantages of the assay is the occurrence of false positives due to non-specific interactions and some weak interactions are not always detected by this assay (Bruckner *et al.*, 2009). In addition, if the interaction cannot take place in the nucleus (where the reporter gene is transcribed), this could result in false negatives.

Performing co-localisation with fluorescence microscopy is occasionally used to provide supporting evidence for the interaction of two or more proteins. The two proteins that might be interacting are expressed in cells attached to fluorescent proteins with separate emission wavelengths (GFP and variants of DsRed are usually used; Piston and Kremers, 2007). Alternatively, the proteins may be detected using primary antibodies raised in different species of animals and secondary antibodies conjugated to separate fluorophores. However, this requires cell fixation and precludes live cell microscopy. Using a fluorescence (or, ideally,

confocal) microscope, images taken at different wavelengths corresponding to the excitation/emission wavelengths of the fluorophores are merged with each other to determine if there is any overlap in fluorescence which may indicate co-localisation of the two proteins (depending on the nature of the fluorophore and resolution). Co-localisation, in turn, may be used as supporting evidence for interaction in the context of a living cell. Although the resolution achievable with fluorescence microscopy is constantly being refined, typically it is several hundred nanometres while proteins are only a few nanometres in size. Therefore fluorescence microscopy can only determine if the proteins are in proximity, not necessarily if they are interacting. Electron microscopy has a higher resolution, however labelling is difficult and this type of microscopy can only be performed on fixed and resin embedded cells (D'Amico and Skarmoutsou, 2008). To overcome these limitations, Förster Resonance Energy Transfer (FRET) and Bioluminescence Resonance Energy Transfer (BRET) are used. Both these techniques can be used in live cells, are designed to directly detect protein-protein interactions and can be adapted to be used in high-throughput screening for use in drug discovery (Boute *et al.*, 2002).

1.6.1 FRET and BRET assays

FRET and BRET assays have already proven useful in high-throughput drug screening to find inhibitors of protein-protein interactions (Couturier and Deprez, 2012), in addition to being used for monitoring intracellular calcium ion levels (Zhang *et al.*, 2002), testing for protein kinase activity (Ting *et al.*, 2001) and drug discovery aimed at G protein-coupled receptors (Milligan, 2004).

1.6.2 FRET assays

To perform a FRET assay, appropriate donor and acceptor fluorescent molecules are attached to the proteins of interest. If the two proteins interact with each other, the energy flows from one fluorescent molecule (the donor) to the other (acceptor) by non-radiative transfer (Förster,

1948). This transfer will only occur if the distance separating the proteins is less than 100Å and if there is sufficient overlap between the emission spectrum of the donor molecule and the excitation spectrum of the acceptor molecule (Piston and Kremers, 2007). The effectiveness of the assay depends on the inverse of power to the sixth of distance between and the alignment of dipoles in the both the donor and acceptor: ($E = \frac{1}{1\left(\frac{r}{Ro}\right)^6}$), where E=FRET efficiency, r=distance between donor and acceptor, Ro=distance at which the energy transfer efficiency is 50%. Therefore, slight changes in distance and orientation of the fluorophores can have a large effect on the signal (Milligan, 2004). Consequently, the closer and better aligned the two fluorophores are the higher the FRET efficiency, leading to an improved detection rate (Piston and Kremers, 2007). These parameters make FRET a practical assay to determine protein-protein interactions in a high throughput format. The assay can be performed *in vitro* using purified proteins attached to compatible donor and acceptor fluorophores. However, fusion of the interacting proteins to donor and acceptor fluorescent proteins and their co-expression in cells allows for the detection of protein interactions in live cells by fluorescence microscopy or using a fluorimeter or fluorescence plate reader.

1.6.3 Limitations of the FRET assay

There are limitations with FRET assays which can theoretically lead to the assay being misread and the results being misinterpreted. To perform a FRET assay in a fluorimeter or plate reader, the sample is illuminated using the excitation wavelength of the donor fluorophore and the fluorescence emission measured at the emission wavelengths of the donor and acceptor fluorophores, respectively. The FRET signal is obtained by the ratio of the acceptor/donor fluorescence emissions. The assumption is that the acceptor fluorescence emission is due to its excitation by the donor fluorophore emission. Close proximity of the fluorophores (due to the interaction of the attached proteins) thus yields higher FRET signals. The two main concerns

are using donor and acceptor fluorophores of different quantum yields (brightness) and cross-talk and bleed-through between the two fluorophores. Cross-talk occurs when the acceptor fluorophore is excited by the wavelength chosen to excite the donor fluorophore, leading to misleading results. Bleed-through occurs when either or both of the fluorophores have broad emission spectra, thus leading to the detection of donor emission at the acceptor emission wavelength or *vice versa* (Chen *et al.*, 2006). This can be exacerbated if one of the fluorophores has a higher quantum yield than the other. Therefore, choosing the correct FRET pair of fluorophores is crucial. When using fluorescent proteins (FPs) as the FRET pair, the parameters that need to be met are as follows: the FPs should not be too large – larger FPs means the photons from the donor have to travel a longer distance to reach the acceptor, thus decreasing FRET efficiency, while also increasing the risk that fusion to the interaction partners compromises the affinity of the interaction; the excitation and emission spectra cannot be too wide, to reduce the occurrence of bleed-through; there has to be minimal interaction between the FPs to ensure that FRET signals obtained reflect interaction of their respective fusion partners; brighter FPs are preferable due to better detection of the signal (Piston and Kremers, 2007).

For this project, the donor fluorophore used was cyan fluorescent protein (CFP) and the acceptor was yellow fluorescent protein (YFP). Although this FRET pair still has cross-talk and bleed-through it is considered an optimal pair (Kremers *et al.*, 2006). CFP absorbs lights optimally at 425 nm and emits light at 485 nm, while YFP absorbs light at 485 nm and emits light at 535 nm. The FRET assay is thus performed by reading the fluorescence using excitation/emission wavelengths of 425 nm/485 nm (CFP) and 425 nm/535 nm (YFP) and calculating the YFP/CFP emission ratios

1.6.4 BRET assays

Bioluminescence resonance energy transfer (BRET) is another method widely used to monitor protein-protein interactions. It involves resonance energy transfer between a bioluminescent donor and a fluorescent acceptor (Xie *et al.*, 2011). Since the donor emits photons intrinsically, fluorescence excitation is unnecessary, therefore BRET avoids some of the problems associated with fluorescence resonance energy transfer (FRET), such as photobleaching, auto-fluorescence and direct excitation of the acceptor fluorophore (Xie *et al.*, 2011). To perform a BRET assay, the two proteins of interest are fused to an energy donor (a luciferase bioluminescent enzyme) and an energy acceptor (fluorescent protein). If the proteins come into close proximity to each other (up to 100Å), a non-radiative transfer of energy from the excited state luciferase energy donor to the fluorescent protein acceptor occurs after addition and the subsequent oxidation of the luciferase substrate (Wu and Brand, 1994). Similar to the FRET assay, BRET signals are calculated as the ratio of acceptor to donor emissions. The most common BRET pair and the pair that was used in this study is *Renilla* luciferase (Rluc), which oxidizes the substrate coelenterazine and emits photons at 475 nm, and yellow fluorescent protein (YFP) as the energy acceptor (Pfleger and Eidne, 2006). This BRET pair has the advantage of higher quantum yields and therefore higher sensitivity to aid in signal detection (Gersting *et al.*, 2012). To perform a BRET assay, coelenterazine is added to the sample and the emission of Rluc (475+/-30nm) and YFP (535+/-30nm) is recorded using a spectrometer and the ratio is calculated (Pfleger and Eidne, 2006). As with the FRET assay, the BRET assay can be used to detect protein interactions in live cells by co-expressing the respective Rluc and YFP fusion proteins in cells.

As stated in the problem statement (section 1.5), the overall aim of this project was to explore assay formats that can be used, firstly, to detect Hsp90-Hop interactions and, secondly, are plate-based to facilitate screening of compound collections for inhibitors of the interaction.

FRET and BRET assay formats were chosen since they enable the detection of protein interactions in live cells, thus more closely mimicking the endogenous Hsp90-Hop interaction for screening purposes. The *P. falciparum* Hsp90 and Hop proteins were focused on with anti-malarial drug discovery in mind, but mammalian Hsp90 and Hop was included in the study for two reasons: to act as a control for inhibitor specificity during compound screening experiments; to attempt to establish an assay that can alternatively be used for potential anti-cancer compound screening. To achieve the aims, the following objectives were pursued:

1) Preparation of mammalian cell expression plasmid constructs suitable for FRET and BRET assays. This involved cloning experiments to fuse the coding sequences of YFP to human Hsp90 and *P. falciparum* Hsp90 as well as their C-terminal domains and to fuse *Renilla* luciferase and CFP sequences to murine Hop and *P. falciparum* Hop as well as their TPR2A domains in a mammalian expression plasmid (pEGFP-C1) backbone.
2) Culturing and transient transfection of HeLa cells in 96-well plates with the expression constructs to determine if the respective Hsp90-Hop interactions (full-length Hsp90-Hop and C-domain-TPR2A domain) can be detected using FRET or BRET assays.

To simplify the assay format and improve compound screening throughput, an additional *in vitro* protein-based FRET assay format was explored for detecting the interaction of the Hsp90 C-terminal domains and Hop TPR2A domains. To enable this, the following objectives were pursued:

1) Preparation of *E. coli* plasmids for the expression of His-tagged proteins. This involved cloning experiments to insert coding sequences of the human and *P. falciparum* C-terminal domains fused to YFP and murine and *P. falciparum* TPR2A domains fused to CFP in a pET-28a plasmid backbone.

2) Small scale expression experiments to determine the extent to which the respective fusion proteins were expressed in a soluble form in *E. coli.*
3) Large scale expression and purification of the recombinant proteins using Ni-NTA affinity chromatography.
4) Using the purified proteins to perform FRET assays in 96-well plates to determine if the respective *P. falciparum* and mammalian domain interactions can be detected.

CHAPTER 2

METHODS

2.1 PREPARING PLASMID CONSTRUCTS

2.1.1 Primers, plasmids and cloning strategies (Additional details in Appendix I)

This study required the preparation of four sets of expression plasmid constructs. Three of these were required for the HeLa cell FRET and BRET assays:

1) pCFP-mHop, pCFP-*Pf*Hop, pCFP-mTPR2A, pCFP-*Pf*TPR2A
2) pRluc-mHop, pRluc-*Pf*Hop, pRluc-mTPR2A, pRluc-*Pf*TPR2A
3) pYFP-hHsp90, pYFP-*Pf*Hsp90, pYFP-hCdom, pYFP-*Pf*Cdom

The pCFP, pRluc and pYFP plasmid backbones contain the coding sequences of cyan fluorescent protein (CFP – Cerulean variant), *Renilla* luciferase (Rluc) and yellow fluorescent protein (YFP – Venus variant) respectively, upstream of the multiple cloning site of the mammalian expression plasmid pEGFP-C1 (ClonTech). The plasmids were previously prepared (H.C. Hoppe, unpublished) and donated for this study by PCR amplifying the respective coding sequences from pCerulean N1 (CFP; Addgene plasmid 27795), pBIND (Rluc; Promega) and pISH-Venus (YFP; Addgene plasmid 15865) and using them to replace the EGFP sequence between the *Age*I and *Bgl*II sites of pEGFP-C1. Two additional constructs donated for this study were FRET and BRET positive controls (pFRET, pBRET) containing, respectively, the CFP sequence cloned into the *Kpn*I/*Bam*HI sites downstream of the YFP sequence in pYFP and the YFP sequence cloned into the *Kpn*I/*Bam*HI sites downstream of Rluc in pRluc, thereby creating YFP-CFP and Rluc-YFP fusion constructs.

The coding sequences of murine Hop (mHop; *Mus musculus* stress-induced phosphoprotein 1; NCBI reference sequence NM_016737.2), the murine Hop TPR2A domain (mTPR2A; amino acids 223 – 352), *P. falciparum* Hop (*Pf*Hop; PlasmoDB reference number PF3D7_1434300)

and the *Pf*Hop TPR2A domain (*Pf*TPR2A amino acids 233 – 367) had previously been cloned (H.C. Hoppe) into the *Sal*I and *Xba*I sites of the mammalian 2-hybrid plasmid pACT (Promega; GenBank accession number AF264723) and made available for this study. Also donated for this study by H.C. Hoppe were the coding sequences of the human Hsp90 α isoform (hHsp90; *Homo sapiens* HSP90AB1; NCBI reference sequence NM_001271969.1), *P. falciparum* Hsp90 (*Pf*Hsp90; PlasmoDB reference number PF3D7_0708400), human Hsp90 C-terminal domain (hCdom; amino acids 629-724) and *Pf*Hsp90 C-terminal domain (*Pf*Cdom; amino acids 656 – 744) cloned into the *Sal*I and *Xba*I sites of the mammalian 2-hybrid plasmid pBIND (Promega; GenBank accession number AF264722). The *P. falciparum Pf*Hsp90 and *Pf*Hop sequences had previously been codon-optimised for expression in human cells by Genscript.

To prepare the pCFP and pRluc constructs listed above (construct sets 1 and 2), the Hop and TPR2A domain sequences were excised from the corresponding donated pACT plasmids with *Kpn*I and *Sal*I and cloned into the *Kpn*I/*Xho*I sites of pCFP and pRluc (this study). To prepare the pYFP constructs (construct set 3), the donated pBIND plasmids were used as templates to PCR amplify the Hsp90 and C-domain sequences (primers listed in Table 1, below), digest the PCR products with *Bam*HI and *Xho*I and clone them into the *Bam*HI/*Xho*I sites of pYFP (this study).

A fourth set of plasmid constructs was required for expressing recombinant YFP- and CFP-fusion proteins in *E. coli* for the exploration of an *in vitro* FRET assay:

4) pET-YFP-hCdom, pET-YFP-*Pf*Cdom, pET-CFP-mTPR2A, pET-CFP-*Pf*TPR2A.

The *E. coli* expression plasmid pET-28a (+) (Novagen), which contains a histidine tag-coding sequence upstream of the multiple cloning site, was used as the target plasmid for these constructs. The coding sequences of YFP fused to the N-termini of the C-terminal domains of

human Hsp90 and *Pf*Hsp90 (YFP-hCdom, YFP-*Pf*Cdom) and CFP fused to the N-termini of the TPR2A domains of murine Hop and *Pf*Hop (CFP-mTPR2A, CFP-*Pf*TPR2A) were PCR amplified from the corresponding mammalian pCFP and pYFP FRET expression plasmids (plasmid sets 1 and 3) described above, digested with *Nhe*I and *Xho*I and cloned into the *Nhe*I/*Xho*I sites of pET-28a. An additional negative control plasmid (pET-YFP) was prepared by PCR, amplifying the YFP sequence from pYFP and cloning it into the *Nhe*I/*Xho*I sites of pET28a.

Primers used for preparing the constructs in set 3 (pYFP constructs) and set 4 (pET constructs), the pET-YFP negative control, as well as primers used for verifying the cloning of hHsp90 and *Pf*Hsp90 C-domain constructs, are listed in Table 1. Primers were synthesised by Integrated DNA Technologies®, USA, and supplied as lyophilized preparations at a 25 nmol scale. Primers were reconstituted in Tris-EDTA (TE) buffer solution (10 mM Tris-HCl, 1 mM EDTA, pH 8.0) to create a 100 µM stock concentration.

Table 1: Constructs, primers and templates used in this project. Restriction sites are underlined in the primer sequences and include *Bam*HI and *Xho*I for the pYFP constructs and *Nhe*I and *Xho*I for the pET constructs

Construct	Template	Forward primer	Reverse primer
pYFP-hCdom	pBIND-hHsp90	5'-AATGGGTCGCGGATCC AACCCTGACCACCCCATTGT G-3'	5'-GGTGGTGGTGCTCGAG CTAATCGACTTCTTCCATC GGAGAC-3'
pYFP-*Pf*Cdom	pBIND-*Pf*Hsp90	5'-ATTGGGTCGCGGATCC GAGATTAACGCAAGACAC CCC-3'	5'GGTGGTGGTGCTCGAG TCAATCGACTTCCTCCAT CTTGCTATC-3'
pYFP-hHsp90	pBIND-hHsp90	5'CACCTCGAG AGATGCCTGAGGAAGTG-3'	5'GGTGGTGGTGCTCGAG TCAATCGACTTCCTCCAT CTTGCTATC-3'
pYFP-*Pf*Hsp90	pBIND-*Pf*Hsp90	5'CACCTCGAG AGATGTCCACTGAGACTT-3'	5'-CACGGATCC TCAATCGACTTCCTCCAT-3'
Verifying pYFP-hCdom	pYFP-hCdom	5'CAGCCATATGGCTAGC ATGGTGAGCAAGGGCGA GGAG 3'	5'GGTGGTGGTGCTCGAG TCAATCGACTTCCTCCAT CTTGCTATC-3'
Verifying pYFP-*Pf*Cdom	pYFP-*Pf*Cdom	5'CAGCCATATGGCTAGC ATGGTGAGCAAGGGCGA GGAG 3'	5'GGTGGTGTTGCTCGAG CTAATCGACTTCTTCCAT GCGAGAC-3'
pET-YFP	pYFP	5'CAGCCATATGGCTAGC ATGGTGAGCAAGGGCGA GGAG 3'	5'GGTGGTGGTGCTCGAG TTACTTGTACAGCTCGT CCATGCCG 3'
pET-YFP-hCdom	pYFP-hCdom	5'CAGCCATATGGCTAGC ATGGTGAGCAAGGGCGA GGAG 3'	5'GGTGGTGGTGCTCGAG CTAATCGACTTCTTCCAT GCGAGACG 3'
pET-YFP-*Pf*Cdom	pYFP-*Pf*Cdom	5'CAGCCATATGGCTAGC ATGGTGGCAAGGGCGAG GAG 3'	5'GGTGGTGGTGCTCGAG TCAATCGACTTCCTCCAT CTTGC 3'
pET-CFP-mTPR2A	pCFP-mTPR2A	5'CAGCCATATGGCTAGC ATGGTGAGCAAGGGCGA GGAG 3'	5'GGTGGTGGTGCTCGAG TTACAAGCGCTCCTGTT CCTTCAG 3'
pET-CFP-*Pf*TPR2A	pCFP-*Pf*TPR2A	5'CAGCCATATGGCTAGC ATGGTGAGCAAGGGCGA GGAG 3'	5'GGTGGTGGTGCTCGAGT TACTCTTTCTCCTTGCGCC TTTCCAG 3'

2.1.2 Polymerase chain reaction (PCR)

PCR was performed using a hot-start protocol with 5 x KAPA HiFi buffer, KAPA dNTP mix (0.2 mM), DNA template (0.5 µl purified plasmid), primers (3 µM) and 0.5 units of HiFi DNA polymerase (KAPA). The total volume was made up to 50 µl with water. Prior to initiating the PCR cycle, the sample was heated at 94°C for two min, followed by the addition of the DNA polymerase. The following PCR cycle was used:

94°C	0:40 min (denaturation phase)
60-64°C	0:45 min (annealing phase)
70°C	2:00 min (extension phase)

The cycle was repeated 30 times, with one final extension step of 5:00 min at 70°C. After agarose gel analysis (section 2.1.5 below), the PCR product was purified using a Nucleospin Gel and PCR Clean-up kit (Macherey-Nagel) according to the manufacturer's instructions in preparation for restriction digestion.

2.1.3 Alkaline lysis plasmid miniprep

To purify plasmids from *E. coli* cultured from a glycerol stock or from a colony on a plate, an alkaline lysis plasmid miniprep was performed. A scraping of the glycerol stock or a picked colony was placed in 5 ml LB broth with appropriate antibiotic (50 µg/ml ampicillin or kanamycin) and grown up with shaking overnight at 37°C. The *E. coli* cells were pelleted in a microfuge tube at 3099x*g* for three min and the pellet was re-suspended in 100 µl GTE buffer (30 mM glucose, 25 mM Tris, 10 mM EDTA, 10 µg/ml RNase, pH 8.0). A volume of 200 µl NaOH/SDS lysis solution (0.2 N NaOH, 1% (w/v) SDS) was added, the tube agitated to ensure complete cell lysis and 150 µl 5 M potassium acetate was subsequently added and mixed thoroughly. This mixture was centrifuged at 15458x*g* for five min, 400 µl of the supernatant was removed and placed in a fresh microfuge tube, 800 µl absolute ethanol was added

and the DNA was pelleted at 15458x*g* for six min. The pellet was washed using 70% ethanol and air dried before it was dissolved in 50 µl water.

2.1.4 Restriction digestion

ThermoFisher Scientific FastDigest™ enzymes were used for all restriction digests of PCR products and plasmids. Reactions were carried out in a total volume of 25 µl containing 1 unit of each enzyme, 10 µl of the PCR product or the plasmid miniprep, 2.5 µl 10X ThermoFisher Scientific FastDigest buffer and the balance made up with milliQ water. All digestion reactions were incubated at 37°C for two h.

2.1.5 Agarose gel electrophoresis

To prepare an 0.8% agarose gel, 0.4 g of SeaKem® LE Agarose (Lonza) was dissolved in 50 ml of TBE buffer (0.277 M Tris, 0.22 M boric acid, 0.013 M EDTA) by briefly heating the mixture in a microwave oven and 12 µg of ethidium bromide (1mg/ml stock in water) was added. The gel was poured into a casting tray and allowed to solidify. Samples were mixed with sample buffer (TBE buffer containing 30% [v/v] glycerol and 0.25% [w/v] bromophenol blue) in a 5:1 ratio and applied to the gel along with a 1 kb DNA ladder (New England Biolabs). The gel was run in TBE buffer at 80 V until the bromophenol blue front had migrated approximately two thirds of the length of the gel. DNA bands were visualised on a UV transilluminator and images captured with a ChemiDoc™ XRS+ gel documentation system (Bio-Rad). For cloming purposes, restriction digested plasmid, insert and PCR product bands were purified from the gel using a Nucleospin Gel and PCR Clean-up kit (Macherey-Nagel) according to the manufacturer's instructions.

2.1.6 Ligation reactions

Ligation reactions were performed, using the restriction-digested and gel-purified plasmids, inserts and PCR products according to their concentrations determined using a NanoDrop 2000

spectrophotometer (ThermoFisher Scientific), using a 3-fold molar excess of insert and 200 ng plasmid. Reactions were carried out in a total volume of 20 µl containing 10 µl 2x ligase buffer and 1 µl (1 unit) T4 DNA ligase (Promega) and incubated overnight in icy water.

2.1.7 Transforming *E. coli* cells

2.1.7.1 Preparing competent cells

In this study, XL10-Gold *E. coli* cells (Stratagene) were used for cloning experiments and BL21 (DE3) (New England Biolabs) for protein expression.

Untransformed *E. coli* cells (from a frozen stock) were cultured overnight in 5 ml LB broth at 37°C with shaking. The following day, the 5 ml *E. coli* suspension was split into two flasks containing 100 ml LB broth each. These cultures were grown with shaking at 37°C until the OD_{600} reached 0.6-0.8. The cultures were then centrifuged at 3913x*g* for 10 min to pellet the *E. coli* cells. Each of the *E. coli* pellets was re-suspended in 4 ml RF-1 buffer (0.1 M KCl, 50 mM $MnCl_2$, 30 mM potassium acetate, 10 mM $CaCl_2$, 15% [v/v] glycerol, pH 5.8) and incubated on ice for 20 min. These suspensions were centrifuged at 3578x*g* for 10 min and the pellet was re-suspended in 3 ml RF-2 buffer (10 mM HEPES, 10 mM KCl, 75 mM $CaCl_2$, 15% [v/v] glycerol). The suspensions were aliquoted into cryotubes and stored at minus 80°C.

2.1.7.2 Transformation

To transform the *E. coli* cells, 10 µl of a ligation reaction (or 0.1 µl purified plasmid) was added to 50 µl of thawed competent cells and mixed gently in a chilled microfuge tube. The mixture was incubated on ice for 30 min and was then incubated at 42.5°C for 60 seconds. The mixture was returned to ice for five min. Thereafter, 500 µl LB broth was added to the tube and it was incubated at 37°C for one hour. An aliquot of 100 µl of this mixture was plated on an LB-agar plate with 50 µg/ml the appropriate antibiotic and the plate was incubated at 37°C overnight.

2.2 HELA CELL CULTURING AND TRANSFECTION

2.2.1 Thawing HeLa cells

A cryotube of frozen HeLa cells (Cellonex, South Africa) was removed from a -80^{o}C freezer and allowed to thaw at room temperature before being transferred to a 15 ml tube containing 10 ml culture medium (section 2.2.3). The suspension was centrifuged at 300x*g* for three min to pellet the cells. The supernatant was discarded and the cell pellet was re-suspended in 5 ml medium and transferred to a T25 flask that was subsequently incubated in a 5% CO_2 37°C incubator.

2.2.2 Cryopreserving HeLa cells

Four ml of Trypsin/EDTA solution (Lonza, Switzerland) was added to a culture flask containing semi-confluent cells and the flask was returned to the incubator for approximately five min. The flask was viewed under an inverted light microscope to ensure that the cells had detached from the bottom surface of the flask. The suspension of cells was transferred to a 15 ml tube and centrifuged at 300x*g* for three min to pellet the cells. The supernatant was aspirated off and the cell pellet was re-suspended in 1 ml cryopreservation solution (10% dimethyl sulfoxide [DMSO] in fetal bovine serum), placed in a cryotube and stored in a -80°C freezer.

2.2.3 Routine culturing

HeLa cells were grown in Dulbecco's modified Eagle's medium (DMEM) with 5 mM L-glutamine (Lonza) supplemented with 10% fetal bovine serum (Biowest) and 1% penicillin, streptomycin and Fungizone (Lonza) in a 37°C, 5% CO_2 incubator. When the cells became confluent, the medium was aspirated, 4 ml Trypsin/EDTA solution was added and the flask placed in the incubator for approximately five min. The flask was viewed under an inverted light microscope to ensure that the cells had detached. Most of the cell suspension was then

aspirated off, leaving only a thin layer in the corners of the flask. Five ml of medium was added to the flask and it was returned to the incubator.

2.2.4 Plating HeLa cells in 96-well plates

When the HeLa cells in the flask had reached a 60-80% confluency, the medium was aspirated off, 5 ml trypsin/EDTA was added and the flask was placed in the incubator for approximately five min. Once the cells had detached from the bottom of the flask, they were pelleted in a 15 ml tube at 300x*g* for three min. The cells were re-suspended in 5 ml medium. The concentration of the cells in this suspension was counted using a haemocytometer (Neubauer chamber), using an inverted microscope. Subsequently, the cells were diluted in medium to a concentration of $1x10^5$ cells/ml for plating in a 96-well plate. An aliquot of 100 µl of this diluted suspension was transferred into each well of a 96-well plate, to give a final concentration of $1x10^4$ cells per well. The plate was placed back in the incubator and incubated overnight.

2.2.5 Transfection of HeLa cells using Xfect

After the cells had been plated and left overnight, 2.5 µg total plasmid DNA was mixed with Xfect buffer (ClonTech) in a microfuge tube to bring the total volume to 50 µl. Xfect polymer (0.75 µl) was then added and mixed thoroughly. The mixture was incubated at room temperature for 10 min, after which 10 µl/well of the mixture was added to the cells in the plate and the plate returned to the 5% CO_2 37ºC incubator. The medium containing the Xfect-DNA mixture was removed from the cells after four h and replaced with 150 µl of fresh medium. The plate was returned to the incubator and left overnight.

2.3 PERFORMING HELA CELL FRET AND BRET ASSAYS

2.3.1 FRET assay

The day after the HeLa cells in 96-well plates had been transfected with FRET plasmids using the Xfect transfection protocol described above (2.2.5), the media was removed from the wells and replaced with 50 µl phosphate-buffered saline (PBS: 10 mM sodium phosphate, 2.7 mM KCl, 0.137 M NaCl, pH 7.4). Fluorescence was read in a Spectramax M3 reader (Molecular Dynamics). The cells were excited at 425 nm and emission was read at 485 nm and 535 nm. The FRET signal was obtained by dividing the emission at 535 nm by that at 485 nm after having subtracted background readings obtained from wells of untransfected cells.

2.3.2 BRET assay

As in the case of the FRET assay, the BRET assay was performed the day after transfecting HeLa cells with BRET plasmids using Xfect. The media in the wells was removed and replaced with 50 µl PBS containing a 1:50 dilution of *Renilla*-Glo luciferase assay substrate (Promega). Luminescence was read using a Spectramax M3 plate reader (Molecular Devices) at emission wavelengths of 485 nm and 535 nm. BRET signals were calculated from the ratio of the 535 nm/485 nm readings, after having subtracted background readings obtained from wells containing untransfected cells.

2.4 PROTEIN EXPRESSION IN *E. coli*

2.4.1 Small-scale expression

Once the correct pET plasmid constructs had been created, they were transformed into BL21(DE3) (New England Biolabs) competent *E. coli* cells using the protocol described above (2.1.7.2) and plated onto LB plates containing 50 µg/ml kanamycin. The plates were left at 37°C overnight and the resulting colonies were picked and cultured in 5 ml of LB broth containing 50 µg/ml of kanamycin overnight at 37°C. The next day, the broth was used to

inoculate two sets of fresh LB broth (5 ml with 50 µg/ml kanamycin) with 1/20th of the pre-culture which were cultured at 37°C until OD_{600} 0.6 – 0.8 was reached. Expression in one of the cultures was then induced with 1 mM Isopropyl β-D-1-thiogalactopyranoside (IPTG; Sigma-Aldrich), and the other culture was left un-induced as a control. Both cultures were incubated for a further 3.5 h at 37°C, after which the cultures were centrifuged at 8050x*g* for six min and the supernatant was discarded. The pellets (induced and un-induced) were re-suspended in 500 µl of PBS buffer and sonicated twice (kept on ice in between sonication cycles) at 60 Hertz for 30 seconds using a Vibra Cell ™ (Sonic and Materic Inc.). The sonicated suspensions were centrifuged at 20,000x*g* for 10 min to separate out the soluble and insoluble fractions. The soluble fractions (supernatants) were transferred to separate microfuge tubes, and the insoluble pellets were re-suspended in 500 µl PBS buffer. These fractions were mixed with 4X SDS-PAGE sample buffer and run on a 12% SDS-PAGE separating gel with a 4% stacking gel according to Laemmli (1970) (section 2.5 below). The gel was stained with Coomassie stain for three h and de-stained until the protein bands became clear. The gel was photographed using a ChemiDoc XRS gel documentation system (Bio-Rad).

Owing to the fact that the pET 28a plasmid displayed "leaky expression" in the BL21 cells and the proteins appeared to be expressed with and without induction with IPTG, an alternative control had to be used to confirm the proteins were being expressed. For the control, un-transformed BL21 *E. coli* cells were used. A Bradford's assay (see section 2.4.5 below) was performed to ensure that the control and the sample had the same protein concentrations before loading onto the SDS-PAGE gel.

2.4.2 Large-scale protein purification

Transformed BL21 cells were cultured in 5 ml LB broth with 50 µg/ml kanamycin overnight. The following day, 250 ml of fresh LB broth with 50 µg/ml kanamycin was inoculated with 2.5 ml of the overnight culture. This culture was incubated until OD_{600} reached 0.6 – 0.8, 1mM

ITPG was added and culturing continued for a further 3.5 h. The culture was centrifuged at 3913x*g* for 10 min and the supernatant was discarded. The pellet was re-suspended in 10 ml lysis buffer (50 mM NaH_2PO_4, 300 mM NaCl, 10 mM imidazole, pH 8) per 1 g of wet bacterial pellet, lysozyme was added to a final concentration of 1 mg/ml and the suspension was left on ice for 20 min. The suspension was then sonicated at 60 Hertz for one min using a Vibra Cell™ probe sonicator and centrifuged at 30678x*g* for 30 min. The supernatant was poured into a syringe and filtered using 0.4 µm and 0.2 µm filters sequentially and a sample was collected for SDS-PAGE analysis. A Ni-NTA super flow column (Qiagen) was equilibrated with 5 ml lysis buffer, the cleared lysate was added to the column and a sample of the flow-through was removed for SDS-PAGE analysis. The column was washed twice with 5 ml lysis buffer and a sample of each wash was taken for SDS-PAGE analysis. The protein was eluted with 2.7 ml elution buffer (50 mM NaH_2PO_4, 300 mM NaCl, 500 mM imidazole, pH 8) and a sample removed for SDS-PAGE analysis. All samples were mixed with SDS-PAGE sample buffer and analysed on 12% SDS-PAGE gels to determine whether protein purification was successful (section 2.5).

2.4.3 Stripping and re-charging the nickel-NTA column

After elution, the Ni-NTA super-flow column was rinsed with distilled water, stripping buffer (20 mM sodium phosphate, 500 mM NaCl, 50 mM EDTA, pH 7.4) was applied and allowed to run through it. The column was rinsed again with water and re-charging buffer (0.1 M $NiSO_4$) was applied. The column was rinsed a final time in water and stored in 50% ethanol at 4°C.

2.4.4 Desalting the protein

To remove the excess imidazole from the protein eluted from the Ni-NTA column and perform buffer exchange, a PD-10 desalting column (GE Healthcare) was washed with 25 ml Tris-buffered saline (TBS: 50 mM Tris-HCl, 150 mM NaCl, pH 7.5), 2.5 ml of the protein eluate

was applied to the column and the protein was eluted with 3.5 ml TBS buffer. A Bradford's assay was performed to determine the amount of protein present in the sample.

2.4.5 Bradford's assay

A standard curve was prepared, using serial dilutions of bovine serum albumin (BSA; Roche) in TBS: 2 mg/ml, 1.5 mg/ml, 1 mg/ml, 0.75 mg/ml, 0.5 mg/ml, 0.25 mg/ml and 0.125 mg/ml. Five µl of each dilution was added to 250 µl of Bradford Reagent (Sigma-Aldrich) in a 96-well plate. The plate was left to develop for 10 min and the absorbance was read at 595 nm, using a Spectramax M3 plate reader. A standard curve of BSA concentration vs. Abs_{595} was prepared, using Microsoft Excel. To determine the level of protein in the samples, 5µl of the sample was added to 250 µl Bradford Reagent, the absorbance was read at 595 nm and the concentration of protein was determined using the standard curve.

2.5 SDS-PAGE AND WESTERN BLOTTING

2.5.1 SDS-PAGE

To create a 12% resolving gel, a gel sandwich using Bio-Rad Mini-PROTEAN II casting components was set up. Four ml of 30% acrylamide (0.3 g/ml acrylamide, 0.008 g/ml *bis*-acrylamide in water) was added to 2.5 ml lower gel buffer (1.5 M Tris, 0.01 M SDS, pH 8.8) and 3.5 ml distilled water. To initiate polymerisation, 7µl of tetramethylethylenediamine (TEMED) and 35 µl of 10% (w/v) ammonium persulfate (APS) was added. The gel solution was poured into the gel sandwich and a thin layer of isopropanol was added to the top. To create the 4% stacking gel, 0.7 ml 30% acrylamide was added to 1.25 ml stacking gel buffer (0.5 M Tris, 0.01 M SDS, pH 6.8) and 3 ml distilled water, followed by the addition of 6 µl TEMED and 25 µl ammonium persulfate (APS). The isopropanol was removed from the top of the polymerised resolving gel and the stacking gel solution was poured on top, a well comb

was added and the gel left to set. Samples were mixed in a 3:1 ratio with 4X SDS-PAGE sample buffer (5% [v/v] 2-mercaptoethanol, 0.02% [w/v] bromophenol blue, 30% [v/v] glycerol, 10% [w/v] SDS in 250 mM Tris-HCl, pH 6.8), incubated at 95°C for five min and applied to the gel. The gel was run at a constant voltage of 120 V in a Bio-Rad Mini-PROTEAN II apparatus. When electrophoresis was complete, the gel was removed from the apparatus and incubated in Coomassie stain solution (45% water, 45% methanol, 10% acetic acid and 0.5 g/l Coomassie blue R-250) for three h and de-stained using Coomassie de-stain solution (10% acetic acid, 45% methanol, 45% water).

2.5.2 Western blotting

After having run an SDS-PAGE gel, it was removed from the apparatus and incubated in transblot buffer (0.025 M Tris, 0.19 M glycine, 10% methanol) for 15 min. The gel was placed in a Bio-Rad Mini-PROTEAN II transblot sandwich with an Amersham Hybond ECL™ nitrocellulose blotting membrane and transblotted at 90 V for an hour. The membrane was removed from the sandwich, incubated with Ponceau S stain, (0.1% [w/v] Ponceau S in 1% [v/v] acetic acid) and de-stained using Ponceau S de-stain (1% acetic acid) to confirm successful transfer of the proteins.

For probing with antibodies, the blot was incubated in blocking buffer (TBS containing 0.1% [v/v] Tween 20, 1% [w/v] BSA and 2% [w/v] milk powder) and subsequently incubated overnight at 4°C with the appropriate primary antibody: rabbit anti-actin (Santa-Cruz Biotechnologies), mouse anti-GFP (Santa-Cruz Biotechnologies) or rabbit anti-*Renilla* luciferase (ThermoFisher Scientific) diluted 1000-fold in blocking buffer. The blot was then washed four times with washing buffer (TBS + 0.1% Tween 20) and incubated with secondary antibody (goat anti-rabbit-HRP or goat anti-mouse-HRP [Seracare] diluted 1:5000 in blocking buffer) for one hour at room temperature. The blot was rewashed four times in washing buffer and the bands were detected using a colorimetric TMB peroxidase substrate (Seracare).

To detect His-tagged proteins, the HCL Hybond membrane was incubated with blocking buffer (TBS containing 0.1% Tween 20, 1% BSA, 2% milk powder and 10 mM imidazole) overnight at 4°C. The next day, HisDetector™ Nickel-HRP (KPL) (1 in 5000 dilution in blocking buffer) was added to the blot and it was incubated at room temperature for one hour. The blot was then washed four times with blocking buffer and the bands visualised by adding TMB membrane peroxidase substrate (Seracare).

2.6 FRET ASSAY WITH PURIFIED PROTEINS

Fifty µl of each purified protein (YFP-hCdom [1.87 µM], YFP-*Pf*Cdom [3.8 µM], CFP-mTPR2A [5.41 µM], CFP-*Pf*TPR2A [6.4 µM] or YFP [5.28 µM]) was placed in separate wells of a black 96-well plate. Each protein then underwent a two-fold serial dilution in TBS containing 0.1% BSA across the 12 wells of the 96-well plate row. The CFP fluorescence was read using excitation and emission wavelengths of 425 nm and 485 nm respectively, and the YFP fluorescence using 485 nm and 535 nm in a Synergy Mx plate reader (BioTek). A blank of buffer without protein was used and the fluorescence value obtained with it subtracted from the corresponding readings in the wells containing proteins. Each fluorescence value for each YFP fusion protein dilution was compared to that obtained with the corresponding CFP fusion protein (*i.e.*, YFP-hCdom with CFP-mTPR2A and YFP-*Pf*Cdom with CFP-*Pf*TPR2A). To prepare for the FRET assay, the proteins were diluted in TBS containing 0.1% BSA to obtain similar YFP and CFP fluorescence values. To perform the FRET assay, 50 µl of the CFP-mTPR2A dilution was added to five wells of a 96-well black plate and mixed with 50 µl of YFP-hCdom and this was repeated for the *Pf* proteins. Negative control wells contained CFP-*Pf*TPR2A and YFP and background control wells buffer without protein. This resulted in final concentrations of 0.12 µM YFP-hCdom + 0.34 µM CFP-mTPR2A, 0.24 µM YFP-*Pf*Cdom + 0.41 µM CFP-*Pf*TPR2A and 0.33 µM YFP + 0.41 µM CFP-*Pf*TPR2A). After incubating for 20 min at room temperature, the fluorescence was read at 425/485 nm (excitation/emission

wavelengths) and again at 425/535 nm. The average fluorescence values obtained from background control wells (buffer without protein) were subtracted from the readings obtained in corresponding experimental wells. The emission values at 535 nm were divided by the values at 485 nm to obtain the FRET signals.

2.6.1 Inhibiting the *Pf*Cdom – *Pf*TPR2A interaction with a TPR2A peptide

Based on a TPR2A peptide described by Horibe, *et al.* (2011) which contains the human Hop TPR2A domain amino acid sequence responsible for binding to the C-terminal EEVD motif of Hsp90, a peptide containing the corresponding *Pf*TPR2A sequence (amino acids 318 – 330: AKLYNRLAISYIN) was custom synthesized by Genscript (Hong Kong) and prepared as a 1 mM stock solution in DMSO. The YFP-*Pf*Cdom protein and the TPR2A peptide were mixed in a 96-well black plate to yield concentrations of 0.38 µM and 200 µM for the protein and peptide respectively, in a volume of 50 µl. The plate was left at room temperature rocking on a MiniMix^{TM} rocker (Enduro^{TM}). After 20 min, 50 µl of the CFP-*Pf*TPR2A domain was added to achieve final concentrations of 0.19 µM YFP-*Pf*Cdom, 0.41 µMCFP-*Pf*TPR2A and 100 µM peptide. The peptide inhibitor was also included in the background and negative control wells (buffer alone and YFP + CFP-*Pf*TPR2A respectively) and an uninhibited reaction containing DMSO without peptide was included as a positive control. The fluorescence values were read at 425/535 nm and 425/485 nm. As before, the FRET signal was calculated by first subtracting the background control values and dividing the emission readings at 535 nm by those at 485 nm.

CHAPTER 3
EXPLORING HELA CELL FRET AND BRET ASSAYS TO DETECT HSP90-HOP INTERACTIONS

3.1 Preparation of FRET and BRET assay plasmids.

To be able to perform FRET and BRET assays, appropriate reporter proteins need to be attached to the proteins of interest. Therefore, the gene coding sequences of the full-length mammalian and *Plasmodium falciparum* Hop and Hsp90 proteins and their respective TPR2A and C-domains were cloned into the plasmids pRluc, pCFP and pYFP containing the sequences of *Renilla* luciferase (Rluc), cyan fluorescent protein (CFP; Cerulean variant) and yellow fluorescent protein (YFP; Venus variant), respectively. The plasmids enable the mammalian cell expression of proteins of interest fused at the N-terminus to the reporter proteins (the plasmids were donated by Prof H. Hoppe and are described in the Methods section 2.1.1. and Appendix I).

3.1.1 Cloning of the human and malarial Hop and TPR2A sequences in pCFP and pRluc.

For this study, the Hop and TPR2A sequences were fused to Rluc (for BRET assays) and CFP (for FRET assays) respectively. The Hop and TPR2A sequences had previously been cloned into a pACT plasmid (donated by Prof. H. Hoppe – see Methods section 2.1.1 for a description) and were used in this study for sub-cloning. The pRluc and pCFP plasmids were restricted with the enzymes *Kpn*I and *Xho*I and the following pACT plasmids were restricted with *Kpn*I and *Sal*I to obtain the coding sequences of Hop and TPR2A: pACT-*Pf*Hop (*P. falciparum* Hop), pACT-mHop (murine Hop), pACT-mTPR2A (murine TPR2A domain) and pACT-*Pf*TPR2A (*P. falciparum* TPR2A domain).

The restriction digests were run on an 0.8% TAE agarose gel, the coding sequence inserts were excised, purified and ligated with the restricted pRluc and pCFP target plasmids, thus creating 8 new constructs (pRluc and pCFP respectively containing the coding sequences of the full-length Hop proteins and the TPR2A domains of murine and *P. falciparum* Hop). The ligation reactions were used to transform competent *E. coli* XL-10 Gold cells and plated on LB-kanamycin agar plates. Selected colonies were picked, cultured overnight and their recombinant plasmids isolated by alkaline lysis miniprep for diagnostic restriction digests. Plasmids were digested with *Bam*HI and *Bgl*II to determine if the inserts had ligated into the plasmid. The expected sizes of the inserts were: mHop: 1629 bp, *Pf*Hop: 1692 bp, mTPR2A: 390 bp, *Pf*TPR2A: 430bp. The expected plasmid backbone sizes were: pCFP: 4645 bp, pRluc: 4845 bp. The diagnostic digest results are shown in Fig. 1 and Fig. 2 for the pCFP and pRluc constructs, respectively.

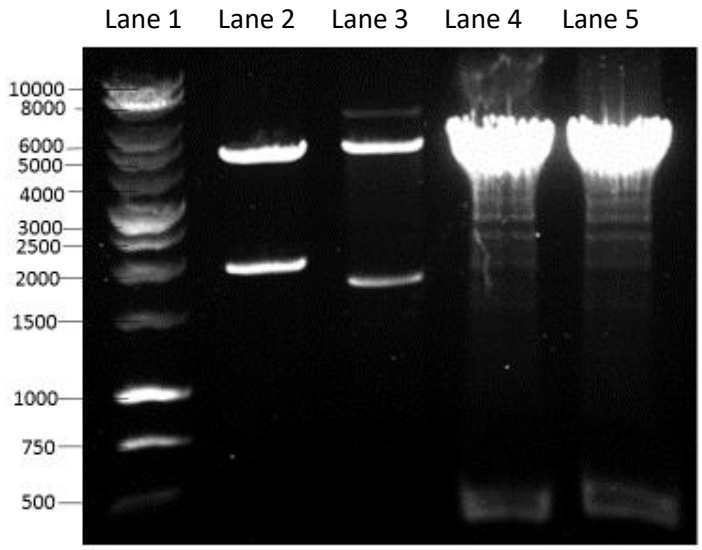

Figure 1: Diagnostic digest performed on pCFP fusion constructs. An alkaline lysis plasmid miniprep was performed on colonies that were cultured overnight to isolate potential pCFP fusion plasmids. The plasmids were subsequently restricted with the restriction enzymes *Bam*HI and *Bgl*II and analysed on a 0.8% agarose gel stained with ethidium bromide and viewed using a UV transilluminator. Lane 1: Marker (1 kb DNA ladder [Promega]), Lane 2: pCFP-*Pf*Hop, Lane 3: pCFP-mHop, Lane 4: pCFP-mTPR2A, Lane 5: pCFP-*Pf*TPR2A.

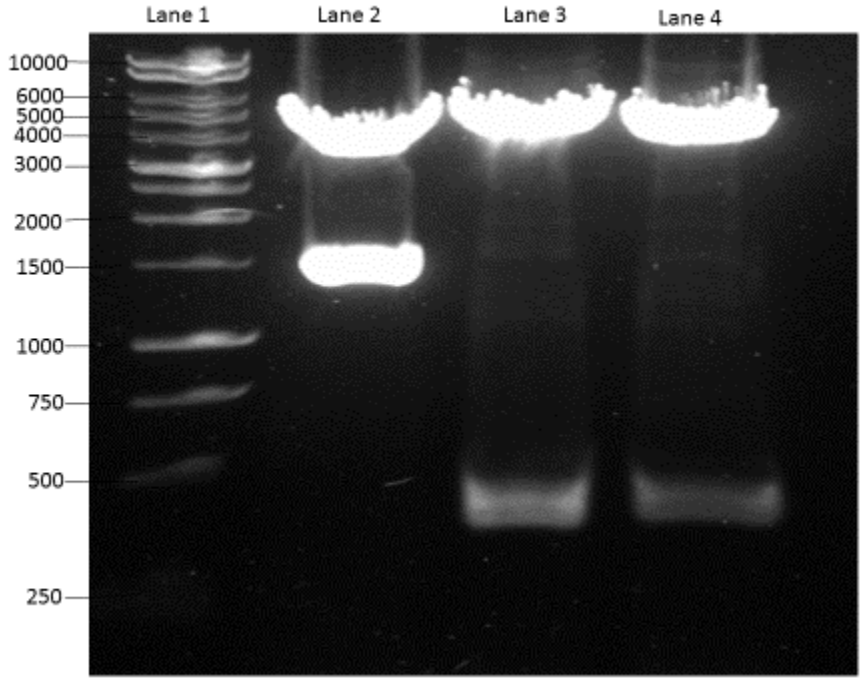

Figure 2: Diagnostic digest performed on pRluc fusion constructs. An alkaline lysis plasmid mini prep was performed on colonies that were cultured overnight to isolate potential pRluc fusion plasmids. The plasmids were subsequently restricted with the restriction enzymes *Bam*HI and *Bgl*II and analysed on an 0.8% agarose gel stained with ethidium bromide and viewed using a UV transilluminator. Lane 1: Marker (1 kb DNA ladder [Promega]), Lane 2: pRluc-*Pf*Hop, Lane 3: pRluc-mTPR2A, Lane 4: pRluc-*Pf*TPR2A.

With the exception of pRluc-mHop which was not successfully obtained (not shown), all lanes contain the expected sizes of inserts present in the plasmid, showing that cloning was successful.

3.1.2 Cloning hHsp90 and *Pf*Hsp90 sequences into pYFP

The coding sequences of human Hsp90 (hHsp90) and *P. falciparum* Hsp90 (*Pf*Hsp90) had previously been cloned into a pBIND plasmid (donated by Prof. H. Hoppe; described in Methods section 2.1.1). The plasmids did not contain compatible restriction sites for sub-cloning the inserts in pYFP, thus a PCR cloning approach was used. The Hsp90 coding

sequences were PCR amplified from the template plasmids pBIND-hHsp90 and pBIND-*Pf*Hsp90 using forward and reverse primers containing *Xho*I and *Bam*HI restriction sites respectively (Fig. 3). The PCR reactions were run on an agarose gel and the appropriate bands excised, purified and restricted with *Xho*I and *Bam*HI. Simultaneously, pYFP was restriction digested with *Xho*I and *Bam*HI and purified and the PCR products and plasmids were ligated, used to transform *E. coli* cells and plated on LB-kanamycin agar plates. The resulting colonies were propagated overnight, plasmids isolated by alkaline lysis miniprep and a diagnostic restriction digest was performed using *BamHI* and *Xho*I (Fig. 4). The expected sizes of the hHsp90 and *Pf*Hsp90 coding sequences were 2172 bp and 2235 bp, respectively, and 4600 bp for the pYFP plasmid backbone.

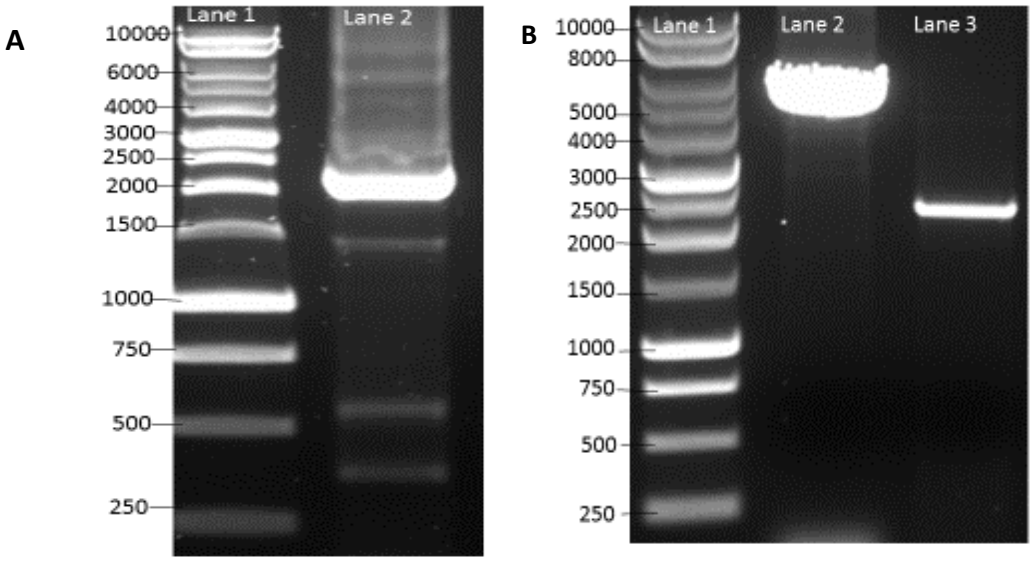

Figure 3: PCR reaction amplifying the hHsp90 and *Pf*Hsp90 coding sequences. The PCR products were analyzed on an 0.8% agarose gel stained with ethidium bromide and viewed using a UV transilluminator. (**A**) Lane 1: 1 kb DNA ladder [Promega]), Lane 2: PCR of hHsp90. (**B**) Lane 1: 1 kb DNA ladder [Promega]), Lane 2: unrelated sample, Lane 3: PCR of *Pf*Hsp90.

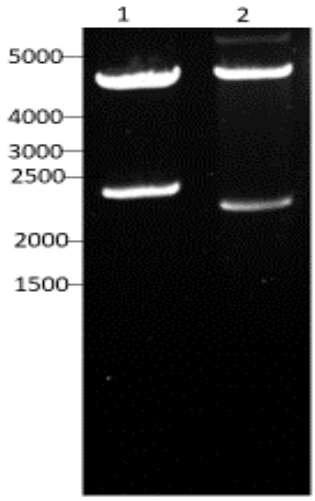

Figure 4: Diagnostic digest performed on pYFP fusion constructs. An alkaline lysis plasmid miniprep was performed on colonies that were cultured overnight to isolate potential pYFP fusion plasmids, which were subsequently restricted with the restriction enzymes *Bam*HI and *Bgl*II and analysed on an 0.8% agarose gel stained with ethidium bromide and viewed using a UV transilluminator. Lane 1: pYFP-*Pf*Hsp90, Lane 2: pYFP-hHsp90.

3.1.3 Cloning hCdom and *Pf*Cdom sequences in pYFP

In order to clone the human Hsp90 C-domain (hCdom) and *P. falciparum* Hsp90 C-domain (*Pf*Cdom) coding sequences into the pYFP vector, a PCR reaction was performed using forward and reverse primers with *Xho*I and *Bam*HI restriction sites respectively and the templates pBIND-hHsp90 and pBIND-*Pf*Hsp90 (Fig. 5). Expected amplicon sizes for hCdom and *Pf*Cdom were 290 bp and 273 bp, respectively.

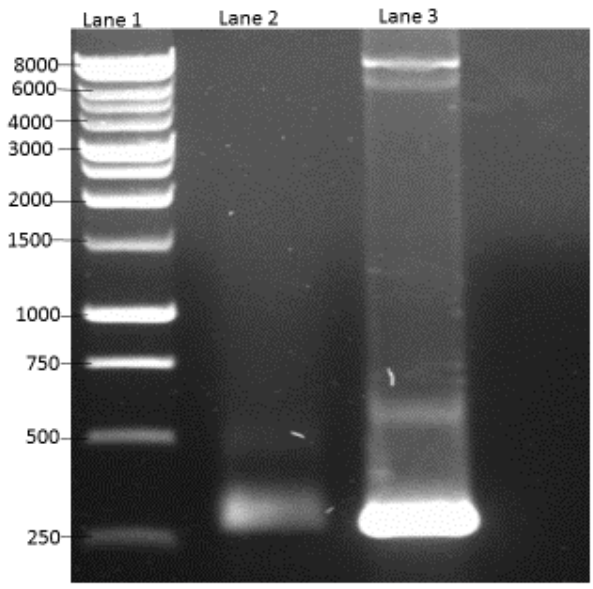

Figure 5: PCR reaction amplifying the hCdom and *Pf*Cdom DNA sequences. The PCR reactions were analysed on an 0.8% agarose gel stained with ethidium bromide and viewed using a UV transilluminator. Lane 1: marker (1 kb DNA ladder [Promega]), Lane 2: hCdom, Lane 3: *Pf*Cdom.

.

The PCR products were gel purified after restriction with *Xho*l and *Bam*HI. The vector, pYFP, was restricted with *BglI*I and *Sal*I and gel purified and the PCR products and vector ligated. The ligation reactions were used to transform *E. coli* cells and plated on LB-agar plates containing kanamycin. The resulting colonies were picked and cultured overnight, an alkaline lysis plasmid miniprep was performed and a restriction digest was performed with the restriction enzymes *Age*I and *Kpn*I to determine if the insert had ligated into the plasmid (Fig. 6). The *Age*I site is upstream of the YFP coding sequence and *Kpn*I downstream of the Cdom inserts. The digest should therefore release the YFP sequence fused to the Cdom insert from the plasmid backbone. This was done since the small sizes of the Cdom inserts complicates agarose gel analysis. For comparison, the pYFP plasmid was also restricted with *Age*I and *Kpn*I and run alongside the C-domain constructs in the diagnostic agarose gel. Successful cloning of the C-domain inserts should have resulted in restriction fragments slightly larger than YFP (990 bp and 1007 bp for YFP-*Pf*Cdom and YFP-hCdom respectively; 717 bp for YFP).

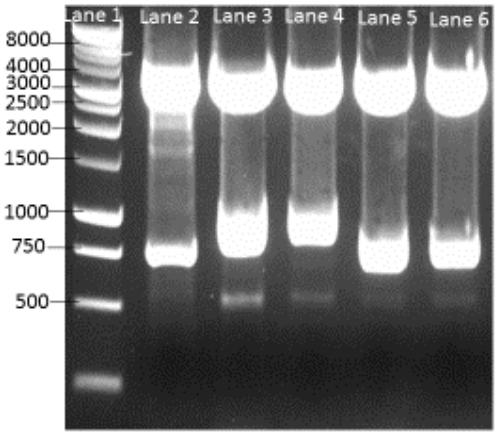

Figure 6: Diagnostic digest performed on YFP C-domain fusion constructs. An alkaline lysis plasmid miniprep was performed on *E. coli* cells harbouring potential YFP-C-domain fusion constructs and subsequently restricted with the restriction enzymes *Bam*HI and *Age*I and analysed on a 0.8% agarose gel stained with ethidium bromide and viewed using a UV transilluminator. Lane 1: Marker (1 kb DNA ladder [Promega]), Lane 2: pYFP, Lane 3-4: pYFP-*Pf*Cdom, Lane 5-6: pYFP-hCdom.

The digests of the *Pf*Cdom plasmids (Fig. 6, lanes 3-4) yielded inserts larger than YFP alone (Fig. 6, lane 2), suggesting the presence of the *Pf*Cdom insert in the plasmids, however the hCdom inserts (Fig. 6, lanes 5-6) could not be distinguished from YFP alone. A PCR reaction was subsequently performed to verify the cloning.

The recombinant plasmids obtained from 4 colonies of *E. coli* transformed with the pYFP-hCdom ligation reaction and 2 colonies transformed with pYFP-*Pf*Cdom were used as templates. In the PCR reaction, forward and reverse primers were used that annealed to the 5' end of the YFP sequence and 3' ends of the Cdom inserts, respectively (Fig. 7). Expected sizes of amplicons were 1007 bp for YFP-hCdom (Fig. 7A) and 990 bp for YFP-*Pf*Cdom (Fig. 7B).

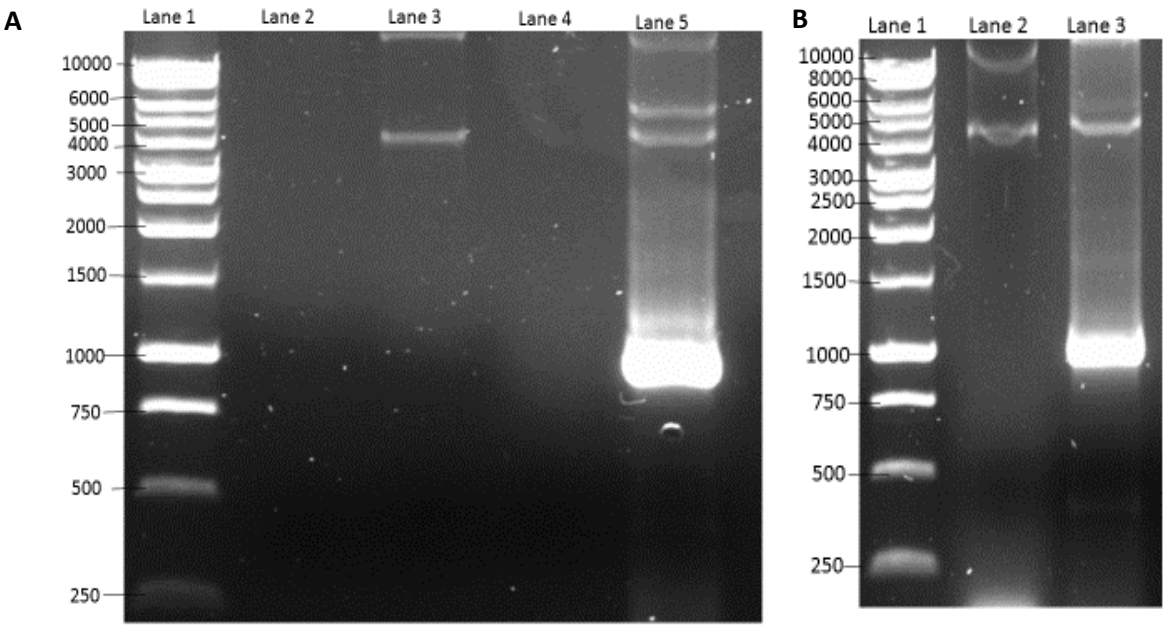

Figure 7: PCR reactions verifying the cloning of pYFP-hCdom and pYFP-*Pf*Cdom. The PCR products were analysed on an 0.8% agarose gel stained with ethidium bromide and visualised with a UV transilluminator. (**A**) Lane 1: Marker (1 kb DNA ladder [Promega]), Lane 2-5: PCR reactions of pYFP-hCdom. (**B**) Lane 1: Marker, Lanes 2-3: PCR reactions of pYFP-*Pf*Cdom.

One plasmid from each of the YFP-hCdom and YFP-*Pf*Cdom colonies yielded positive PCR reactions (Fig. 7A, lane 5; Fig. 7B, lane 3), indicating the presence of the Cdom inserts. Further confirmation was obtained by sequencing of the purified plasmid multiple cloning sites (Inqaba Biotech).

In summary, the cloning experiments yielded 11 plasmid constructs for use in mammalian cell BRET and FRET assays:

pRluc-*Pf*Hop, pRluc-*Pf*TPR2A, pRluc-mTPR2A (BRET assay);

pCFP-*Pf*Hop, pCFP-mHop, pCFP-*Pf*TPR2A, pCFP-mTPR2A (FRET assay);

pYFP-*Pf*Hsp90, pYFP-hHsp90, pYFP-*Pf*Cdom, pYFP-hCdom (BRET and FRET assay).

3.2 Performing the BRET assay

To explore whether *P. falciparum* and mammalian Hsp90-Hop interactions can be detected in HeLa cells using a BRET assay format, HeLa cells were plated at a density of $1x10^4$ cells in 100 µL medium per well in a Greiner white/clear bottom 96-well plate. The following day cells were transfected with BRET plasmids using Xfect transfection reagent (Clontech). After 24 h, the medium was replaced with 50 µL Rluc substrate (coelenterazine reagent, Promega; 1 in100 dilution in PBS) and after a 10 min incubation period, luminescence readings were obtained at 535 nm (YFP stimulated emission) and 485 nm (*Renilla* luciferase emission) in a Molecular Devices Spectramax M3 plate reader. Background readings were obtained from wells containing untransfected cells and subtracted from the other values and BRET signals calculated as the ratio of the emissions at 535 nm and 485 nm (Fig. 8). As a positive control, cells were transfected with pBRET – a plasmid containing the YFP coding sequence directly fused to Rluc (donated by Prof. H. Hoppe; Methods section 2.1.1). Negative control wells were co-transfected with pRluc and pYFP (*i.e.* plasmids containing the respective reporter protein coding sequences alone).

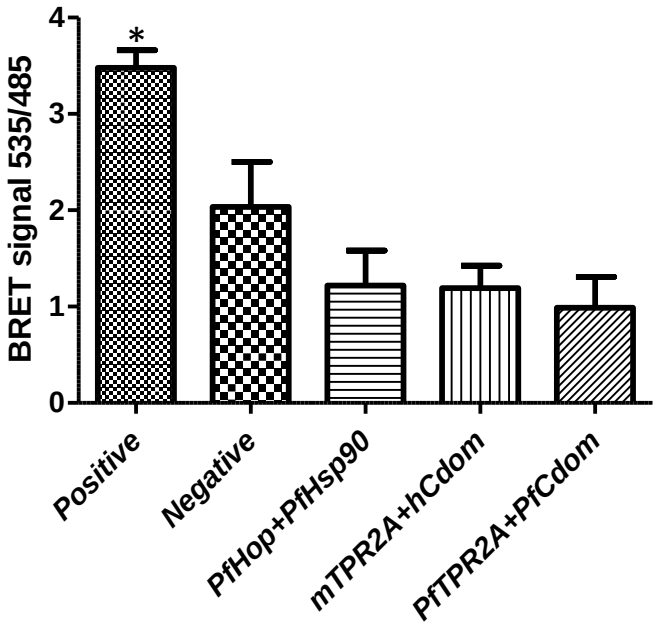

Figure 8: HeLa cell BRET assay using *P. falciparum* and mammalian Hsp90 and Hop constructs. HeLa cells were co-transfected with expression plasmids for Rluc-*Pf*Hop + YFP-*Pf*Hsp90, Rluc-mTPR2A + YFP-hCdom and Rluc-*Pf*TPR2A + YFP-*Pf*Cdom. Emission was measured at 535 nm and 485 nm and the 535 nm/485 nm ratio calculated to obtain BRET signals. Positive control wells were transfected with pBRET plasmid and negative control wells with pYFP and pRluc plasmids. The bargraphs show the mean BRET signals ± standard deviation for 5 wells (n = 5). *$p<0.05$ compared to negative control.

The representative experiment presented in Fig. 8 shows that, while a BRET signal could be obtained with the positive control (Rluc-YFP fusion), none of the Hsp90-Hop partners yielded a detectable BRET signal compared to the negative control (YFP and Rluc expressed separately). The lower signals obtained with the Hsp90/Hop constructs compared to the negative control may have been due to lower relative expression levels of the YFP fusion proteins (535 nm emission) vs. the Rluc fusion proteins (485 nm emission), resulting in reduced 535/485 nm ratios. The results suggested that, either the *P. falciparum* full-length Hsp90 and Hop proteins and the corresponding C-domain and TPR2A domain don't interact in HeLa cells, or the expression levels of the proteins were insufficient to generate BRET signals. The same applies to the mammalian C-domain and TPR2A domain.

3.3 Performing the FRET assay

Having failed to detect Hsp90-Hop interactions in HeLa cells using the BRET assay, FRET assays were performed to determine if it is a more suitable assay format. HeLa cells were plated at a density of $1x10^4$ cells in 100 µL medium per well in a Greiner white/clear bottom 96-well plate. The following day cells were transfected with FRET plasmids using Xfect transfection reagent (Clontech). After 24 h, the plate was read in a Molecular Devices Spectramax M3 plate reader in well scanning bottom read mode. The medium was replaced with 50 µL PBS and fluorescence readings were obtained using excitation/emission wavelength pairs of 425 nm/535 nm (YFP stimulated emission) and 425 nm/485 nm (CFP emission). FRET signals were calculated as the ratio of the 535 nm/485 nm emissions, after subtracting background fluorescence readings obtained from wells containing untransfected cells (Fig. 9). As a positive control, cells were transfected with a pFRET plasmid (donated by Prof. H. Hoppe; Methods section 2.1.1) containing the coding sequence of YFP directly fused to CFP. Negative control wells were co-transfected with pYFP and pCFP (*i.e*. the reporter proteins not fused to suspected interaction partners).

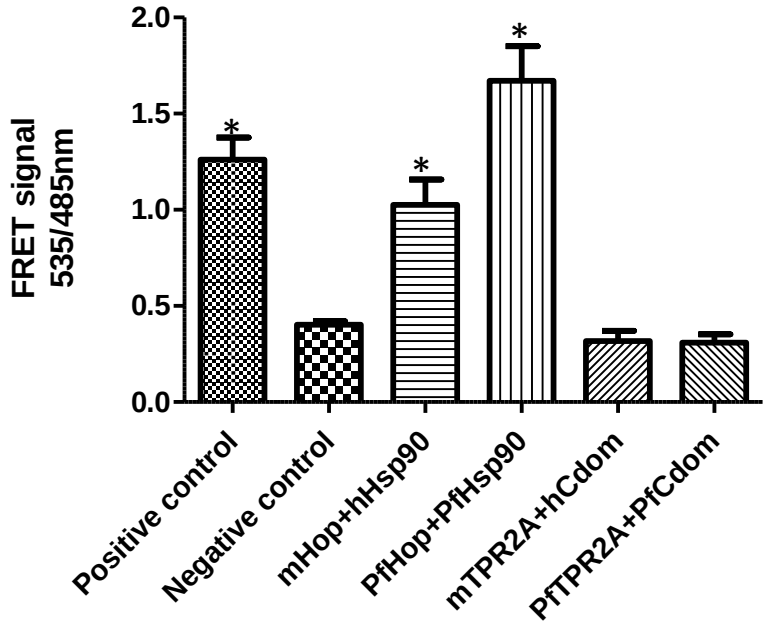

Figure 9: HeLa cell FRET assay using *P. falciparum* and mammalian Hsp90 and Hop constructs. HeLa cells were co-transfected with expression plasmids for CFP-mHop + YFP-hHsp90, CFP-*Pf*Hop + YFP-*Pf*Hsp90, CFP-mTPR2A + YFP-hCdom, CFP-*Pf*TPR2A + YFP-Cdom and YFP + CFP (negative control), as well as a YFP-CFP fusion (positive control). Fluorescence at 425-535nm (stimulated YFP emission) and 425-485 nm (CFP) was measured and the 535 nm/485 nm ratio calculated to obtain FRET signals. Graphs represent the mean and standard deviation of 5 wells per transfection (n=5). $^{*}p<0.05$ compared to negative control.

In the representative experiment shown in Fig. 9, the positive control FRET signal was more robustly detected (compared to the negative control) than the signals obtained for the positive control in BRET experiments (Fig. 8). In addition, unlike the BRET experiments, an interaction could be detected for the full-length *P. falciparum* and mammalian Hsp90-Hop pairs. By contrast, the C-domain/TPR2A domain pairs failed to produce a FRET signal above the negative control for both malaria and mammalian constructs. This suggests that the full-length proteins may interact with a higher affinity than the respective minimal interaction domains and/or that the expression levels of the YFP-Cdom/CFP-TPR2A proteins were insufficient to yield a FRET signal.

3.4 Performing Western blotting to determine protein expression

To determine why there was no detectable FRET signal for the TRP2A/Cdom interaction for both mammalian and malarial constructs, as well as why the BRET assay failed to produce signals for the Hsp90-Hop interactions, western blotting was performed to gauge protein expression. HeLa cells were transfected with the plasmids and subsequently mixed with SDS-PAGE loading buffer and proteins separated on a 12% SDS-PAGE gel. Subsequently, the gel was transblotted onto a nitrocellulose membrane and the proteins detected using the following antibodies: mouse anti-GFP for YFP and CFP fusion proteins, rabbit anti-*Renilla* luciferase for Rluc fusion proteins and rabbit anti-actin as a loading control. The secondary antibodies used were goat anti-mouse or goat anti-rabbit Ig conjugated to horseradish peroxidase (HRP) and they were visualised using a colorimetric TMB membrane peroxidase substrate.

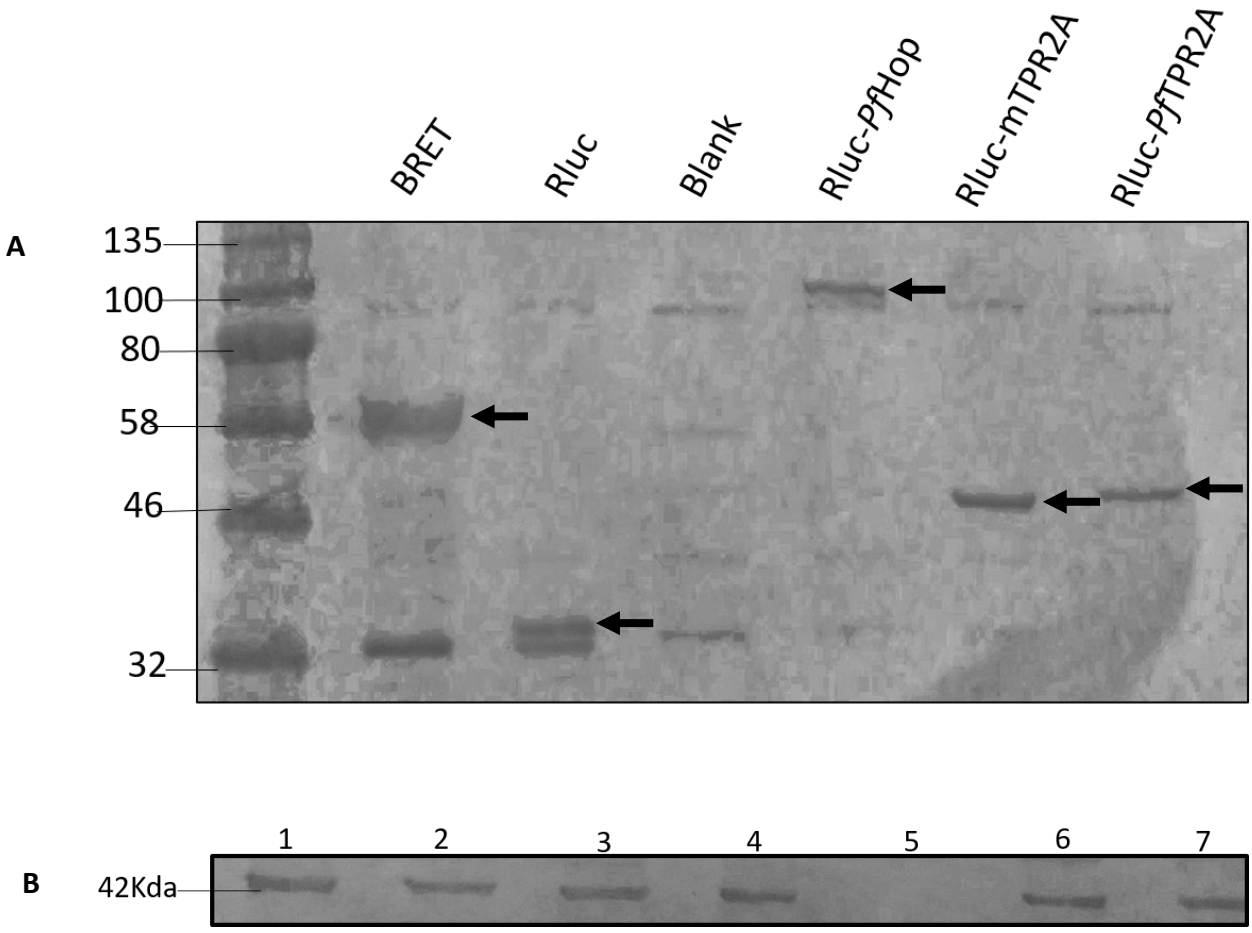

Figure 10: Western blotting to detect Rluc fusion protein expression in HeLa cells. (A) HeLa cells transfected with Rluc fusion constructs were mixed with SDS-PAGE loading buffer and analysed on a 12% SDS gel. The proteins were transblotted onto a nitrocellulose membrane and probed using rabbit anti-Rluc primary antibodies and anti-rabbit secondary antibodies conjugated to HRP which were visualised with TMB membrane peroxidase substrate. Lane 1: Marker (Broad Range Protein Ladder, New England Biolabs), Lane 2: BRET positive control (Rluc fused to YFP), Lane 3: Rluc, Lane 4: untransfected cells, Lane 5, Rluc-*Pf*Hop, Lane 6: Rluc-mTPR2A, Lane 7: Rluc-*Pf*TR2A. **(B)** A parallel blot was probed with rabbit anti-actin antibodies followed by HRP-conjugated goat anti-rabbit secondary antibodies and TMB membrane peroxidase substrate. Lane 1: BRET positive control, Lane 2: Rluc, Lane 3: Rluc-*Pf*Hop, Lane 4: Rluc-mTRR2A, Lane 5: Blank, Lane 6: Rluc-*Pf*TPR2A, Lane 7: untransfected cells.

For the Rluc western blotting experiment (Fig. 10), the expected sizes of the proteins were: BRET (YFP fused to Rluc): 60.9 kDa, Rluc: 34.4 kDa, Rluc-*Pf*Hop: 97 kDa, Rluc-mTPR2A: 48.84 kDa, Rluc-PfTPR2A: 50.32 kDa. The antibody cross-reacted with some cellular proteins

as shown by the presence of faint bands in the untransfected (blank) cell lane which correspond to bands in the other lanes. However, there is a more intense band correlating with the expected Rluc fusion protein sizes in each lane (arrows), suggesting that all the proteins were being expressed. Although a smaller apparent degradation product corresponding to the size of Rluc was present in the BRET lane, the BRET band (Rluc-YFP fusion positive control) was the most intense compared to the other Rluc fusion proteins, which could potentially mean that more protein was being expressed and would correlate with the BRET assay results where only the positive control produced a detectable BRET signal (Fig. 8). To ensure that this was not due to unequal loading of the lanes, a second blot with the Rluc fusion proteins was also probed with rabbit anti-actin antibodies (Fig. 10B). This suggested that the cell samples used for blotting contained equivalent amounts of protein.

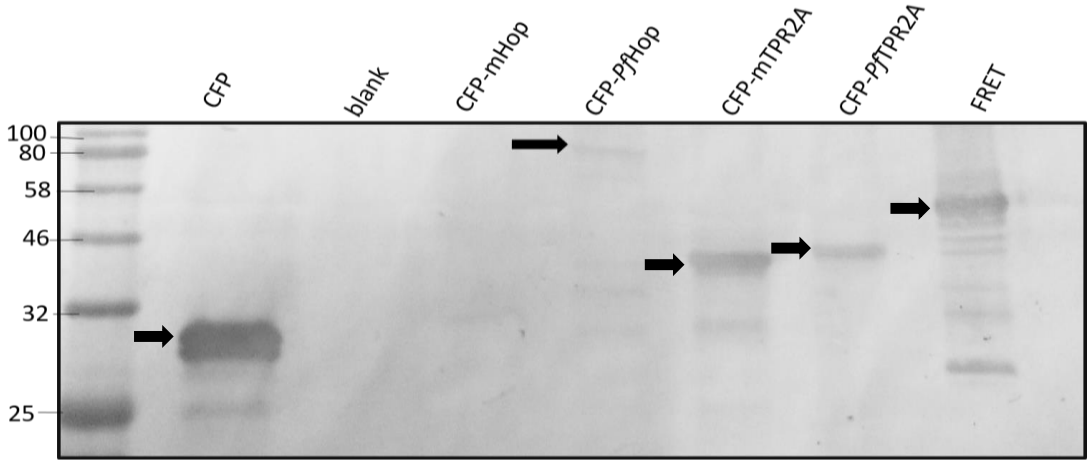

Figure 11: Western blotting to detect CFP fusion protein expression in HeLa cells. HeLa cells transfected with CFP fusion constructs were mixed with SDS-PAGE loading buffer and analysed on a 12% SDS gel. The proteins were transblotted onto a nitrocellulose membrane and probed using mouse anti-GFP primary antibodies and anti-mouse secondary antibodies conjugated to HRP which was visualised with TMB membrane peroxidase substrate. Lane 1: Marker (Broad Range Protein Ladder, New England Biolabs), Lane 2: CFP, Lane 3: Blank, Lane 4: CFP-mHop, Lane 5: CFP-*Pf*Hop, Lane 6: CFP-mTPR2A, Lane 7: CFP-*Pf*TPR2A, Lane 8: FRET (YFP-CFP positive control).

For the western blotting analysis of CFP fusion proteins (Fig. 11), the expected sizes of the proteins were: FRET (YFP-CFP positive control): 53 kDa, CFP: 26.5 kDa, CFP-mHop: 86.8 kDa, CFP-*Pf*Hop: 89.1 kDa, CFP-mTPR2A: 40.9 kDa, CFP-*Pf*TPR2A: 42.4 kDa. Due to the presence of a band in the expected size in most lanes (arrows), it suggests that the respective proteins were being expressed, despite the presence of apparent degradation products in the CFP, CFP-mTPR2A and FRET lanes. The exception was CFP-mHop which was not detected, compared to the faint band corresponding to CFP-*Pf*Hop (lane 5, arrow).

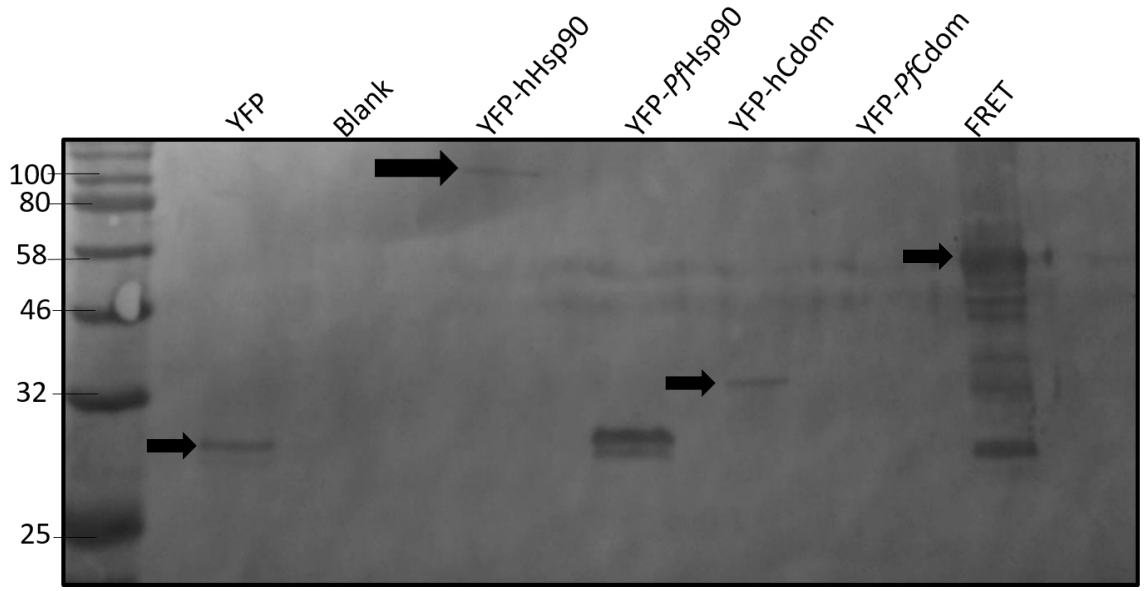

Figure 12: Western blotting to detect YFP fusion protein expression in HeLa cells. HeLa cells transfected with YFP fusion constructs were mixed with SDS-PAGE loading buffer and analysed on a 12% SDS gel. The proteins were transblotted onto a nitrocellulose membrane and probed using mouse anti-GFP primary antibodies and anti-mouse secondary antibodies conjugated to HRP which was visualised with TMB membrane peroxidase substrate. Lane 1: Marker (Broad Range Protein Ladder, New England Biolabs), Lane 2: YFP, Lane 3: Blank, Lane 4: YFP-hHsp90, Lane 5: YFP-*Pf*Hsp90, Lane 6:YFP-hCdom, Lane 7: YFP-*Pf*Cdom, Lane 8: FRET (YFP-CFP positive control).

For the western blotitng analysis of YFP fusion protein expression (Fig. 12), expected sizes of the proteins were: FRET: 53 kDa, YFP: 26.5 kDa,YFP-hHsp90: 106.9kDa, YFP-*Pf*Hsp90:

109.2 kDa, YFP-hCdom: 37.2 kDa, YFP-*Pf*Cdom: 36.6 kDa. A feint band shows the detection of YFP-hHsp90 (arrow). YFP-hCdom, YFP and FRET were also detected (smaller arrows), although the latter contained degradation products, as was found in the CFP expression experiments. In the case of YFP-*Pf*Hsp90, a prominenent degradation product corresponding in size to YFP was present, but the full length protein as well as the C-domain construct (YFP-*Pf*Cdom) could not be detected.

In summary, for the BRET constructs expression of the Rluc fusion proteins could be confirmed (*Pf*Hop, *Pf*TPR2A and mTPR2A; Fig. 10). However, the same could not be said for the corresponding YFP fusion proteins. The human C-domain was detected, but not the *Pf* C-domain, while *Pf*Hsp90 appeared to be degraded (Fig. 12). This could explain the absence of BRET signals for the *Pf* proteins in the BRET experiments. In the case of the mammalian C-domain-TPR2A domain interaction, the absence of a BRET signal may be due to the low affinity of the interaction (see Chapter 4). However, the western botting results do not correlate with the FRET assay results. CFP-*Pf*Hop expression could be detected (Fig. 11) and a *Pf*Hop-*Pf*Hsp90 FRET signal was obtained (Fig. 9), despite the presence of YFP-*Pf*Hsp90 as a degradation product. Similarly, YFP-hHsp90 expression was detected (Fig. 12) and an hHsp90-mHop FRET signal was obtained (Fig. 9), despite the absence of detectable CFP-mHop expression (Fig. 11). One possibility is that the western blotting detection of the intact large YFP-*Pf*Hsp90 and CFP-mHop proteins (109 kDa and 87 kDa repsectively) was compromised by the high percentage acrylamide SDS-PAGE gel used to resolve the smaller YFP and CFP proteins and thus poor transfer of the larger proteins to the membrane during transblotting and/or the lack of correlation between the blotting results and FRET experiments reflects inherent inconsistencies in inter-experimental cell transient transfection and protein expression

efficiencies. Given these obstacles, an alternative protein-based FRET assay format was explored (Chapter 4).

CHAPTER 4:

ESTABLISHING AN *IN VITRO* PROTEIN-BASED FRET ASSAY FOR *P. FALCIPARUM* HSP90-HOP INTERACTION

In the previous chapter, cell-based BRET and FRET assay formats were explored as a means to detect the interactions of malaria and mammalian Hsp90 and Hop proteins and their respective interaction domains (C-domains and TPR2A domains). BRET experiments failed to yield positive interaction results. The FRET experiments demonstrated that interaction of the full-length malaria and mammalian Hsp90 and Hop proteins could be detected in the context of live cells using this assay format. However, the experiments required repeated transient transfections of HeLa cells with expression plasmids which makes them prone to problems with intra- and inter-experimental reproducibilty, as suggested by the relatively large error bars (inter-well variations in FRET and BRET signals) and failure to robustly detect protein expression by western blotting. This is not ideal, given that the overall goal of the project was to attempt to develop an assay that can be used to screen compounds for inhibitors of Hsp90-Hop intercations, with a particular emphasis on *P. falciparum* for the discovery of potentially novel anti-malarials. While the HeLa cell FRET assay can potentially be used as a secondary assay to validate "hit" compounds for inhibition of Hsp90-Hop interaction, we explored the possibility of developing an alternative *in vitro* FRET assay using purified proteins as a more practical primary assay for compound screening.

Development of an *in vitro* protein-based assay required the expression and purification of recombinant proteins using *E. coli*. To simplify protein expression and purification, we opted to use the smaller C-domains and TPR2A domains of the *P. falciparum* and mammalian proteins as opposed to the full-length proteins (using full-length Hsp90 and Hop fused to YFP and CFP respectively would have required the successful expression and purification of proteins of approx. 110 kDa and 90 kDa in size). To enable expression in *E. coli*, YFP-hCdom, YFP-*Pf*Cdom, CFP-mTPR2A and CFP-*Pf*TPR2A coding sequences were cloned into the *E. coli* expression plasmid pET-28a(+) which inroduces a histidine tag at the N-terminus of the protein for affinity purification using Ni-NTA columns.

4.1 Preparation of pET expression plasmids

Primers were used to PCR amplify the Cdom and TPR2A coding sequences of both mammalian and *P. falciparum* Hsp90 and Hop, fused to YFP and CFP at the 5' end respectively, using the pYFP-Cdom and pCFP-TPR2A FRET constructs previously prepared for the HeLa cell experiments as templates. Negative control sequences (CFP and YFP separately) were also amplified using the pYFP and pCFP plasmids used in the HeLa cell experiments as templates. Each primer was designed to have *Nhe*I and *Xho*I sites (forward and reverse primers, respectively) for ligation into the pET plasmid. PCR reactions were analysed using ethidium bromide-stained 0.8% agarose gels (Fig. 16). Expected sizes of the amplicons were: YFP and CFP: 717 bp (Fig. 16A, lanes 2 and 3), CFP-mTPR2A and CFP-*Pf*TPR2A: 1107 bp and 1147 bp (Fig. 16A, lanes 4 and 5), YFP-hCdom and YFP-*Pf*Cdom: 1008 bp and 990 bp (Fig. 16B, lanes 2 and 3).

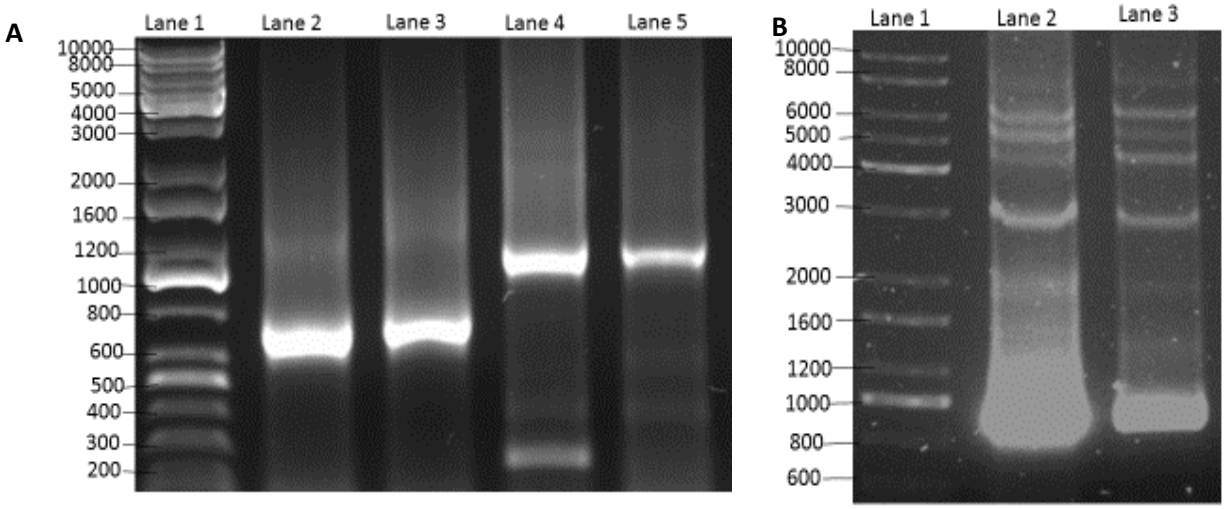

Figure 13: PCR reactions amplifying the DNA sequences used for pET cloning. The PCR reactions were analysed on an 0.8% agarose gel stained with ethiduim bromide and viewed using a UV transilluminator. **(A)** Lane 1: Marker (1 kb ladder, Promega) Lane 2: YFP, lane 3: CFP, lane 4: CFP-mTPR2A, Lane 5: CFP-*Pf*TPR2A. **(B)** Lane 1: Marker (1 kb ladder Promega), Lane 2: YFP-hCdom, Lane 3: YFP-*Pf*Cdom.

The PCR products were purified from agarose gels using a Nucleospin Gel and PCR Clean-up kit (Macherey-Nagel), restricted with *Nhe*I and *Xho*I and re-purified. In parallel, pET28a was restricted with *Nhe*I and *Xho*I and gel purified using the Nucleospin Gel and PCR Clean-up kit. The digested and purified PCR products and pET plasmid were ligated together in a 3:1 molar ratio (insert:plasmid) using T4 DNA ligase (Promega). The ligation reactions were transformed into XL10-Gold *E. coli* cells and plated on kanamycin-LB plates. Colonies were picked and propagated in LB broth containing 50 ng/µl kanamycin. Alkaline lysis plasmid minipreps were performed to obtain plasmids from selected colonies and restriction digests with *Nhe*I and *Xho*I were performed and analysed on an 0.8% agarose gel to confirm the presence of the expected inserts (Fig. 14). Expected sizes were: pET plasmid backbone: 5369 bp (Fig. 14, all lanes), YFP: 717 bp (Fig. 14A, lanes 2-3), , CFP-*Pf*TPR2A: 1147bp (lanes 4-6), CFP-mTPR2A: 1107 bp (lane 7), YFP-hCdom: 1007 bp (Fig. 14B, lane 2) YFP-*Pf*Cdom: 990 bp (Fig. 14B, lane 3).

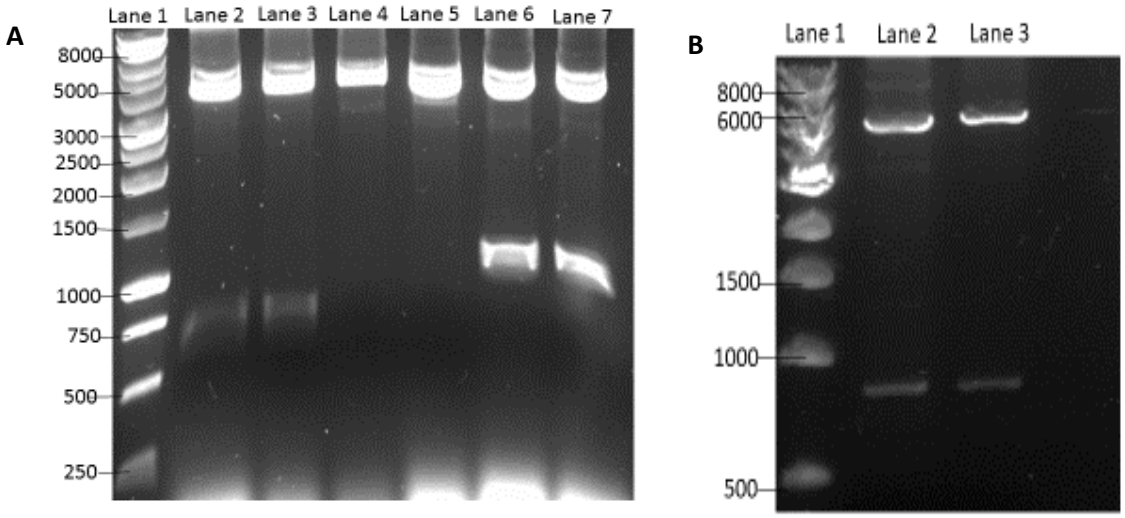

Figure 14: Restrcion digestion performed on pET recombinant plasmids. An alkaline lysis was performed on cultured *E. coli* colonies containing potential pET recombinant constructs,subsequently restricted with *Nhe*I and *Xho*I restriction enzymes and analysed on an 0.8% agarose gel stained with ethidium bromide and viewed using a UV transilluminator. (**A**) Lane 1: Marker (1 kb DNA ladder, Promega), Lanes 2-3: pET-YFP, Lanes 4-6: pET-CFP-*Pf*TPR2A, Lane 7: pET-CFP-mTPR2A. (**B**) Lane 1: Marker (1 kb DNA ladder, Promega), Lane 2: pET-YFP-Cdom, Lane 3: pET-YFP *Pf*Cdom

Two colonies contained pET plasmids with expected YFP inserts (Fig. 14A, lanes 2-3) and one colony each the CFP-*Pf*TPR2A, CFP-mTPR2A (Fig. 14A, lanes 6 and 7), YFP-hCdom and YFP-*Pf*Cdom (Fig, 14B, lanes 2 and 3) inserts.

4.2 Small-scale protein expression analysis

To determine if the expected recombinant proteins could be expressed in *E. coli* and whether they were present as soluble proteins vs. insoluble inclusion bodies, small-scale expression analysis was conducted using 5 ml bacterial cultures. The pET plasmid constructs were transformed into BL21(DE3) competent cells and plated onto LB plates containing 50 µg/ml kanamycin. The plates were left at 37 degrees C overnight. The resulting colonies were picked and propagated in 5 ml LB broth containing 50 ug/ml of kanamycin. This broth was used to innoculate 2 sets of fresh 5 ml LB broth (with kanamycin) with 1/20 of the pre-culture and was incubated at 37 degrees C until OD_{600} 0.4 – 0.6 was reached. Expression in one set was then induced by adding 1 mM IPTG, while the other set was left un-induced and culturing was continued at 37 degrees C for a further 4 h. The cultures were centrifuged at 6000 rpm for 6 mins in a microfuge and the bacterial pellet was resuspended in 500 µl PBS buffer. This resuspended pellet was probe sonicated at 60 Hrtz for 30 secs and centrifuged again to separate out the solube (supernatant) and insoluble (pellet) fractions. The pellets were resuspended in a volume of PBS equal to the supernatant, the fractions were mixed with SDS-PAGE sample buffer and run on a 12% SDS-PAGE gel which was stained with Coomassie stain to visualise protein bands. Alternatively, proteins were transblotted onto nitrocellulose membranes, stained with Ponceau S to visualise protein bands and probed with a mouse anti-GFP monoclonal antibody to detect recombinant protein expression (the anti-GFP antibody cross-reacts with YFP and CFP). Alternatively, western blotting was perfomed with a Ni-NTA-HRP cojugate to detect His-tagged proteins (HisDetector™, SeraCare).

For the initial expression analysis, *E. coli* transformed with pET-YFP was used. Using a Coomassie-stained SDS-PAGE gel, no differences could be observed in the protein content of

the IPTG induced and non-induced samples (*i.e.* the presence of a distinct YFP band in the induced samples - not shown). Western blotting was therefore performed with an anti-GFP antibody to determine the presence of expressed YFP in the samples (Fig. 16). As shown in the Ponceau S-stained blot (Fig. 16A), a prominent band corresponding to the expected size of YFP (26.5 kDa) was present in both the induced and non-induced soluble protein fractions. Western blotting confirmed that this band contained YFP (Fig. 22B). YFP is thus expressed in a soluble form in the pET-YFP transformed *E. coli* cells.

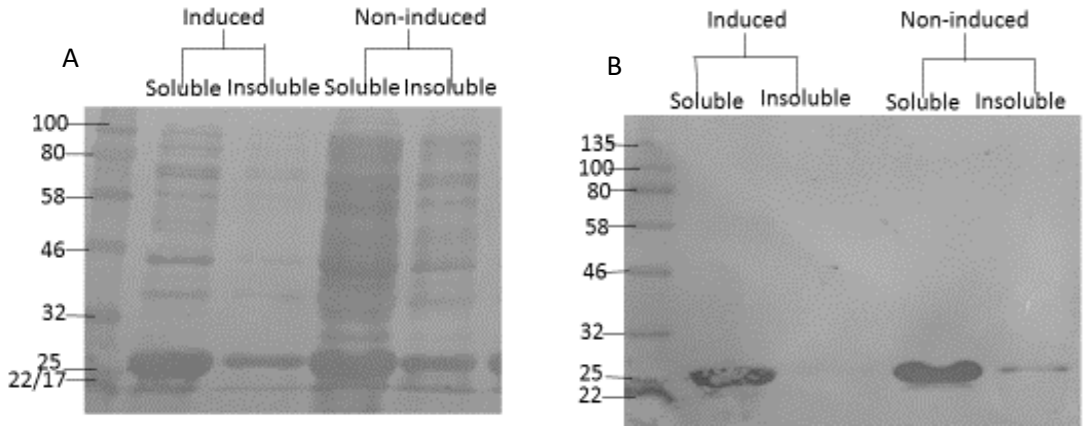

Figure 15: Western blotting analysis of YFP expression. IPTG induced and non-induced pET-YFP transformed *E. coli* soluble and insoluble fracions were run on a 12% SDS-PAGE gel, transblotted onto a Hybond ECL nitrocellulose membrane and probed with a mouse anti-GFP antibody. **(A)** Nitrocellulose membrane stained with Ponceau S**. (B)** Western blot using mouse anti-GFP primary antibody and goat anti-mouse-HRP secondary antibodies, visualized with a colorimetric TMB peroxidase substrate. The sizes of protein size markers (in kDa) are indicated on the left.

Due to the fact that the pET 28a plasmid displayed "leaky expression" in the BL21(DE3) cells and the YFP protein was being expressed with and without induction with ITPG, for subsequent experiments an alternative control was used to determine whether the correct protein was being

expressed in tranformed cells. For the control, untransformed BL21 cultures were used. A Bradford's assay was performed to ensure that the untransformed control and tranformed experimental samples were diluted to the same protein concentration before SDS-PAGE gel loading. For the next experiment, expression of the FRET positive control (CFP fused at its C-terminus to YFP) was analysed. As with the YFP expression experiment, differences in protein content in IPTG induced and non-induced samples could not be discerned by Coomassie staining, hence western blotting was performed with the anti-GFP antibody (Fig. 16B). The Ponceau S-stained blot showed the presence of a unique band (compared to untransformed cells) corresponding to the size of the CFP-YFP fusion protein (53 kDa) in the soluble and insoluble fractions of both induced and non-induced pET-FRET transformed cells (Fig. 16A, left 4 lanes). Probing with the anti-GFP antibody confirmed that this band represented the positive control protein (Fig. 16B). Though the protein was also present in the insoluble fraction, it was concluded to be sufficiently soluble to proceed to purification.

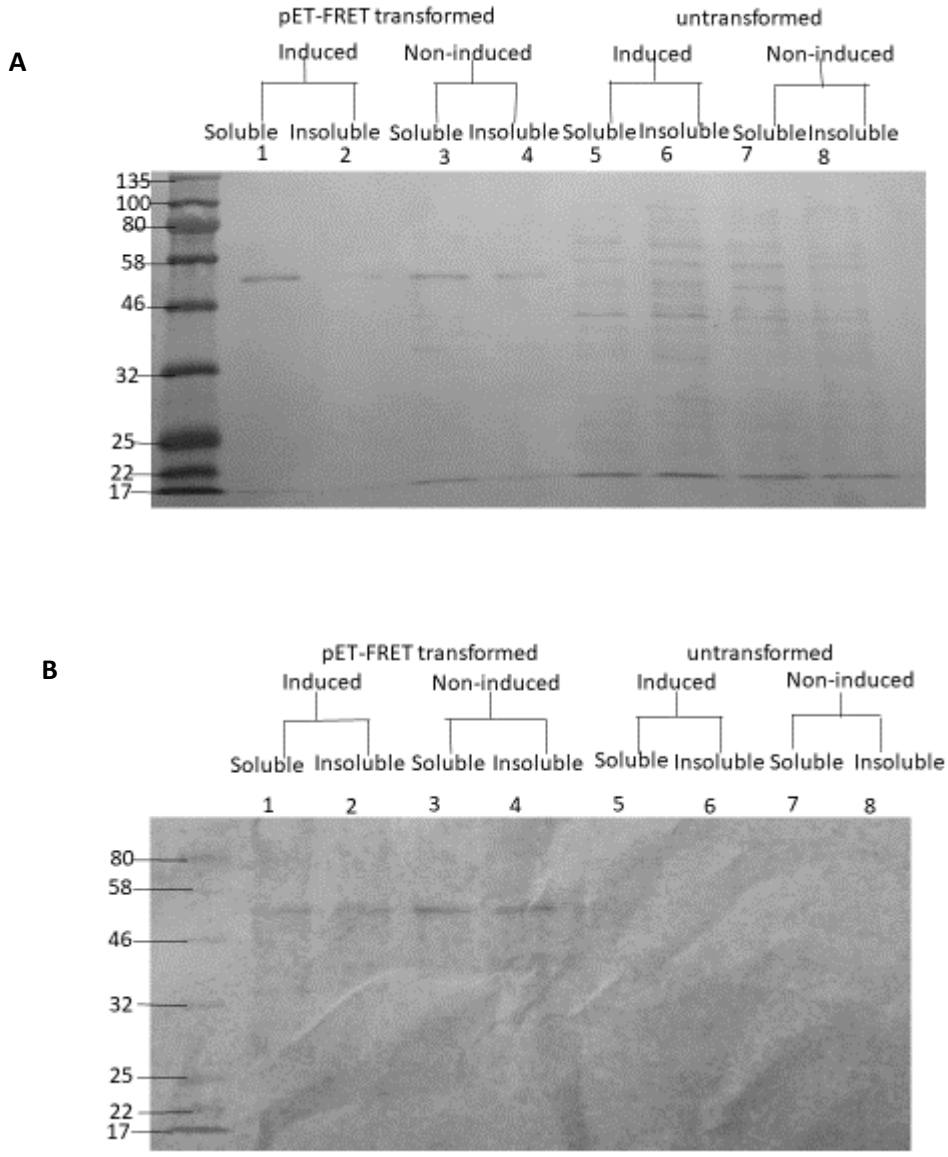

Figure 16: Western blotting analysis of CFP-YFP (FRET control) expression. The soluble and insoluble fractions of IPTG induced and non-induced pET-FRET transformed *E. coli* (lanes 1-4) and untransformed *E. coli* (lanes 5-8) were run on a 12% SDS-PAGE gel and transblotted onto a nitrocellulose membrane. **(A)** Ponceau-stained nitrocellulose membrane. **(B)** Western blot using mouse anti-GFP primary antibodies and goat anti-mouse-HRP secondary antibodies visulised with TMB peroxidase substrate. The sizes of protein size markers (in kDa) are indicated on the left.

Seeing as the pET 28a plasmid had again displayed leaky expression when analysing the CFP-YFP samples and there was no difference between induced and non-inducd samples (Fig. 16), for the expression analysis of the rest of the proteins induction with ITPG was not performed, but untransformed BL21 cells were still used as a control. For the next experiment, expression of the mammalian domains (CFP-mTPR2A and YFP-hCdom) was analysed using a Coomassie stained SDS-PAGE gel and a second gel that was used for western blotting using a nickel-HRP conjugate for detecting His-tagged proteins (HisDetector, SeraCare) (Fig. 17). Predicted sizes of the recombinant proteins were 41 kDa (CFP-mTPR2A) and 37 kDa (YFP-hCdom). In the case of CFP-mTPR2A, a prominent unique band was present in the soluble fraction in the expected size range in the Coomassie-stained gel (Fig. 17A, arrow). Western blotting confirmed the presence of a His-tagged protein at this position (Fig. 17B). The blot also showed a significant amount of CFP-mTPR2A in the insoluble fraction. However, this may be symptomatic of poor *E. coli* lysis by the sonication protocol used here, as evidenced by the similarity of the protein content in the soluble and insoluble fractions in the Coomassie-stained gel. The "insoluble" fraction may thus have contained unlysed cells, leading to an under-estimation of protein solubility. The Coomassie-stained gel also suggested the presence of YFP-hCdom in the soluble fraction (Fig. 17A, arrow) and the western blot of the YFP-hCdom samples (Fig. 17B) confrimed this.

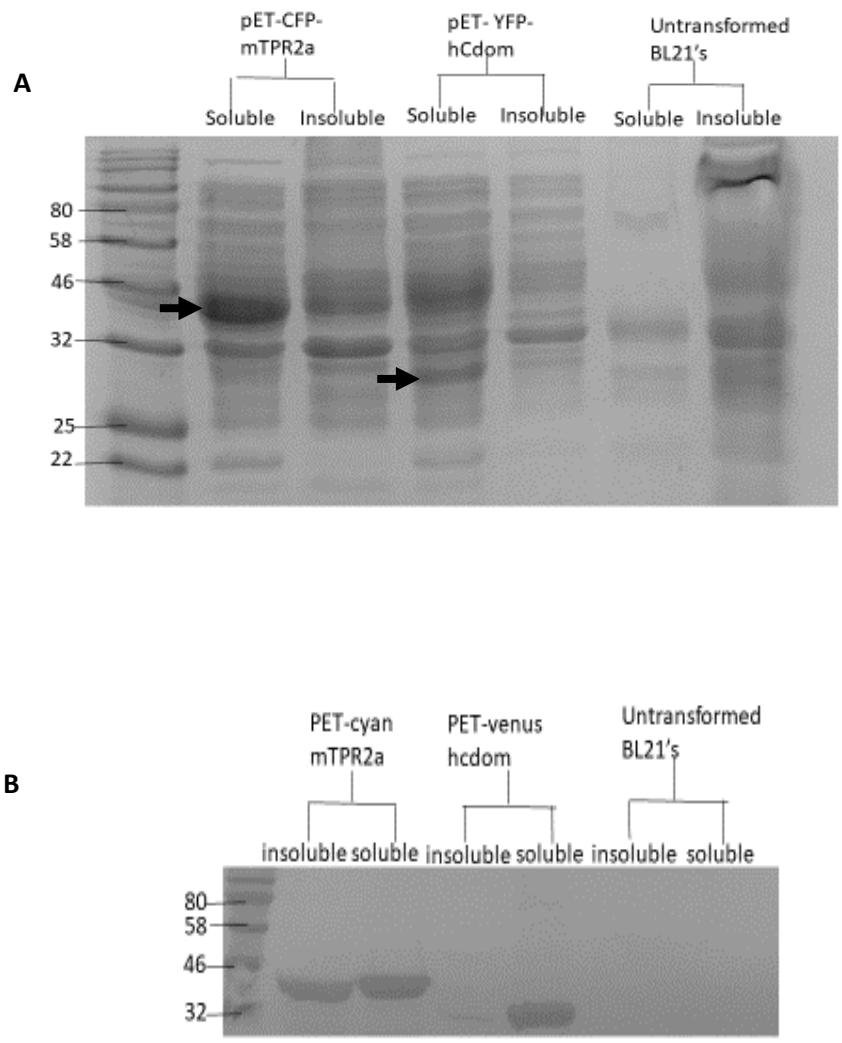

Figure 17: SDS-PAGE and western blotting analysis of CFP-mTPR2A and YFP-hCdom expression. Soluble and insoluble fractions of *E. coli* transformed with pET-CFP-mTPR2A and pET-YFP-hCdom and untransformed cells were run on 12% SDS-PAGE gels. **(A)** Gel stained with Coomassie. (**B**) Western blot performed on a parallel gel using a Ni-NTA-HRP conjugate (HisDetector), visualised with TMB membrane peroxidase substrate. Sizes of protein standards in kDa are indicated on the left.

Virtually identical results were obtained analysing the expression of the *P. falciparum* domains (CFP-*Pf*TPR2A, YFP-*Pf*Cdom) (Fig. 18). Predicted recombinant protein sizes were 42 kDa and 36.5 kDa for the TPR2A and Cdom fusion proteins respectively. CFP-*Pf*TPR2A was prominent in both the soluble and insoluble fracions of pET-CFP-TPR2A transformed cells as

determined by SDS-PAGE (Fig. 18A, arrow) and blotting (Fig. 18B). As with the murine TPR2A expression experiment, the amount of CFP-*Pf*TPR2A in the insoluble fraction may have been attributable to inclomplete *E. coli* lysis. As with the YFP-hCdom samples , the western blot of YFP-*Pf*Cdom samples (Fig. 18B) showed the presence of a YFP-*Pf*Cdom protein only in the soluble fraction.

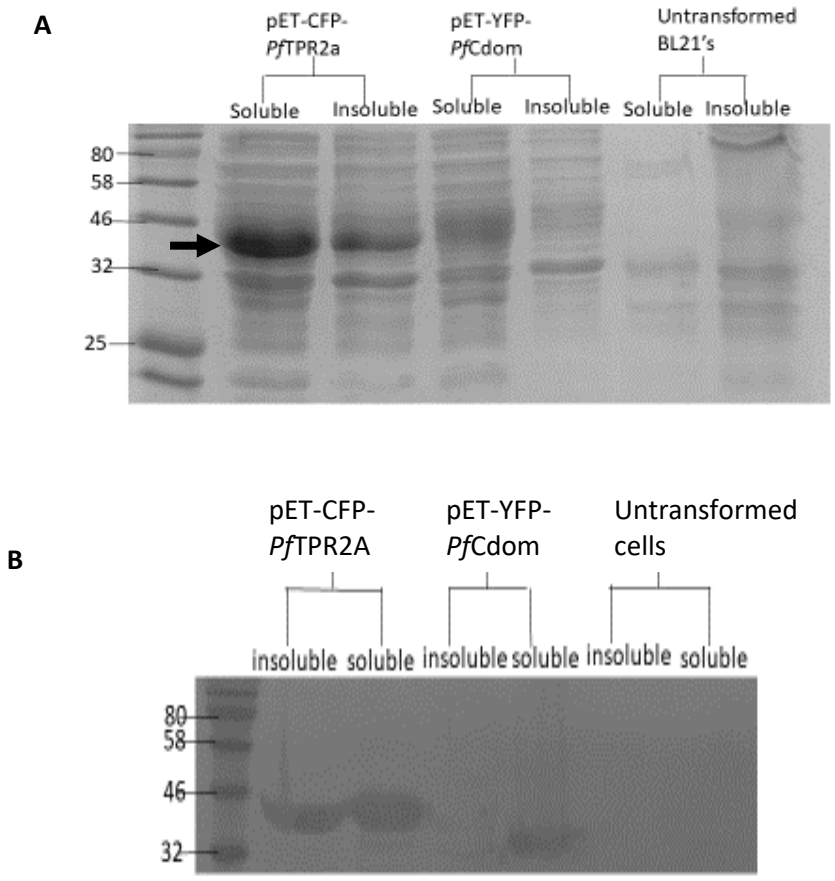

Figure 18: SDS-PAGE and western blotting analysis of CFP-*Pf*TPR2A and YFP-*Pf*Cdom expression. Soluble and insoluble fractions of *E. coli* transformed with pET-CFP-*Pf*TPR2A and pET-YFP-*Pf*Cdom and untransformed *E. coli* were run on 12% SDS-PAGE gels. **(A)** Gel stained with Coomassie. **(B)** Western blot using Ni-NTA-HRP (HisDetector) with TMB membrane peroxidase substrate.

In summary, the expression analyses suggested that sufficient CFP-YFP, YFP, CFP-mTPR2A, CFP-*Pf*TPR2A ,YFP-hCdom and YFP-*Pf*Cdom proteins were expressed in the *E. coli* soluble fractions to proceed to protein purification.

4.3 Protein purification

To be able to perform assays with the proteins, a large scale protein expression and purification was performed.

To purify the recombinant proteins from soluble fractions, BL21(DE3) cells transformed with the respective pET plasmids were propagated in 5 ml LB broth with kanamycin overnight. Two hundred and fifty ml of fresh LB broth with kanamycin was inoculated with 2.5 ml of the overnight culture. Culturing was continued at 37 degrees C until an OD_{600} of 0.4 - 0.6 was achieved. Although the previous experiments had shown ample protein expression in the absence of IPTG induction, 1 mM ITPG was added to ensure maximal expression and culturing at 37 degrees °C continued for a further 4 h before pelleting the cells by centrifugation.

The pellet was re-suspended in 10 ml lysis buffer (50 mM NaH_2PO_4, 300 mM NaCl, 10 mM imidazole, pH 8) per 1 g of wet bacterial pellet, lysozyme was added to a final concentration of 1 mg/ml and the suspension was left on ice for 20 mins. The lysate was then sonicated and centrifuged at 30678x*g* for 30 mins. The cleared supernatant was filtered and a sample was collected for SDS-PAGE analysis. A Ni-NTA super flow pre-packed column containing 1.5 ml packed resin (Qiagen) was equilibrated with 5 ml lysis buffer, the cleared lysate was added to the column and a sample of the flow-through was removed for SDS-PAGE analysis. Samples were also removed for SDS-PAGE analysis from two subsequent washing steps with lysis buffer. The protein was eluted with two consecutive elution steps using elution buffer (lysis buffer containing 500 mM imidazole) and samples removed for analysis. All samples were analysed on 12% SDS-PAGE gels which were stained with Coomassie to determine if protein

purification was successful.

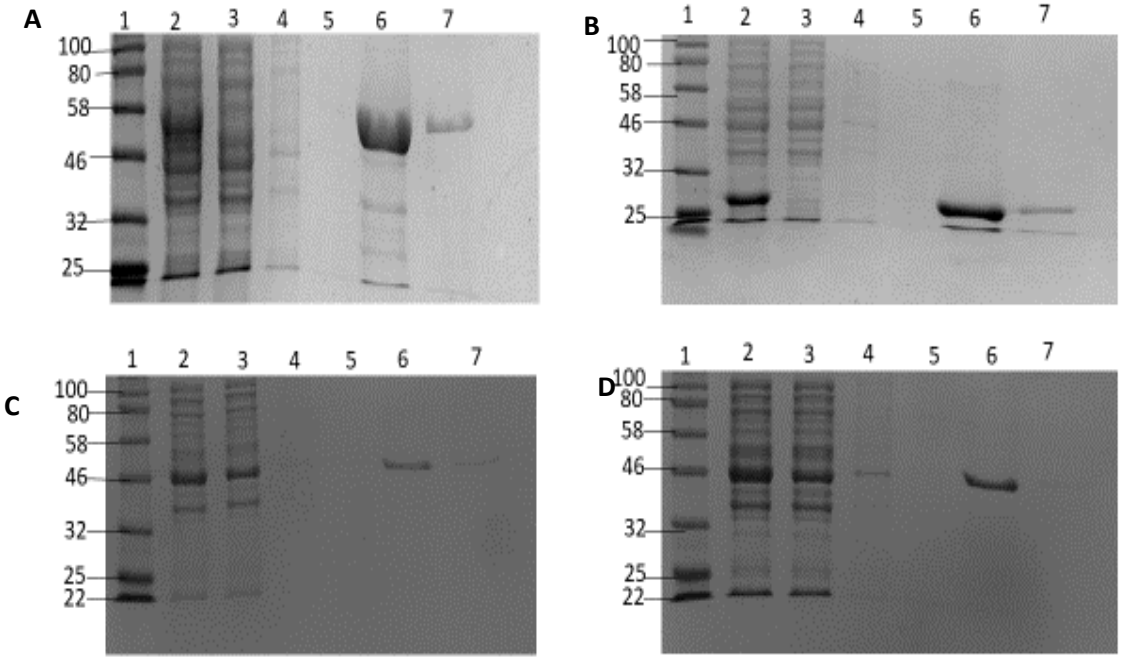

Figure 19: SDS-PAGE analysis of the purification of the FRET positive control (CFP-YFP) (A), YFP (B), CFP-mTPR2A (C) and CFP-*Pf*TPR2A (D). Samples obtained from Ni-NTA column affinity purification were run on 12% SDS-PAGE gels and stained wth Coomassie. Lane 1: Marker (kDa), Lane 2: Soluble lysate, Lane 3: Column flow-through, Lane 4: Wash 1, Lane 5: Wash 2, Lane 6: Elution 1, Lane 7: Elution 2.

Figure 19 shows the purification results obtained for the CFP-YFP fusion protein (FRET positive control; Fig. 19A), YFP (Fig. 19B), CFP-mTPR2A (Fig. 19C) and CFP-*Pf*TPR2A (Fig. 19D). Predicted recombinant sizes for the respective proteins (including the N-terminal extension and histidine tag encoded by the pET-28a plasmid) were:

CFP-YFP: 53 kDa

YFP: 26.5 kDa

CFP-mTPR2A: 41 kDa

CFP-*Pf*TPR2A: 42.4 kDa

All proteins were purified to a high degree as shown by the presence of prominent bands of the expected size in the elution samples (lanes 6) and the absence of contaminating proteins. The CFP-YFP sample did contain smaller proteins (likely degradation products of the full-length protein and/or contaminating *E. coli* proteins; Fig. 19A, lane 6), but these were present at very low concentrations relative to the purified protein. YFP also contained a comparitively low concentration of a low molcular weight protein running at the gel front (Fig. 19B, lane 6). In the case of both TPR2A proteins, some of the recombinant protein was possibly still present in the column flow-through (Fig. 19C and D, lanes 3) suggesting relatively inefficient binding to the column or exceeding of column binding capacity, but more likely the band represents a prominent *E. coli* protein migrating at the same position in the gel (a prominent band just below the 46 kDa marker was also present in the lysate and flow-through of the CFP-YFP and YFP samples – Fig. 19A and B, lanes 2 and 3).

The results of the purification of *Pf*Cdom and hCdom are shown in Fig. 20. Predicted sizes of the recombinant proteins were:

YFP-hCdom: 37.2 kDa

YFP-*Pf*Cdom: 36.6 kDa

The purification experiments yielded pure proteins migrating at the position of the 32 kDa marker (Fig. 20, lane 6).

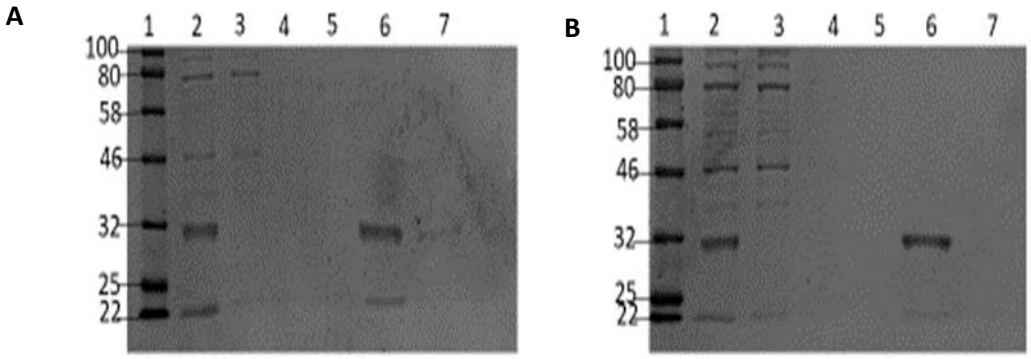

Figure 20 SDS-PAGE analysis of the purification of YFP-hCdom (A) and YFP-*Pf*Cdom (B). Samples obtained from Ni-NTA affinity purification were run on a 12% SDS-PAGE gel and stained with Coomassie. Lane 1: Marker (kDa), Lane 2: Soluble lysate, Lane 3: Column flow-throuh, Lane 4: Wash 1, Lane 5: Wash 2, Lane 6: Elution 1, Lane 7: Elution 2.

The proteins were desalted using desalting size exclusion coloums from GE Healthcare. The coloumn was eqilibrated with assay buffer (TBS) and 2.5 ml of the protein eluate was added and eluted with 3.5 mL TBS. These desalted proteins were stored at 4°C or in 20% glycerol at -20°C. A Bradfords assay was used to determine protein concentration.

4.4 FRET assay with Purified Proteins

In preparation for FRET assays, the purified and desalted proteins were individually placed in a black 96 well plate at different dilutions. The proteins underwent two-fold serial dilutions starting at half their original concentrations: YFP-hCdom (0.94 µM), YFP-*Pf*Cdom (1.9 µM), CFP-mTPR2A (2.70 µM), CFP-*Pf*TPR2A (3.20 µM), YFP (2.64 µM). The fluorescence obtained with the different dilutions of the flourescent proteins was read according to their wavelenghts: The YFP proteins were read at 485/535 nm (excitation/emisison) and the CFP proteins at 425/535 nm. Based on the fluorescence readings, the proteins were prepared as dilutions that yielded similar flourescence values. This was done in an attempt to minimise the

problems commonly experienced with FRET assays that can obscure signals – cross-talk (excitation of the YFP acceptor fluorophore by the wavelength intended to exclusively excite the CFP donor) and bleed-through (detection of donor emission in the acceptor emission wavelength range and *vice versa*). For example, if the CFP fluorescence partner is present in a large quantum yield excess, due to overlap in the CFP and YFP emission spectra, large 'YFP emission' may be detected during CFP excitation even in the absence of a protein interaction and could obscure YFP emissions caused by FRET. Conversely, an excess in the YFP partner and an inadvertent excitation of YFP by the wavelength intended to excite CFP (425 nm) due to excitation spectrum overlap may result in excessive YFP emission that is not attributable to FRET.

Having equalised the protein fluorescence emissions, a FRET assay was subsequently performed using 0.23 µM YFP-hCdom + 0.68 µM CFP-mTPR2A and 0.48 µM YFP-*Pf*Cdom + 0.81 µM CFP-*Pf*TPR2A (Fig. 22). As a negative control, 0.66 µM YFP + 0.81 µM CFP-*Pf*TPR2A was used.

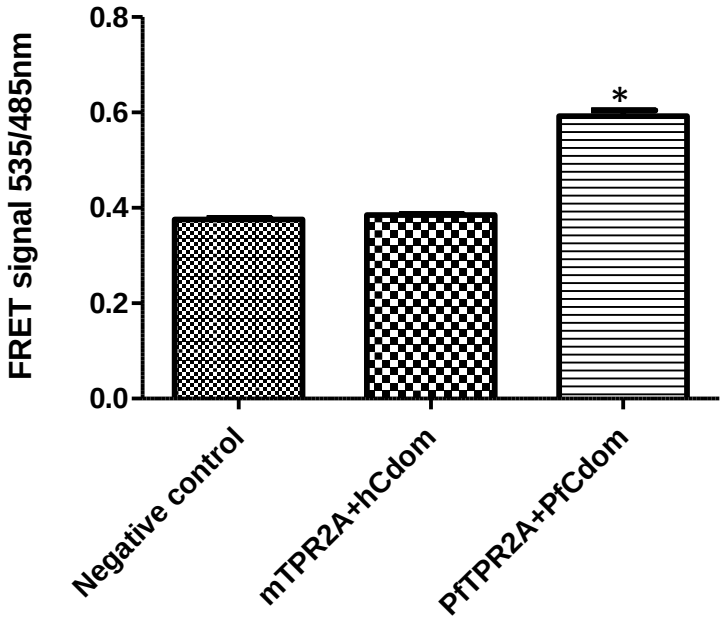

Figure 21: FRET assay with purfied fusion proteins. YFP and CFP fusion proteins were mixed together in assay buffer in a black 96 well plate. The fluorescence was read at 425-535 nm (FRET) and 425-485 nm (CFP) for the interaction of CFP-mTPR2A + YFP-hCdom and CFP-*Pf*TPR2A + YFP-*Pf*Cdom. The negative control was YFP mixed with CFP-*Pf*TPR2A. To obtain the final FRET reading, the fluorescence readings at 535 nm were divided by the readings at 485 nm after deduction of background values (wells without protein). The bargraphs show the mean FRET signals ± standard deviation for 5 wells (n = 5). *p<0.05 compared to negative control.

While the assay failed to show a FRET signal above the negative control using the mammalian proteins, the *P. falciparum* interaction was detected. To estimate the robustness of the assay, the Z' factor was calculated using the following formula:

$$\boldsymbol{Z' = 1 - \frac{3(\sigma p + \sigma n)}{|\mu p - \mu n|}}$$

where σp and σn are the positive interaction and negative control standard deviations, respectively and μp and μn the respective mean FRET signals. It was calculated to be 0,53. Since this value is above 0,5 which is the acknowledged standard for a robust assay, this assay

was able to confidently detect the postive interaction of the *Pf* domains compared to the negative controls (Zhang *et al.*, 1999).

4.4.1 TPR peptide inhibition assay

To confirm that the positive FRET signal for the interaction between the CFP-*Pf*TPR2a and the YFP-*Pf*Cdom proteins was due to protein interaction and explore whether the assay could potentially be used to identify inhibitors of the interaction, a peptide inhibitor based on a peptide designed by Horibe *et al.,* (2011) was used. The original Horibe peptide contained the amino acid sequence of the human TRP2A domain which is thought to bind to the CEEVD motif of the C-terminus of Hsp90. For this study, a peptide containing the corresponding *Pf*TPR2A domain sequence was custom prepared and supplied by Genscript and included in the assay at a final concentration of 100µM (Fig. 22). To control for effects the peptide might have on CFP and YFP fluorescence emissions, it was also included in the negative control sample.

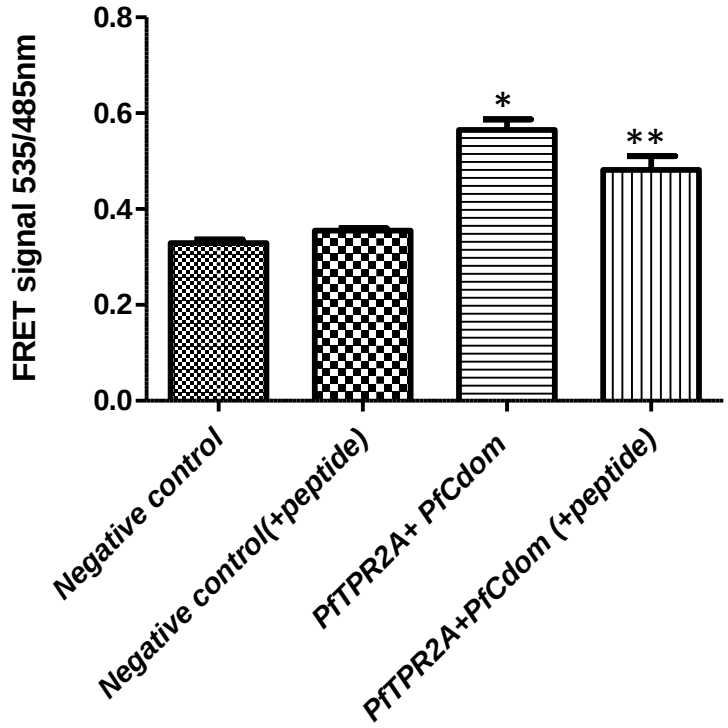

Figure 22: FRET assay with purified fusion proteins in the presence of a TPR peptide inhibitor. The YFP-*Pf*Cdom protein (0.38 µM) was incubated with 200 µM of the TPR peptide, followed by the addition of the CFP-*Pf*TPR2A binding partner (final concentrations: YFP-*Pf*Cdom – 0.19 µM, CFP-*Pf*TPR2A – 0.4 µM, TPR peptide – 100 µM). The uninhibited reaction was performed in the same way, but with vehicle control (DMSO) instead of peptide. The negative control with and without peptide contained 0.33 µM YFP instead of YFP-*Pf*Cdom. The fluorescence was read at 425-535 nm (FRET) and 425-485 nm (CFP). To obtain the final FRET reading, the fluorescence readings at 535 nm were divided by the readings at 485 nm after deduction of background values obtained from wells without protein. The bargraph show the mean FRET signals ± standard deviation for 3 wells (n = 3). *$p<0.05$ (compared to negative control); **$p<0.05$ (compared to un-inhibited reaction)

The FRET signal for the interaction between CFP-*Pf*TPR2A and YFP-*Pf*Cdom decreased by 53.7 % in the presence of the inhibitor, suggesting th**a**t the observed positive FRET signal is due to the interaction of the *P. falciparum* C-domain and TPR2A domain and that the TPR peptide containing the *Pf*TPR2A sequence is capable of inhibiting the interaction.

For further confirmation, the experiment was repeated with varying TPR peptide concentrations (Fig. 23).

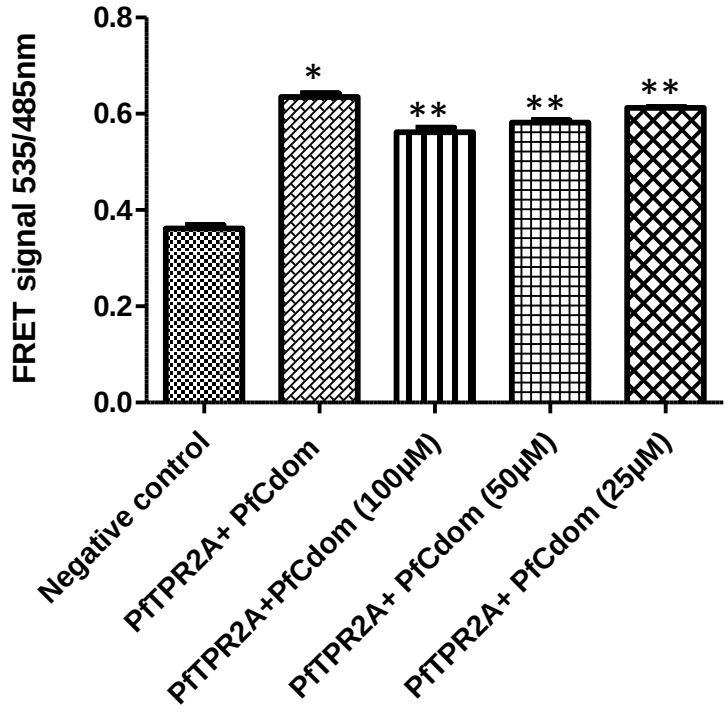

Figure 23: FRET assay with purified fusion proteins with the presence of varying concentrations of TPR peptide inhibitor. The YFP-*Pf*Cdom protein was incubated with varying concentrations of the TPR peptide (200 µM, 100 µM and 50 µM) followed by the addition of the CFP-*Pf*TPR2A domain to yield final TPR peptide concentrations of 100 µM, 50 µM and 25 µM. An uninhibited reaction (no peptide) and negative control reaction (YFP instead of YFP-*Pf*Cdom) was also included. The fluorescence was read at 425-535 nm (FRET) and 425-485nm (CFP) and the final FRET signals by dividing the fluorescence readings at 535 nm with those at 485 nm after deduction of background values obtained from wells without protein. The bar graphs show the mean FRET signals ± standard deviation for 3 wells (n = 3). *$p<0.05$ (compared to negative control); **$p<0.05$(compared to uninhibited reaction)

The *Pf*Cdom and *Pf*TPR2A interaction FRET signal showed a dose dependant recovery with reduced concentrations of the TRP peptide inhibitor. At the lowest concentration of inhibitor (25 µM) the FRET signal of *Pf*Cdom and PfTPR2A was still lower than the FRET signal of the un-inhibited reaction. This experiment further supports the conclusion that the observed positive FRET signal for *Pf*TR2A and *Pf*Cdom is due to the interaction of these protein domains.

CHAPTER 5

DISCUSSION AND CONCLUSION

5.1 DISCUSSION

Even though great inroads have been made to reduce the number of deaths from malaria, the increase in drug and insecticide resistance means that new drug compounds as well as novel drug targets are always in demand. In this study, the drug target focused on was inhibiting the protein-protein interaction (P-PI) between the highly expressed heat shock protein, Hsp90, and its co-chaperone, Hop. To achieve this, it was attempted to create an assay to confirm the interaction of these two proteins and which could potentially be used to detect small drug-like molecule inhibitors of the interaction.

Interaction of the malarial *Pf*Hsp90 and *Pf*Hop in cultured parasite lysates was previously demonstrated by co-immunoprecipitation and gel filtration column co-elution of the proteins (Gitau, *et al.*, 2011). In addition, the *Pf*Cdom was shown to bind to the *Pf*Hop TPR2A domain in *E. coli* using a GFP-complementation ("split-GFP") assay (Zininga, *et al.*, 2015). In principle, the latter assay format conforms to the requirements of a high-throughput assay. However, the interaction takes place in *E. coli* bacteria. The chemical characteristics of compounds capable of penetrating bacterial cell walls often differ significantly from those required for compounds to diffuse across eukaryotic cell membranes (Davis *et al.*, 2014). Consequently, employing the assay in a screen may rule out compounds that are, in fact, able to enter parasites and inhibit *Pf*Hsp90-*Pf*Hop interaction (and *vice versa*, *i.e.*, select for compounds that are incapable of penetrating parasites). In this study, we explored the use of mammalian cell-based assays that should more closely mimic the context of malaria parasites. BRET and FRET assay formats were chosen due to their widespread use for detecting protein interactions in mammalian cells.

To provide an overview of how the BRET assay format works: when the donor reporter protein, the luciferase Rluc, oxidises coelenterazine (substrate), it emits light at 485 nm. This light is absorbed by the acceptor reporter protein YFP (Venus variant used in this study), which emits light at 535 nm. Two proteins each attached to the respective reporter proteins can be said to interact if the two reporter proteins are in close enough proximity for an increased emission at 535 nm to be read after the addition of the coelenterazine substrate. The BRET assay in this study was performed in HeLa cells using full-length *Pf*Hsp90 + *Pf*Hop, as well as *Pf*Cdom + *Pf*TPR2A (the *Pf*Hsp90 C-terminal and *Pf*Hop TPR2A domains, respectively) and hCdom + mTPR2A (human Hsp90 C-terminal and murine Hop TPR2A domains) as interaction partners. After several attempts, only the positive control (Rluc fused directly to YFP) yielded positive BRET signals, with the other interaction pairs yielding signals lower than the negative control (the reporters Rluc and YFP expressed as separate individual proteins). When a western blot was performed on cells transfected with the YFP-fusion constructs using anti-GFP antibodies, it could not detect the YFP-*Pf*Hsp90 and YFP-*Pf*Cdom proteins, potentially explaining the lack of BRET signals, although all the Rluc-fusion proteins were detected using anti-Rluc antibodies. Low expression of proteins is not an uncommon problem, however (Gersting, *et al.,* 2012). One explanation for this may be differences in HeLa cell transfection efficiency with the plasmid pairs in individual wells and from one experiment to the next. Increased expression of the proteins may be achievable by increasing transient transfection efficiency (increasing the percentage of cells successfully transfected and/or the plasmid copy number in individual cells) by using alternative transfection reagents or host cells. The transfection reagent used in this study was Xfect (Clontech), which uses a cell-penetrating peptide to enable the DNA to enter the cell. Other transfection methods include: lipofection (the use of liposomes to cross the phospholipid bilayer), calcium phosphate co-precipitation of DNA onto the cell membrane, electroporation (the use of short electric impulses to make the cell membrane more

permeable) and optical transfection (the use of a laser to create a small perforation in the membrane). Alternative host cell lines include COS-7 cells (African green monkey fibroblasts), HEK293 (human embryonic kidney) cells, NIH 3T3 cells (mouse embryo fibroblasts) and CHO K1 (Chinese hamster ovary) cells. Choosing an appropriate cell line to transfect depends on what is expected from the cells, *e.g*. high production of recombinant proteins, the type of transfection used and the transfection protocol implemented (Chen and Okayama, 1987).

Conceivably another reason for failing to detect interaction signals may have been that endogenous Hsp90 and Hop proteins in HeLa cells were binding to the expressed fusion proteins and outcompeting their mutual binding. Despite low recombinant protein expression levels, conceptually a very sensitive means to determine if the Hsp90 and Hop Rluc and YFP fusion proteins are interacting in transiently transfected cells may be to perform immuno-precipitation of the YFP fusion protein from cell lysates using anti-GFP antibody coated beads and detecting co-precipitation of the Rluc fusion partner using Rluc luminescent substrates. This approach, however, would be cumbersome in a drug-screening scenario. A possible solution to the low and/or variable protein expression levels may be rather to create stable cell lines with the plasmid pairs, *i.e*. cell lines that have incorporated the expression plasmids into their genomes and in which the proteins are constantly expressed (Paddison, *et al.,* 2002). For the BRET assays, however, the procedure is complicated by the fact that two plasmids – not one – would need to be successfully incorporated and their respective proteins expressed in appropriate ratios in individual cells.

From a cell-based screening point of view, disrupting a P-PI is hard to achieve and, therefore, in the past, the assays developed were *in vitro* biochemical assays that allowed the test compound to be added to the reaction before sequentially adding the protein interaction

partners. The compound is thus present before the interaction takes place. In living cells, however, a fast-inducible protein-expression system needs to be introduced in BRET to allow the compound to be added before the target interaction can take place (Corbel, *et al.*, 2011). This approach was followed to identify inhibitors of the cdk5 and p25 protein interaction in yeast cells stably transformed with inducible expression plasmids (Corbel, *et al.*, 2011). Mammalian expression plasmids with inducible promoters include the Tet-on systems, ecdysone systems and derivatives and Qmate^{TM}. This is not required if the studied interaction can be naturally induced, such as by the interaction of signalling receptors and their effectors upon ligand addition. Inducible expression also allows a donor saturation assay that can be performed to characterise the P-PIs and to separate the positives from spurious interactions. An inducible assay allows one to control the levels of BRET proteins to get the optimum ratio of acceptor to donor. An acceptor (YFP) to donor (Rluc) expression ratio is chosen that produces a half maximal BRET signal. The acceptor to donor levels are increased and the BRET signal is read. Plotted on a graph of acceptor/donor ratio vs BRET signal, a hyperbolic curve symbolises a positive P-PI. A linearly increasing BRET signal (straight line), however, is more likely the product of non-specific interaction caused by random collisions between the proteins (Mercier, *et al.*, 2002).

Finally, BRET assays could be improved by using alternative luciferase enzymes and substrates. In this study, commonly used Rluc and YFP were employed as the reporter pair and coelenterazine as the Rluc substrate. To improve the sensitivity of the BRET assay, different pairings that emit more light can be used. For example, the use of *Gaussia* luciferase (Gluc) with native coelenterazine as substrate or Rluc and enduren (a modified coelenterazine) as substrate emits light 8- to 15-fold brighter than other pairings (Kimura, *et al.*, 2010). The following luciferases and their mutants emit light in the 450-500 nm range and can, therefore,

also be considered for BRET assays in conjunction with YFP: *Vargular* luciferase (Vluc), *Metridia longa* luciferase (Mluc) and *Metridia pacific* luciferase 1 (MPluc1). There is also a new luciferase evolved from a deep-sea shrimp (*Oplophorus gracilirostris*) commercialised by Promega as Nanoluc™. It uses furimazine as a substrate and it is reported to have more than a 100-fold higher luciferase activity than Rluc. As it has a maximum emission peak of 465 nm, it is compatible for use in current BRET assays using YFP as acceptor (Hall, *et al.*, 2012).

Similar to the BRET assay, the FRET assay also depends on the donation of photons from a donor reporter protein to an acceptor reporter protein. While the YFP protein is still used as the acceptor, a variant of CFP is used as the donor. By contrast to the BRET assay, the FRET assay did suggest an interaction of the full-length human and malarial proteins. In addition, the positive control gave a robust FRET signal in comparison to the negative control. Unexpectedly, the C-domains and the TPR2A domains showed no interaction for either malarial or mammalian proteins, even though western blotting showed the expression of the two respective TPR2A domains and the human C-domain. Interestingly, this lack of interaction of the mammalian domains was also found using the purified *E. coli* expressed proteins. In the case of the malarial domains, the lack of an apparent interaction in the HeLa cells contradicts the results that were found using the *E. coli* expressed protein, which could possibly be attributed to the lack of detectable *Pf*Cdom expression in HeLa cells as determined in western blotting. Alternatively, detection of a FRET signal using the full-length Hop and Hsp90 proteins could be indicative of a higher affinity of the interaction, possibly due to the presence of additional interacting regions outside the C-terminal and the TPR2Adomains respectively (Onuoha, *et al.*, 2008). In the western blotting experiments, however, expression of the *Pf*Hop and hHsp90 could be faintly detected, not their respective interaction partners. A degradation product of *Pf*Hsp90 was present on the blot, but it is unclear if degradation occurred in the live

cells or during the lysis procedure in preparation in western blotting. As with the FRET assay using the purified *E. coli* expressed proteins, the veracity of the interactions may need to be confirmed using inhibitors. If the TPR peptide used in this study to inhibit the *E. coli* expressed protein interaction is to be employed for this purpose, it would need to be attached to a cell-penetrating peptide sequence to make it membrane permeable, as was done by Horibe, *et al.*, (2011). In addition, as discussed for the BRET assay, to ameliorate inconsistencies in assay signals and protein expression possibly brought about by variations in transient transfection efficiencies, further pursuit of the cell-based FRET assay might require the preparation of stably transfected cell lines, despite the complications involved in achieving this for the co-expression of two separate proteins in the same cell.

There are additional factors that compromise the accuracy of FRET assays, however. Some of the flaws include fluorescence cross-talk and bleed-through, as described in the Introduction. Another limitation is that the energy transfer is dependent upon the appropriate orientation of the donor and acceptor fluorophores. Occasionally, the conformational orientations of the two interacting proteins may lock them in a position that is unfavourable for energy transfer between the fluorophores that are fused to their ends. In this way, the two proteins might be interacting but not allowing the two fluorophores to get close enough to each other for an energy transfer to take place (Xu, *et al.*, 1998). A negative FRET result would, therefore, not necessarily mean that the two proteins are not interacting. A possible way to solve this would be to clone the fluorophores on both the C- and N-termini of the respective interacting proteins and to determine which combination can detect the protein-protein interaction. In this study, the YFP and CFP fluorophores were fused to the N-termini of the Hsp90 and Hop proteins respectively. In the case of Hsp90, this is a prerequisite owing to the requirement of the C-terminal MEEVD sequence for Hop binding. A model of Hsp90-Hop interaction (Southworth

and Agard, 2011) suggests that, in the case of Hop, an N-terminally fused CFP should place it in a better position for FRET interaction with the YFP fused to Hsp90 N-terminus, but this could be explored experimentally with C-terminal Hop-CFP fusions.

In the FRET experiments using the *E. coli* expressed and purified proteins, it was observed that the interaction between *Pf*Cdom and *Pf*TPR2A yielded a significant and reproducible positive FRET signal in comparison to the negative control. By contrast, an interaction between the mammalian hCdom and mTPR2A proteins could not be detected. Interestingly, similar results were found in an alternative assay format developed with purified proteins in a parallel project (Lynn Wambua, MSc dissertation submitted). In this format, the His-tagged C-domain proteins were immobilised on nickel-coated plates and binding to glutathione-S-transferase (GST)-tagged TPR2A domains detected using a GST enzyme assay. While hCdom and mTPR2A interaction could be confidently detected, it consistently yielded signals significantly lower than the interaction of the corresponding malarial domains. It might be insightful to perform *in silico* modelling and docking studies to make an attempt at identifying the molecular basis for this apparent difference in interaction affinity. To confirm the observed interaction between the two malarial proteins, a peptide based on the peptide described by Horibe, *et al.* (2011) which mimics the sequence of the TPR2A domain responsible for Hsp90 binding was designed and used as an inhibitor. At a final peptide concentration of 100 µM, there was a significant decrease in the FRET signal obtained by the interaction between *Pf*Cdom and *Pf*TPR2A in comparison to the uninhibited reaction. From a general drug discovery point of view, a concentration of 100 µM is high, considering that drug discovery projects are typically stimulated by compounds displaying inhibitory concentrations <10 µM. In the Horibe, *et al.*, (2011) study, a concentration of 140 µM of the human peptide was required to inhibit the interaction of human Hsp90 and the human Hop TPR2A domain in surface plasmon resonance

(SPR) experiments. This could suggest that mimicking the TPR2A domain sequence responsible for EEVD motif binding with competitive peptide inhibitors may not be an optimal strategy for disrupting Hsp90-Hop interaction.

The relatively small difference between the FRET signals of the negative control and the test reactions could be explained by the fact that the FRET assay technique is often plagued by background "noise" (including fluorescence cross-over and bleed-through described previously), making it problematic to observe positive signals (Woehler *et al.*, 2010). By using purified proteins, however, sufficient accuracy could be achieved consistently to produce Z' factor values of over 0.5, meaning that the assay is sufficiently robust for drug screening (Zhang, *et al.*, 1999). In addition, the assay requires minimal liquid handling steps, no other reagents are required besides the interacting recombinant proteins and results can be obtained using a standard fluorescence plate reader. Based on these considerations, the assay may be a convenient primary screening format for identifying potential *P. falciparum* Hsp90-Hop interaction inhibitors.

5.2 CONCLUSION

In conclusion, the FRET assay in HeLa cells showed promising interactions between the two full-length mammalian and *P. falciparum* Hsp90 and Hop proteins. Owing to the failure to detect expression of all the individual fusion proteins by western blotting, however, validation of the observed interactions with an inhibitor or a preparation of stable cell lines would need to be implemented. By contrast, using purified *E. coli* expressed proteins in an FRET assay format showed promising detection of *P. falciparum* C-domain and TPR2A domain interactions with Z' factor values suitable for a compound screening assay.

However, there is still room for improvement of assay sensitivity and robustness. In this study, protein concentrations in the assay were chosen to equalise the quantum yields of the YFP and CFP fluorophores of the respective interaction partners. Careful titration of the concentration ratios of the interacting proteins may result in improved FRET signals. In addition, 425 nm, 485 nm and 535 nm were selected as the respective CFP excitation, CFP emission and YFP emission wavelengths. Whether these are the most optimal wavelengths in the current assay format was not explored. Further optimisation of incubation conditions to maximise interaction of the C-domain/TPR2A domain partners was also not attempted. TBS (pH 7.5) containing 0.1% BSA was used as buffer and incubations carried out for 20 minutes at room temperature before obtaining FRET readings in this study. The effect of pH, incubation temperature and incubation time on FRET assay performance may be further explored, as well as buffer composition, *e.g.* using HEPES or phosphate instead of Tris, KCl instead of NaCl and including divalent cations.

REFERENCES

Acharya, P., Kumar, R. & Tatu, U. 2007, "Chaperoning a cellular upheaval in malaria: Heat shock proteins in *Plasmodium falciparum*", *Molecular and Biochemical Parasitology*, vol. 153, no. 2, pp. 85-94.

Alag, R., Bharatham, N., Dong, A., Hills, T., Harikishore, A., Widjaja, A.A., Shochat, S.G., Hui, R. & Ho, S.Y. 2009, "Crystallographic structure of the tetratricopeptide repeat domain of *Plasmodium falciparum* FKBP35 and its molecular interaction with Hsp90 C-terminal pentapeptide", *Protein Science*, vol. 18, no. 10, pp. 2115-2124.

Anadu, N.O., Davisson, V.J. & Cushman, M. 2006, "Synthesis and anticancer activity of brefeldin A ester derivatives", *Journal of Medicinal Chemistry*, vol. 49, no. 13, pp. 3897-3905.

Ardi, V.C., Alexander, L.D., Johnson, V.A. & McAlpine, S.R. 2011, "Macrocycles that inhibit the binding between heat shock protein 90 and TPR-Containing proteins", *ACS Chemical Biology*, vol. 6, no. 12, pp. 1357-1366.

Arkin, M.R. & Wells, J.A. 2004, "Small-molecule inhibitors of protein-protein interactions: Progressing towards the dream", *Nature Reviews Drug Discovery*, vol. 3, no. 4, pp. 301-317.

Baba, M., Nishimura, O., Kanzaki, N., Okamoto, M., Sawada, H., Iizawa, Y., Shiraishi, M., Aramaki, Y., Okonogi, K., Ogawa, Y., Meguro, K. & Fujino, M. 1999, "A small-molecule, nonpeptide CCR5 antagonist with highly potent and selective anti-HIV-1 activity", *Proceedings of the National Academy of Sciences of the United States of America*, vol. 96, no. 10, pp. 5698-5703.

Banerji, U. 2009, "Heat shock protein 90 as a drug target: Some like it hot", *Clinical Cancer Research*, vol. 15, no. 1, pp. 9-14.

Banumathy, G., Singh, V., Pavithra, S., Tatu U. 2003, “Heat shock protein 90 is essential for *Plasmodium falciparum* growth in human erythrocytes,” *Journal Biological Chemistry*, vol. 278 no. 1, pp. 18336–18345.

Balu, B. & Adams, J.H. 2007, "Advancements in transfection technologies for Plasmodium", *International Journal for Parasitology*, vol. 37, no. 1, pp. 1-10.

Berg, T. 2003, "Modulation of protein-protein interactions with small organic molecules", *Angewandte Chemie - International Edition,* vol. 42, no. 22, pp. 2462-2481.

Bird, A. 2007, "Perceptions of epigenetics", *Nature,* vol. 447, no. 7143, pp. 396-398.

Bonetta, L. 2010, "Interactome under construction", *Nature,* vol. 468, no. 7325, pp. 851-854.

Boute, N., Jockers, R. & Issad, T. 2002, "The use of resonance energy transfer in high-throughput screening: BRET versus FRET", *Trends in Pharmacological Sciences,* vol. 23, no. 8, pp. 351-354.

Bozdech, Z. & Ginsburg, H. 2004, "Antioxidant defense in Plasmodium falciparum - Data mining of the transcriptome", *Malaria Journal,* vol. 3.

Brandt, G.E.L. & Blagg, B.S.J. 2009, "Alternate strategies of Hsp90 modulation for the treatment of cancer and other diseases", *Current Topics in Medicinal Chemistry,* vol. 9, no. 15, pp. 1447-1461.

Brinker, A., Scheufler, C., Von Der Mülbe, F., Fleckenstein, B., Herrmann, C., Jung, G., Moarefi, I. & Ulrich Hartl, F. 2002, "Ligand discrimination by TPR domains. Relevance and selectivity of EEVD-recognition in Hsp70·Hop·Hsp90 complexes", *Journal of Biological Chemistry,* vol. 277, no. 22, pp. 19265-19275.

Brown, D. 2007, "Unfinished business: target-based drug discovery", *Drug Discovery Today,* vol. 12, no. 23-24, pp. 1007-1012.

Brückner, A., Polge, C., Lentze, N., Auerbach, D. & Schlattner, U. 2009, "Yeast two-hybrid, a powerful tool for systems biology", *International Journal of Molecular Sciences,* vol. 10, no. 6, pp. 2763-2788.

Calderwood, S.K., Khaleque. A., Sawyer, D.B., Daniel R.Ciocca, D.R.,"Heat shock proteins in cancer: chaperones of tumorigenesis", *Trends in Biochemical Sciences,* vol. 31, no.3, pp. 164-172.

Calderwood, S.K. & Gong, J. 2016, "Heat Shock Proteins Promote Cancer: It's a Protection Racket", *Trends in Biochemical Sciences,* vol. 41, no. 4, pp. 311-323.

Campbell, C.C. 1997, "Malaria: An emerging and re-emerging global plague", *FEMS Immunology and Medical Microbiology,* vol. 18, no. 4, pp. 325-331.

Chen, H., Puhl III, H.L., Koushik, S.V., Vogel, S.S. & Ikeda, S.R. 2006, "Measurement of FRET Efficiency and Ratio of Donor to Acceptor Concentration in Living Cells", *Biophysical Journal*, vol. 91, no. 5, pp. L39-L41.

Chen, S. & Smith, D.F. 1998, "Hop as an adaptor in the heat shock protein 70 (Hsp70) and Hsp90 chaperone machinery", *Journal of Biological Chemistry*, vol. 273, no. 52, pp. 35194-35200.

Cheng, A.C., Coleman, R.G., Smyth, K.T., Cao, Q., Soulard, P., Caffrey, D.R., Salzberg, A.C. & Huang, E.S. 2007, "Structure-based maximal affinity model predicts small-molecule druggability", *Nature Biotechnology*, vol. 25, no. 1, pp. 71-75.

Chen, C. & Okayama, H. 1987, "High-efficiency transformation of mammalian cells by plasmid DNA", *Molecular Cellular Biology*, vol. 7, no. 8, pp.2745-2752.

Chua, C.S., Low, H., Goo, K.-. & Sim, T.S. 2010, "Characterization of Plasmodium falciparum co-chaperone p23: Its intrinsic chaperone activity and interaction with Hsp90", *Cellular and Molecular Life Sciences*, vol. 67, no. 10, pp. 1675-1686.

Chua, C.S., Low, H., Lehming, N. & Sim, T.S. 2012, "Molecular analysis of Plasmodium falciparum co-chaperone Aha1 supports its interaction with and regulation of Hsp90 in the malaria parasite", *International Journal of Biochemistry and Cell Biology*, vol. 44, no. 1, pp. 233-245.

Couturier, C. & Deprez, B. 2012, "Setting up a bioluminescence resonance energy transfer high throughput screening assay to search for protein/protein interaction inhibitors in mammalian cells", *Frontiers in Endocrinology*, vol. 3, no. SEP.

Cowman, A.F., Berry, D. & Baum, J. 2012, "The cellular and molecular basis for malaria parasite invasion of the human red blood cell", *Journal of Cell Biology*, vol. 198, no. 6, pp. 961-971.

Cowen, L.E. & Lindquist, S. 2005, "Cell biology: Hsp90 potentiates the rapid evolution of new traits: Drug resistance in diverse fungi", *Science*, vol. 309, no. 5744, pp. 2185-2189.

Csermely, P., Schnaider, T., Soti, C., Nardai, G. 1998, "The 90-kDa molecular chaperone family: Structure function and clinical applications: A comprehensive review", *Pharmacology & Therapeutics*, vol. 79, no.1, pp. 129-68.

D'Amico, F. & Skarmoutsou, E. 2008, "Quantifying immunogold labelling in transmission electron microscopy", *Journal of Microscopy*, vol. 230, no. 1, pp. 9-15.

D'Andrea, L.D. & Regan, L. 2003, "TPR proteins: The versatile helix", *Trends in Biochemical Sciences*, vol. 28, no. 12, pp. 655-662.

Daelemans, D., Afonina, E., Nilsson, J., Werner, G., Kjems, J., De Clercq, E., Pavlakis, G.N. & Vandamme, A.-. 2002, "A synthetic HIV-1 Rev inhibitor interfering with the CRM1-mediated nuclear export", *Proceedings of the National Academy of Sciences of the United States of America*, vol. 99, no. 22, pp. 14440-14445.

Damsky, C. 2002, "Cell-cell and cell-extracellular matrix adhesion receptors", *Annals of the New York Academy of Sciences*, vol. 961, pp. 154–155.

Davis, T.D., Gerry, C.J. & Tan, D.S. 2014, "General platform for systematic quantitative evaluation of small-molecule permeability in bacteria", *ACS Chemical Biology*, vol. 9, no. 1, pp. 2535-2544.

Dobson, S., Kar, B., Kumar, R., Adams, B. & Barik, S. 2001, "A novel tetratricopeptide repeat (TPR) containing PP5 serine/threonine protein phosphatase in the malaria parasite, Plasmodium falciparum", *BMC Microbiology*, vol. 1, pp. 1-10.

Donnelly, A. & Blagg, B.S.J. 2008, "Novobiocin and additional inhibitors of the Hsp90 C-terminal nucleotide-binding pocket", *Current Medicinal Chemistry*, vol. 15, no. 26, pp. 2702-2717.

Edkins A.L. 2016, "Hsp90 Co-chaperones as Drug Targets in Cancer: Current Perspectives", In: McAlpine S., Edkins A. (eds). Heat Shock Protein Inhibitors. *Topics in Medicinal Chemistry*, vol 19. Springer, Cham

Ellis R.J. 2006, "Molecular chaperones: assisting assembly in addition to folding", *Trends in Biochemical Science, vol.* 31, pp.395–401.

Erlanson, D.A., McDowell, R.S. & O'Brien, T. 2004, "Fragment-based drug discovery", *Journal of Medicinal Chemistry*, vol. 47, no. 14, pp. 3463-3482.

Eggers, D.K., Welch, W.J. & Hansen, W.J. 1997, "Complexes between nascent polypeptides and their molecular chaperones in the cytosol of mammalian cells", *Molecular Biology of the Cell*, vol. 8, no. 8, pp. 1559-1573.

Fields, S. & Song, O. 1989, "A novel genetic system to detect protein-protein interactions", *Nature*, vol. 340, no. 6230, pp. 245-246.

Förster, T. 1948, "Zwischenmolekulare Energiewanderung und Fluoreszenz", *Annalen der Physik*, vol. 437, no. 1-2, pp. 55-75.

Gamo, F.-., Sanz, L.M., Vidal, J., De Cozar, C., Alvarez, E., Lavandera, J.-., Vanderwall, D.E., Green, D.V.S., Kumar, V., Hasan, S., Brown, J.R., Peishoff, C.E., Cardon, L.R. & Garcia-Bustos, J.F. 2010, "Thousands of chemical starting points for antimalarial lead identification", *Nature*, vol. 465, no. 7296, pp. 305-310.

Garg, H., Suri, P., Gupta, J.C., Talwar. G.P., Dubey S. 2016, "Survivin: a unique target for tumor therapy", *Cancel Cell International,* vol 16, no.49.

Gersting, S.W., Lotz-Havla, A.S. & Muntau, A.C. 2012, "Bioluminescence resonance energy transfer: An emerging tool for the detection of protein-protein interaction in living cells", *Methods in Molecular Biology*, vol. 815, no. 1, pp. 253-256.

Gibson, C., Sulyok, G.A.G., Hahn, D., Goodman, S.L., Hölzemann, G. & Kessler, H. 2001, "Nonpeptidic αvβ3integrin antagonist libraries: On-bead screening and mass spectrometric identification without tagging", *Angewandte Chemie - International Edition*, vol. 40, no. 1, pp. 165-169.

Gitau, G.W., Mandal, P., Blatch, G.L., Przyborski, J. & Shonhai, A. 2012, "Characterisation of the Plasmodium falciparum Hsp70-Hsp90 organising protein (PfHop)", *Cell Stress and Chaperones*, vol. 17, no. 2, pp. 191-202.

Hartwell, L.H., Hopfield, J.J., Leibler, S. & Murray, A.W. 1999, "From molecular to modular cell biology", *Nature*, vol. 402, no. 6761 SUPPL. 1, pp. C47-C52.

Hatherley, R., Clitheroe, C.-., Faya, N. & Tastan Bishop, Ö. 2015, "*Plasmodium falciparum* Hop: Detailed analysis on complex formation with Hsp70 and Hsp90", *Biochemical and Biophysical Research Communications*, vol. 456, no. 1, pp. 440-445.

Hill, A.V.S. 2011, "Vaccines against malaria", *Philosophical Transactions of the Royal Society B: Biological Sciences*, vol. 366, no. 1579, pp. 2806-2814.

Hoffmann, J.H., Linke, K., Graf, P.C.F., Lilie, H., Jakob, U,. 2003, "Identification of a redox-regulated chaperone network", *The EMBO Journal*, vol. 23, no.1, pp. 160-168

Hojo, M., Sudo, Y., Ando, Y., Minami, K., Takada, M., Matsubara, T., Kanaide, M., Taniyama, K., Sumikawa, K. & Uezono, Y. 2008, "μ-Opioid receptor forms a functional heterodimer with cannabinoid CB1 receptor: Electrophysiological and fret assay analysis", *Journal of Pharmacological Sciences,* vol. 108, no. 3, pp. 308-319.

Horibe, T., Kohno, M., Haramoto, M., Ohara, K. & Kawakami, K. 2011, "Designed hybrid TPR peptide targeting Hsp90 as a novel anticancer agent", *Journal of Translational Medicine,* vol. 9.

Jackson, D.Y. 2002, "Alpha 4 integrin antagonists", *Current Pharmaceutical Design,* vol. 8, no. 14, pp. 1229-1253.

Jendoubi, M., Dubois, P. & Da Silva, L.P. 1985, "Characterization of one polypeptide antigen potentially related to protective immunity against the blood infection by Plasmodium falciparum in the squirrel monkey", *Journal of Immunology,* vol. 134, no. 3, pp. 1941-1945.

Jeong, H., Mason, S.P., Barabási, A.-. & Oltvai, Z.N. 2001, "Lethality and centrality in protein networks", *Nature,* vol. 411, no. 6833, pp. 41-42.

Johnson, B.D., Schumacher, R.J., Ross, E.D., Toft, D.O. 1998, “Hop modulates hsp70/hsp90 interactions in protein folding”, *Journal Biological Chemistry,* vol. 273, pp. 3679–3686.

Jordan, M.A. 2002, "Mechanism of action of antitumor drugs that interact with microtubules and tubulin", *Current Medicinal Chemistry - Anti-Cancer Agents,* vol. 2, no. 1, pp. 1-17.

Kamal, A.,Thao, L.,Sensintaffar, J.,Zhang, L.,Boehm, M.F.,Fritz, L.C.,Burrows, F.J. 2003, “A high-affinity conformation of Hsp90 confers tumour selectivity on Hsp90inhibitors”, *Nature,* vol. 425, no. 6956, pp. 407-410.

Kelly, T.A., Jeanfavre, D.D., McNeil, D.W., Woska Jr., J.R., Reilly, P.L., Mainolfi, E.A., Kishimoto, K.M., Nabozny, G.H., Zinter, R., Bormann, B.-. & Rothlein, R. 1999, "Cutting edge: A small molecule antagonist of LFA-1-mediated cell adhesion", *Journal of Immunology,* vol. 163, no. 10, pp. 5173-5177.

Kremers G.J., Goedhart J., van Munster E.B. & Gadella T.W., 2006. “Cyan and yellow super fluorescent proteins with improved brightness, protein folding, and FRET förster radius”, *Biochemistry,* vol.45, no.1, pp.6570–6580.

Kunicki, J.B., Petersen, M.N., Alexander, L.D., Ardi, V.C., McConnell, J.R. & McAlpine, S.R. 2011, "Synthesis and evaluation of biotinylated sansalvamide A analogs and their

modulation of Hsp90", *Bioorganic and Medicinal Chemistry Letters,* vol. 21, no. 16, pp. 4716-4719.

Kumar, R., Musiyenko, A. & Barik, S. 2003, "The heat shock protein 90 of Plasmodium falciparum and antimalarial activity of its inhibitor, geldanamycin.", *Malaria Journal [electronic resource]*, vol. 2, no. 1, pp. 30.

LaCount, D.J., Vignali, M., Chettier, R., Phansalkar, A., Bell, R., Hesselberth, J.R., Schoenfeld, L.W., Ota, I., Sahasrabudhe, S., Kurschner, C., Fields, S. & Hughes, R.E. 2005, "A protein interaction network of the malaria parasite Plasmodium falciparum", *Nature,* vol. 438, no. 7064, pp. 103-107.

Laemmli, U.K. 1970, "Cleavage of structural proteins during the assembly of the head of bacteriophage T4", *Nature,* vol. 227, no. 5259, pp. 680-685.

Langdon, S.P (2004). Methods in Molecular Medicine, vol. 88: Cancer Cell Culture: Methods and Protocols Edited by: S. P. Langdon © Humana Press Inc., Totowa, NJ

Last-Barney, K., Davidson, W., Cardozo, M., Frye, L.L., Grygon, C.A., Hopkins, J.L., Jeanfavre, D.D., Pav, S., Qian, C., Stevenson, J.M., Tong, L., Zindell, R. & Kelly, T.A. 2001, "Binding site elucidation of hydantoin-based antagonists of LFA-1 using multidisciplinary technologies: Evidence for the allosteric inhibition of a protein-protein interaction", *Journal of the American Chemical Society*, vol. 123, no. 24, pp. 5643-5650.

Li, J., Soroka, J. & Buchner, J. 2012, "The Hsp90 chaperone machinery: Conformational dynamics and regulation by co-chaperones", *Biochimica et Biophysica Acta - Molecular Cell Research,* vol. 1823, no. 3, pp. 624-635.

Lepourcelet, M., Chen, Y.-.P., France, D.S., Wang, H., Crews, P., Petersen, F., Bruseo, C., Wood, A.W. & Shivdasani, R.A. 2004, "Small-molecule antagonists of the oncogenic Tcf/β-catenin protein complex", *Cancer Cell*, vol. 5, no. 1, pp. 91-102.

Lo Conte, L., Ailey, B., Hubbard, T.J.P., Brenner, S.E., Murzin, A.G. & Chothia, C. 2000, "SCOP: A structural classification of proteins database", *Nucleic Acids Research,* vol. 28, no. 1, pp. 257-259.

Maitland, K. & Newton, C.R.J.C. 2005, "Acidosis of severe falciparum malaria: Heading for a shock?", *Trends in Parasitology*, vol. 21, no. 1, pp. 11-16.

Mercier, J.-., Salahpour, A., Angers, S., Breit, A. & Bouvier, M. 2002, "Quantitative assessment of β1- and β2-adrenergic receptor homo- and heterodimerization by bioluminescence resonance energy transfer", *Journal of Biological Chemistry*, vol. 277, no. 47, pp. 44925-44931.

Milligan, G. 2004, "Applications of bioluminescence- and fluorescence resonance energy transfer to drug discovery at G protein-coupled receptors", *European Journal of Pharmaceutical Sciences*, vol. 21, no. 4, pp. 397-405.

Miyawaki, A., Llopis, J., Heim, R., Michael McCaffery, J., Adams, J.A., Ikura, M. & Tsien, R.Y. 1997, "Fluorescent indicators for Ca2+ based on green fluorescent proteins and calmodulin", *Nature*, vol. 388, no. 6645, pp. 882-887.

Modi, S., Stopeck, A., Linden, H., Solit, D., Chandarlapaty, S., Rosen, N., D'Andrea, G., Dickler, M., Moynahan, M.E., Sugarman, S., Ma, W., Patil, S., Norton, L., Hannah, A.L., & Hudis, C. 2001, "HSP90 Inhibition Is Effective in Breast Cancer: A Phase II Trial of Tanespimycin (17-AAG) Plus Tanrastuzumab in Patients with HER2-Positive Metastatic Breast Cancer Progressing on Trastuzumab", *Clincal Cancer Research*, vol. 17, no. 15, pp. 5132-5139.

Morimoto, R.I., Kroeger, P.E., and Cotto, J.J., 1996, "The transcriptional regulation of heat shock genes: a plethora of heat shock factors and regulatory conditions" *EXS*, vol. 77, no. 1, pp. 139–163.

Nosten, F. & White, N.J. 2007, "Artemisinin-based combination treatment of falciparum malaria", *American Journal of Tropical Medicine and Hygiene*, vol. 77, no. SUPPL. 6, pp. 181-192.

Neckers, L. & Workman, P. 2012, "Hsp90 molecular chaperone inhibitors: Are we there yet?", *Clinical Cancer Research*, vol. 18, no. 1, pp. 64-76.

Nelson, G.M., Huffman, H., and Smith, D.F. 2003, "Comparison of the carboxy-terminal DP-repeat region in the co-chaperones Hop and Hip", *Cell Stress and Chaperones*, vol. **8**, no.1, pp. 125–133.

Odunuga, O.O., Longshaw, V.M. & Blatch, G.L. 2004, "Hop: More than an Hsp70/Hsp90 adaptor protein", *BioEssays*, vol. 26, no. 10, pp. 1058-1068.

Onuoha, S.C., Coulstock, E.T., Grossmann J.G. & Jackson S.E. 2008, “Structural studies on the co-chaperone Hop and its complexes with Hsp90”, *Journal of Molecular Biology*, vol. 379, no. 1, pp. 732-744.

Paddison, P.J., Caudy, A.A. & Gregory J. Hannon, G.J, 2002, “Stable suppression of gene expression by RNAi in mammalian cells”, *Proceedings of the Natural Academy of Sciences USA*, vol. 99, no. 3, pp. 1443-1448

Pallavi, R., Roy, N., Nageshan, R.K., Talukdar, P., Pavithra, S.R., Reddy, R., Venketesh, S., Kumar, R., Gupta, A.K., Singh, R.K., Yadav, S.C. & Tatu, U. 2010, "Heat shock protein 90 as a drug target against protozoan infections: Biochemical characterization of HSP90 from plasmodium falciparum and Trypanosoma evansi and evaluation of its inhibitor as a candidate drug", *Journal of Biological Chemistry*, vol. 285, no. 49, pp. 37964-37975.

Pavithra, S.R., Banumathy, G., Joy, O., Singh, V. & Tatu, U. 2004, "Recurrent fever promotes Plasmodium falciparum development in human erythrocytes", *Journal of Biological Chemistry*, vol. 279, no. 45, pp. 46692-46699.

Pearl, L.H. & Prodromou, C. 2000, "Structure and in vivo function of Hsp90", *Current Opinion in Structural Biology*, vol. 10, no. 1, pp. 46-51.

Pepin K., Momose N., Ishida N., Nagata K. 2001, “Molecular cloning of the horse Hsp90 cDNA and its cimparative analysis with other vertebrate Hsp90 sequences”, *Journal of Veterinary Medical Science*, vol. 63 no. 1, pp.115–124.

Pfleger, K.D. & Eidne, K.A. 2006, "Illuminating insights into protein-protein interactions using bioluminescence resonance energy transfer (BRET).", *Nature Methods*, vol. 3, no. 3, pp. 165-174.

Phizicky, E.M. & Fields, S. 1995, "Protein-protein interactions: Methods for detection and analysis", *Microbiological Reviews*, vol. 59, no. 1, pp. 94-123.

Pimienta, G., Herbert, K.M. & Regan, L. 2011, "A compound that inhibits the HOP-Hsp90 complex formation and has unique killing effects in breast cancer cell lines", *Molecular Pharmaceutics*, vol. 8, no. 6, pp. 2252-2261.

Piston, D.W. & Kremers, G.-. 2007, "Fluorescent protein FRET: the good, the bad and the ugly", *Trends in Biochemical Sciences*, vol. 32, no. 9, pp. 407-414.

Plescia, J., Salz, W., Xia, F., Pennati, M., Zaffaroni, N., Daidone, M.G., Meli, M., Dohi, T., Fortugno, P., Nefedova, Y., Gabrilovich, D.I., Colombo, G. & Altieri, D.C. 2005, "Rational design of shepherdin, a novel anticancer agent", *Cancer Cell,* vol. 7, no. 5, pp. 457-468.

Pratt, W.B. 1998, "The Hsp90-based chaperone system: Involvement in signal transduction from a variety of hormone and growth factor receptors", *Proceedings of the Society for Experimental Biology and Medicine,* vol. 217, no. 4, pp. 420-434.

Prodromou, C. & Pearl, L.H. 2003, "Structure and functional relationships of Hsp90", *Current Cancer Drug Targets,* vol. 3, no. 5, pp. 301-323.

Promega. 2009, “EnduRen TM Live Cell Substrate” *Promega Technical Resources,* TM064

Przyborski, J.M., Nyboer, B. & Lanzer, M. 2016, "Ticket to ride: export of proteins to the Plasmodium falciparum-infected erythrocyte", *Molecular Microbiology,* vol. 101, no. 1, pp. 1-11.

Raj, A., Peskin, C.S., Tranchina, D., Vargas, D.Y. & Tyagi, S. 2006, "Stochastic mRNA synthesis in mammalian cells.", *PLoS Biology,* vol. 4, no. 10.

Ratner, D. 1974, "The interaction of bacterial and phage proteins with immobilized Escherichia coli RNA polymerase", *Journal of Molecular Biology,* vol. 88, no. 2, pp. 373-378,IN15-IN18,379-383.

Riven, I., Kalmanzon, E., Segev, L. & Reuveny, E. 2003, "Conformational rearrangements associated with the gating of the G protein-coupled potassium channel revealed by FRET microscopy", *Neuron,* vol. 38, no. 2, pp. 225-235.

Robineau, S., Chabre, M. & Antonny, B. 2000, "Binding site of brefeldin A at the interface between the small G protein ADP-ribosylation factor 1 (ARF1) and the nucleotide-exchange factor Sec7 domain", *Proceedings of the National Academy of Sciences of the United States of America,* vol. 97, no. 18, pp. 9913-9918.

Rodriguez, A.L., Tamrazi, A., Collins, M.L. & Katzenellenbogen, J.A. 2004, "Design, Synthesis, and in Vitro Biological Evaluation of Small Molecule Inhibitors of Estrogen Receptor α Coactivator Binding", *Journal of Medicinal Chemistry,* vol. 47, no. 3, pp. 600-611.

Rual, J.-., Venkatesan, K., Hao, T., Hirozane-Kishikawa, T., Dricot, A., Li, N., Berriz, G.F., Gibbons, F.D., Dreze, M., Ayivi-Guedehoussou, N., Klitgord, N., Simon, C., Boxem, M.,

Milstein, S., Rosenberg, J., Goldberg, D.S., Zhang, L.V., Wong, S.L., Franklin, G., Li, S., Albala, J.S., Lim, J., Fraughton, C., Llamosas, E., Cevik, S., Bex, C., Lamesch, P., Sikorski, R.S., Vandenhaute, J., Zoghbi, H.Y., Smolyar, A., Bosak, S., Sequerra, R., Doucette-Stamm, L., Cusick, M.E., Hill, D.E., Roth, F.P. & Vidal, M. 2005, "Towards a proteome-scale map of the human protein-protein interaction network", *Nature,* vol. 437, no. 7062, pp. 1173-1178.

Sadigh-Eteghad, S., Sabermarouf, B., Majdi, A., Talebi, M., Farhoudi, M., Mahmoudi, J. 2015, "Amyloid-beta: a crucial factor in Alzheimer's disease", *Medical Principals and Practices,* vol. 24, no. 1 pp. 1-10.

Safeukui, I., Millet, P., Boucher, S., Melinard, L., Fregeville, F., Receveur, M.-., Pistone, T., Fialon, P., Vincendeau, P., Fleury, H. & Malvy, D. 2008, "Evaluation of FRET real-time PCR assay for rapid detection and differentiation of Plasmodium species in returning travellers and migrants", *Malaria Journal,* vol. 7.

Scheufler, C., Brinker, A., Bourenkov, G., Pegoraro, S., Moroder, L., Bartunik, H., Hartl, F.U. & Moarefi, I. 2000, "Structure of TPR domain-peptide complexes: critical elements in the assembly of the Hsp70-Hsp90 multichaperone machine", *Cell,* vol.101, no.2 pp. 199-210.

Schreiber, S.L. & Crabtree, G.R. 1992, "The mechanism of action of cyclosporin A and FK506", *Immunology Today,* vol. 13, no. 4, pp. 136-142.

Sharma, S.V., Settleman,J. 2007, **"**Oncogene addiction: setting the stage for molecularly targeted cancer therapy", *Genes and Development,* vol. 21, no. 24, pp. 3214-3231.

Shonhai, A. 2010, "Plasmodial heat shock proteins: Targets for chemotherapy", *FEMS Immunology and Medical Microbiology,* vol. 58, no. 1, pp. 61-74.

Stoops, J.K.,Holland, R., Yazdi, M.A., Maeng, C., Schroeter, J.P., Klueppelberg, U., Kolodziej, S.J., Baker,T., Reed, L.R. 1997, "On the Unique Structural Organization of the *Saccharomyces cerevisiae* Pyruvate Dehydrogenase Complex", *The Journal of Biological Chemistry,* vol. 272, no. 9, pp. 5757–5764.

Sulyok, G.A.G., Gibson, C., Goodman, S.L., Hölzemann, G., Wiesner, M. & Kessler, H. 2001, "Solid-phase synthesis of a nonpeptide RGD mimetic library: New selective αvβ3 integrin antagonists", *Journal of Medicinal Chemistry,* vol. 44, no. 12, pp. 1938-1950.

Suzuki, A., Knaff, D.B. 2005, “Glutamate synthase: structural, mechanistic and regulatory properties, and role in the amino acid metabolism”, *Photosynthesis Research*, vol. 83 no. 2, pp.191-217.

Ting, A.Y., Kain, K.H., Klemke, R.L. & Tsien, R.Y. 2001, "Genetically encoded fluorescent reporters of protein tyrosine kinase activities in living cells", *Proceedings of the National Academy of Sciences of the United States of America,* vol. 98, no. 26, pp. 15003-15008.

Tun, K.M., Imwong, M., Lwin, K.M., Win, A.A., Hlaing, T.M., Hlaing, T., Lin, K., Kyaw, M.P., Plewes, K., Faiz, M.A., Dhorda, M., Cheah, P.Y., Pukrittayakamee, S., Ashley, E.A., Anderson, T.J.C., Nair, S., McDew-White, M., Flegg, J.A., Grist, E.P.M., Guerin, P., Maude, R.J., Smithuis, F., Dondorp, A.M., Day, N.P.J., Nosten, F., White, N.J. & Woodrow, C.J. 2015, "Spread of artemisinin-resistant Plasmodium falciparum in Myanmar: A cross-sectional survey of the K13 molecular marker", *The Lancet Infectious Diseases,* vol. 15, no. 4, pp. 415-421.

Vasko, R.C., Rodriguez, R.A., Cunningham, C.N., Ardi, V.C., Agard, D.A. & McAlpine, S.R. 2010, "Mechanistic studies of sansalvamide A-amide: An allosteric modulator of Hsp90", *ACS Medicinal Chemistry Letters,* vol. 1, no. 1, pp. 4-8.

Vassilev, L.T., Vu, B.T., Graves, B., Carvajal, D., Podlaski, F., Filipovic, Z., Kong, N., Kammlott, U., Lukacs, C., Klein, C., Fotouhi, N. & Liu, E.A. 2004, "In Vivo Activation of the p53 Pathway by Small-Molecule Antagonists of MDM2", *Science,* vol. 303, no. 5659, pp. 844-848.

Vaughan, C.K., Gohlke, U., Sobott, F., Good, V.M., Ali, M.M.U., Prodromou, C., Robinson, C.V., Saibil, H.R. & Pearl, L.H. 2006, "Structure of an Hsp90-Cdc37-Cdk4 Complex", *Molecular Cell,* vol. 23, no. 5, pp. 697-707.

Wilson, C.G.M., Magliery, T.J. & Regan, L. 2004, "Detecting protein-protein interactions with GFP-fragment reassembly", *Nature Methods,* vol. 1, no. 3, pp. 255-262.

Wang, J., Huang, L., Li, J., Fan, Q., Long, Y., Li, Y. & Zhou, B. 2010, "Artemisinin directly targets malarial mitochondria through its specific mitochondrial activation", *PLoS ONE,* vol. 5, no. 3.

Waugh, D.F., 1954, “Protein-Protein Interactions”, *Advances in Protein Chemistry,* vol. 9, no. 1, pp.325-437.

Welch, W.J. & Feramisco, J.R. 1982, "Purification of the major mammalian heat shock proteins.", *Journal of Biological Chemistry,* vol. 257, no. 24, pp. 14949-14959.

Wells, J.A. & McClendon, C.L. 2007, "Reaching for high-hanging fruit in drug discovery at protein-protein interfaces", *Nature,* vol. 450, no. 7172, pp. 1001-1009.

Wu, P. & Brand, L. 1994, "Resonance energy transfer: Methods and applications", *Analytical Biochemistry,* vol. 218, no. 1, pp. 1-13.

Xie, Q., Soutto, M., Xu, X., Zhang, Y. & Johnson, C.H. 2011, "Bioluminescence resonance energy transfer (BRET) imaging in plant seedlings and mammalian cells.", *Methods in Molecular Biology (Clifton, N.J.),* vol. 680, pp. 3-28.

Yasgar, A., Jadhav, A., Simeonov, A. & Coussens, N.P. 2016, Alphascreen-based assays: Ultra-high-throughput screening for small-molecule inhibitors of challenging enzymes and protein-protein interactions.

Yi, F. & Regan, L. 2008, "A novel class of small molecule inhibitors of Hsp90", *ACS Chemical Biology,* vol. 3, no. 10, pp. 645-654.

Yi, F., Zhu, P., Southall, N., Inglese, J., Austin, C.P., Zheng, W. & Regan, L. 2009, "An alphaScreen TM-based high-throughput screen to identify inhibitors of Hsp90-cochaperone interaction", *Journal of Biomolecular Screening,*vol. 14, no. 3, pp. 273-381.

Young, J.C., Obermann, W.M.J., & Hartl, F.U. 1998, "Specific binding of tetratricopeptide repeat proteins to the C-terminal 12-kDa domain of Hsp90. *Journal of Biological Chemistry*, vol. 273 no.1, pp.18007–18010.

Zhang, J., Campbell, R.E., Ting, A.Y. & Tsien, R.Y. 2002, "Creating new fluorescent probes for cell biology", *Nature Reviews Molecular Cell Biology,* vol. 3, no. 12, pp. 906-918.

Zhang, J., Chung T. & Oldenburg, K. 1999, "A simple statistical parameter for use in evaluation and validation of high throughput screening assays", *Journal of Biomolecular Screening*, vol. 4, no. 1, pp. 67-73.

Zininga, T., Makumire, S., Gitau, G.W., Njunge, J.M., Pooe, O.J., Klimek, H., Scheurr, R., Raifer, H., Prinsloo, E., Przyborski, J.M., Hoppe, H. & Shonhai, A. 2015, "Plasmodium falciparum hop (PfHop) interacts with the Hsp70 chaperone in a nucleotide-dependent fashion and exhibits ligand selectivity", *PLoS ONE,* vol. 10, no. 8.

Zou, J., Guo Y., Guettouche, T., Smith, D.F., Voellmy, R., 1998, “Repression of heat shock transcription factor Hsf1 activation by Hsp90 (Hsp90 complex) that forms a stress-sensitive complex with HSF1”, *Cell*, vol. 94 pp. 471–480.

APPENDIX I – Plasmid constructs and cloning strategies

Mammalian expression plasmids donated for this study:

- **pRluc** – *Renilla* luciferase coding sequence cloned between the AgeI and BglII sites of pEGFP-C1.
- **pCFP** – CFP (Cerulean) coding sequence cloned between the AgeI and BglII sites of pEGFP-C1.
- **pYFP** - YFP (Venus) coding sequence cloned between the AgeI and BglII sites of pEGFP-C1.

pEGFP-C1 (Clontech; shown below) contains the coding sequence of enhanced green fluorescent protein (EGFP) with an upstream cytomegalovirus (CMV) promoter and a downstream multiple cloning site (MCS – the sequence is shown below the plasmid map). It thus allows the expression of a coding sequence cloned into the MCS as protein fused at the N-terminus to EGFP in mammalian cells. To create the above plasmids, the EGFP sequence in pEGFP-C1 was replaced by the coding sequences of Rluc, CFP and YFP respectively.

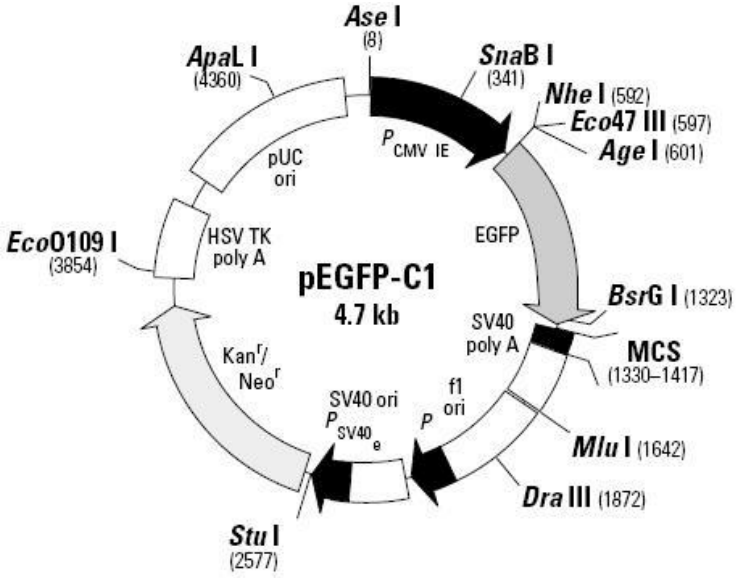

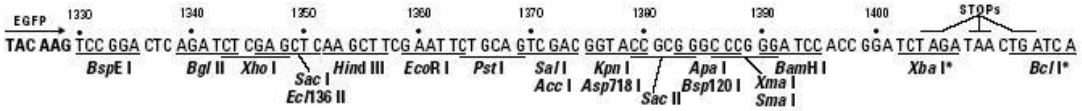

- **pBRET** – Contains the coding sequence of YFP cloned between the KpnI/BamHI sites in the MCS of pRluc.
- **pFRET** – Contains the coding sequence of CFP cloned between the KpnI/BamHI sites in the MCS of pYFP.

The latter two plasmids thus respectively enable the expression of Rluc-YFP and YFP-CFP fusion proteins in mammalian cells for use as BRET and FRET positive controls.

<u>Hsp90 and Hop template plasmids donated for this study</u>:

- **pACT-mHop** – murine Hop coding sequence
- **pACT-*Pf*Hop** – *P. falciparum* Hop coding sequence
- **pACT-mTPR2A** – murine Hop TPR2A domain coding sequence
- **pACT-*Pf*TPR2A** – *P. falciparum* TPR2A domain coding sequence

The Hop and TPR2A coding sequences in the above plasmids were inserted between the SalI and XbaI sites in the multiple cloning region (MCR) of the plasmid pACT (Promega; shown below).

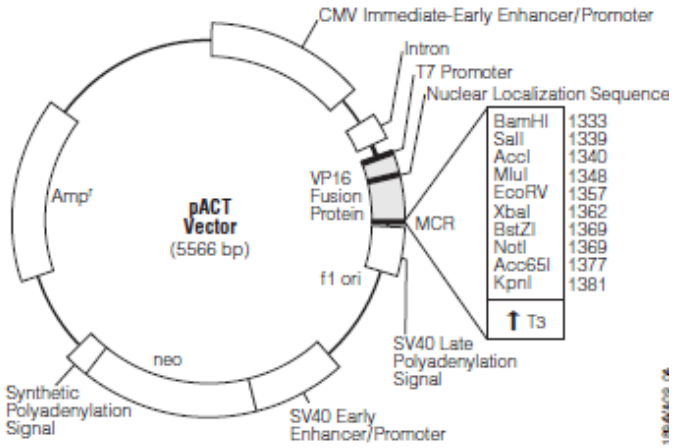

- **pBIND – hHsp90** – human Hsp90 coding sequence
- **pBIND – *Pf*Hsp90** – *P. falciparum* Hsp90 coding sequence

The Hsp90 coding sequences in the above plasmids were inserted between the SalI and XbaI sites of MCR of the plasmid pBIND (Promega; shown below).

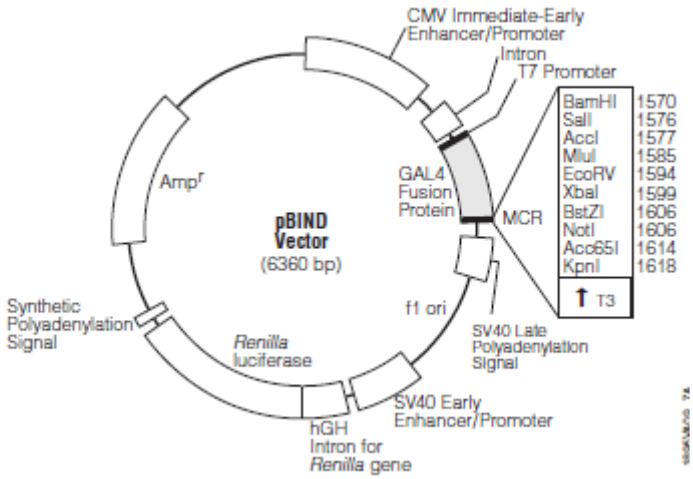

Cloning strategy to prepare mammalian BRET and FRET plasmids

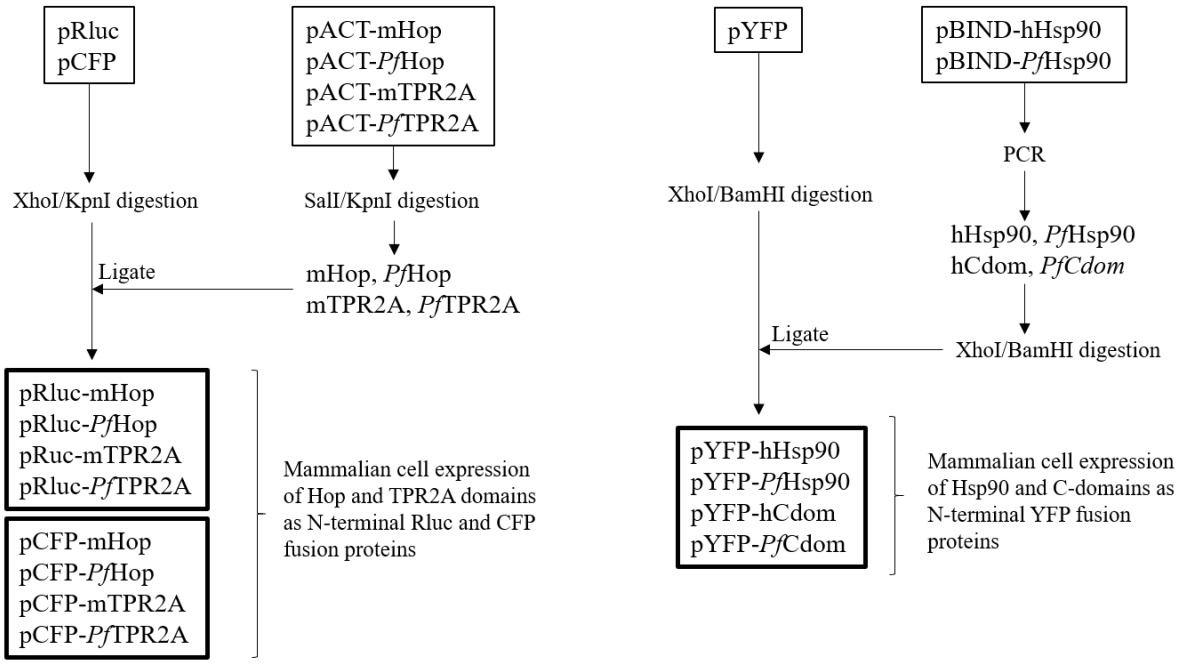

Cloning strategy to prepare *E. coli* expression FRET plasmids

The *E. coli* expression plasmid used in this study was pET-28a(+) (Novagen; plasmid and cloning region shown below). It allows the IPTG-inducible expression of proteins with an N-terminal hexahistidine tag for Ni-NTA affinity purification.

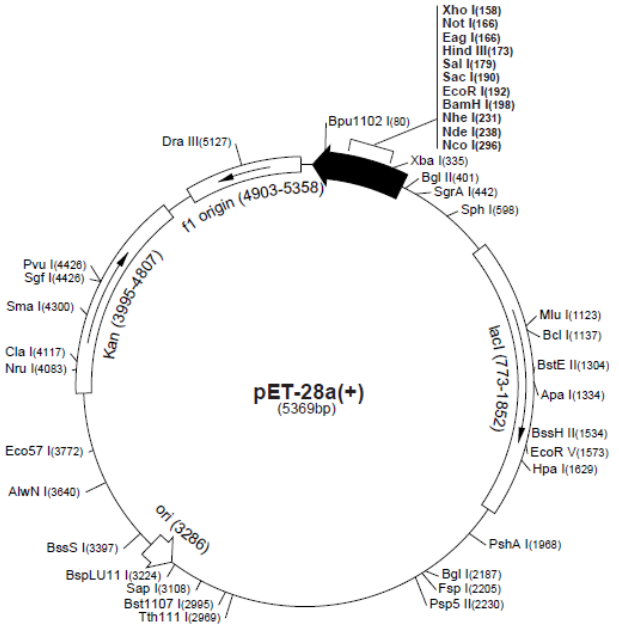
Xho I(158)
Not I(166)
Eag I(166)
Hind III(173)
Sal I(179)
Sac I(190)
EcoR I(192)
BamH I(198)
Nhe I(231)
Nde I(238)
Nco I(296)
Bpu1102 I(80)
Xba I(335)
Bgl II(401)
SgrA I(442)
Sph I(598)
Dra III(5127)
f1 origin (4903-5358)
Pvu I(4428)
Sgf I(4426)
Sma I(4300)
Cla I(4117)
Nru I(4083)
Kan (3995-4807)
pET-28a(+)
(5369bp)
lacI (773-1852)
Mlu I(1123)
Bcl I(1137)
BstE II(1304)
Apa I(1334)
BssH II(1534)
EcoR V(1573)
Hpa I(1629)
Eco57 I(3772)
AlwN I(3640)
ori (3286)
BssS I(3397)
BspLU11 I(3224)
Sap I(3108)
Bst1107 I(2995)
Tth111 I(2969)
PshA I(1968)
Bgl I(2187)
Fsp I(2205)
Psp5 II(2230)

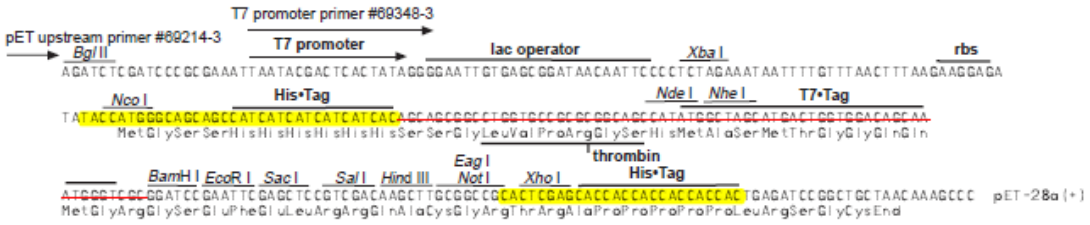
T7 promoter primer #69348-3
pET upstream primer #69214-3
T7 promoter
lac operator
Xba I
rbs
Bgl II
AGATCTCGATCCCGCGAAATTAATACGACTCACTATAGGGGAATTGTGAGCGGATAACAATTCCCCTCTAGAAATAATTTTGTTTAACTTTAAGAAGGAGA
Nco I
His•Tag
Nde I
Nhe I
T7•Tag
TATACCATGGGCAGCAGCCATCATCATCATCATCACAGCAGCGGCCTGGTGCCGCGCGGCAGCCATATGGCTAGCATGACTGGTGGACAGCAA
MetGlySerSerHisHisHisHisHisHisSerSerGlyLeuValProArgGlySerHisMetAlaSerMetThrGlyGlyGlnGln
thrombin
Eag I
BamH I
EcoR I
Sac I
Sal I
Hind III
Not I
Xho I
His•Tag
ATGGGTCGCGGATCCGAATTCGAGCTCCGTCGACAAGCTTGCGGCCGCACTCGAGCACCACCACCACCACCACTGAGATCCGGCTGCTAACAAAGCCC
pET-28a(+)
MetGlyArgGlySerGluPheGluLeuArgArgGlnAlaCysGlyArgThrArgAlaProProProProProLeuArgSerGlyCysEnd

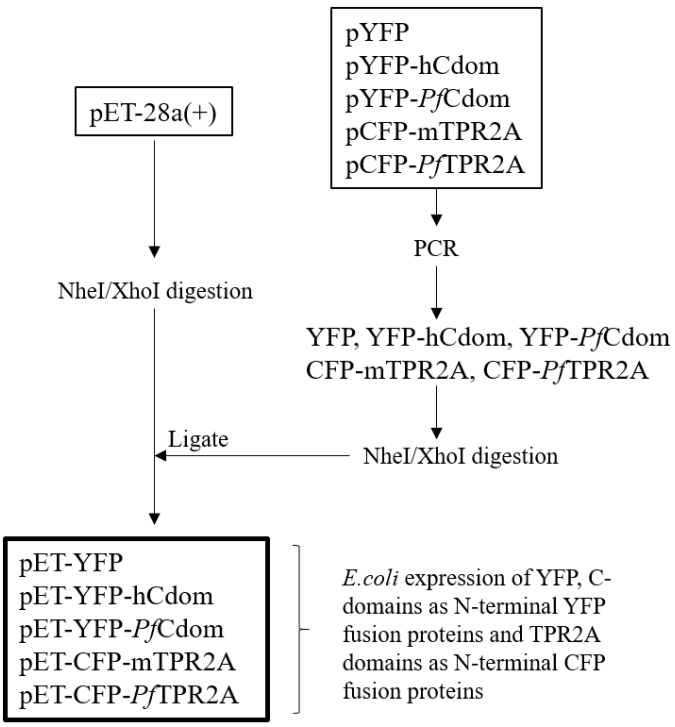
pET-28a(+)
pYFP
pYFP-hCdom
pYFP-*Pf*Cdom
pCFP-mTPR2A
pCFP-*Pf*TPR2A
PCR
NheI/XhoI digestion
YFP, YFP-hCdom, YFP-*Pf*Cdom
CFP-mTPR2A, CFP-*Pf*TPR2A
Ligate
NheI/XhoI digestion
pET-YFP
pET-YFP-hCdom
pET-YFP-*Pf*Cdom
pET-CFP-mTPR2A
pET-CFP-*Pf*TPR2A
E.coli expression of YFP, C-domains as N-terminal YFP fusion proteins and TPR2A domains as N-terminal CFP fusion proteins

Appendix II – Hsp90 and Hop sequences

Human Hsp90 (*Homo sapiens* HSP90AB1; NCBI reference sequence NM_001271969.1).

The sequence of the C-domain is highlighted.

724 amino acids (2172 bases), MW=83152

```
1          ATGCCTGAGGAAGTGCACCATGGAGAGGAGGAGGTGGAGACTTTTGCCTTTCAGGCAGAA
1           M  P  E  E  V  H  H  G  E  E  E  V  E  T  F  A  F  Q  A  E

61         ATTGCCCAACTCATGTCCCTCATCATCAATACCTTCTATTCCAACAAGGAGATTTTCCTT
21          I  A  Q  L  M  S  L  I  I  N  T  F  Y  S  N  K  E  I  F  L

121        CGGGAGTTGATCTCTAATGCTTCTGATGCCTTGGACAAGATTCGCTATGAGAGCCTGACA
41          R  E  L  I  S  N  A  S  D  A  L  D  K  I  R  Y  E  S  L  T

181        GACCCTTCGAAGTTGGACAGTGGTAAAGAGCTGAAAATTGACATCATCCCCAACCCTCAG
61          D  P  S  K  L  D  S  G  K  E  L  K  I  D  I  I  P  N  P  Q

241        GAACGTACCCTGACTTTGGTAGACACAGGCATTGGCATGACCAAAGCTGATCTCATAAAT
81          E  R  T  L  T  L  V  D  T  G  I  G  M  T  K  A  D  L  I  N

301        AATTTGGGAACCATTGCCAAGTCTGGTACTAAAGCATTCATGGAGGCTCTTCAGGCTGGT
101         N  L  G  T  I  A  K  S  G  T  K  A  F  M  E  A  L  Q  A  G

361        GCAGACATCTCCATGATTGGGCAGTTTGGTGTTGGCTTTTATTCTGCCTACTTGGTGGCA
121         A  D  I  S  M  I  G  Q  F  G  V  G  F  Y  S  A  Y  L  V  A

421        GAGAAAGTGGTTGTGATCACAAAGCACAACGATGATGAACAGTATGCTTGGGAGTCTTCT
141         E  K  V  V  V  I  T  K  H  N  D  D  E  Q  Y  A  W  E  S  S

481        GCTGGAGGTTCCTTCACTGTGCGTGCTGACCATGGTGAGCCCATTGGCAGGGGTACCAAA
161         A  G  G  S  F  T  V  R  A  D  H  G  E  P  I  G  R  G  T  K

541        GTGATCCTCCATCTTAAAGAAGATCAGACAGAGTACCTAGAAGAGAGGCGGGTCAAAGAA
181         V  I  L  H  L  K  E  D  Q  T  E  Y  L  E  E  R  R  V  K  E

601        GTAGTGAAGAAGCATTCTCAGTTCATAGGCTATCCCATCACCCTTTATTTGGAGAAGGAA
201         V  V  K  K  H  S  Q  F  I  G  Y  P  I  T  L  Y  L  E  K  E

661        CGAGAGAAGGAAATTAGTGATGATGAGGCAGAGGAAGAGAAAGGTGAGAAAGAAGAGGAA
221         R  E  K  E  I  S  D  D  E  A  E  E  E  K  G  E  K  E  E  E

721        GATAAAGATGATGAAGAAAAACCCAAGATCGAAGATGTGGGTTCAGATGAGGAGGATGAC
241         D  K  D  D  E  E  K  P  K  I  E  D  V  G  S  D  E  E  D  D

781        AGCGGTAAGGATAAGAAGAAGAAAACTAAGAAGATCAAAGAGAAATACATTGATCAGGAA
261         S  G  K  D  K  K  K  K  T  K  K  I  K  E  K  Y  I  D  Q  E

841        GAACTAAACAAGACCAAGCCTATTTGGACCAGAAACCCTGATGACATCACCCAAGAGGAG
281         E  L  N  K  T  K  P  I  W  T  R  N  P  D  D  I  T  Q  E  E

901        TATGGAGAATTCTACAAGAGCCTCACTAATGACTGGGAAGACCACTTGGCAGTCAAGCAC
301         Y  G  E  F  Y  K  S  L  T  N  D  W  E  D  H  L  A  V  K  H

961        TTTTCTGTAGAAGGTCAGTTGGAATTCAGGGCATTGCTATTTATTCCTCGTCGGGCTCCC
321         F  S  V  E  G  Q  L  E  F  R  A  L  L  F  I  P  R  R  A  P

1021       TTTGACCTTTTTGAGAACAAGAAGAAAAAGAACAACATCAAACTCTATGTCCGCCGTGTG
```

```
341          F  D  L  F  E  N  K  K  K  K  N  N  I  K  L  Y  V  R  R  V

1081    TTCATCATGGACAGCTGTGATGAGTTGATACCAGAGTATCTCAATTTTATCCGTGGTGTG
361          F  I  M  D  S  C  D  E  L  I  P  E  Y  L  N  F  I  R  G  V

1141    GTTGACTCTGAGGATCTGCCCCTGAACATCTCCCGAGAAATGCTCCAGCAGAGCAAAATC
381          V  D  S  E  D  L  P  L  N  I  S  R  E  M  L  Q  Q  S  K  I

1201    TTGAAAGTCATTCGCAAAAACATTGTTAAGAAGTGCCTTGAGCTCTTCTCTGAGCTGGCA
401          L  K  V  I  R  K  N  I  V  K  K  C  L  E  L  F  S  E  L  A

1261    GAAGACAAGGAGAATTACAAGAAATTCTATGAGGCATTCTCTAAAAATCTCAAGCTTGGA
421          E  D  K  E  N  Y  K  K  F  Y  E  A  F  S  K  N  L  K  L  G

1321    ATCCACGAAGACTCCACTAACCGCCGCCGCCTGTCTGAGCTGCTGCGCTATCATACCTCC
441          I  H  E  D  S  T  N  R  R  R  L  S  E  L  L  R  Y  H  T  S

1381    CAGTCTGGAGATGAGATGACATCTCTGTCAGAGTATGTTTCTCGCATGAAGGAGACACAG
461          Q  S  G  D  E  M  T  S  L  S  E  Y  V  S  R  M  K  E  T  Q

1441    AAGTCCATCTATTACATCACTGGTGAGAGCAAAGAGCAGGTGGCCAACTCAGCTTTTGTG
481          K  S  I  Y  Y  I  T  G  E  S  K  E  Q  V  A  N  S  A  F  V

1501    GAGCGAGTGCGGAAACGGGGCTTCGAGGTGGTATATATGACCGAGCCCATTGACGAGTAC
501          E  R  V  R  K  R  G  F  E  V  V  Y  M  T  E  P  I  D  E  Y

1561    TGTGTGCAGCAGCTCAAGGAATTTGATGGGAAGAGCCTGGTCTCAGTTACCAAGGAGGGT
521          C  V  Q  Q  L  K  E  F  D  G  K  S  L  V  S  V  T  K  E  G

1621    CTGGAGCTGCCTGAGGATGAGGAGGAGAAGAAGAAGATGGAAGAGAGCAAGGCAAAGTTT
541          L  E  L  P  E  D  E  E  E  K  K  K  M  E  E  S  K  A  K  F

1681    GAGAACCTCTGCAAGCTCATGAAAGAAATCTTAGATAAGAAGGTTGAGAAGGTGACAATC
561          E  N  L  C  K  L  M  K  E  I  L  D  K  K  V  E  K  V  T  I

1741    TCCAATAGACTTGTGTCTTCACCTTGCTGCATTGTGACCAGCACCTACGGCTGGACAGCC
581          S  N  R  L  V  S  S  P  C  C  I  V  T  S  T  Y  G  W  T  A

1801    AATATGGAGCGGATCATGAAAGCCCAGGCACTTCGGGACAACTCCACCATGGGCTATATG
601          N  M  E  R  I  M  K  A  Q  A  L  R  D  N  S  T  M  G  Y  M

1861    ATGGCCAAAAAGCACCTGGAGATCAACCCTGACCACCCCATTGTGGAGACGCTGCGGCAG
621          M  A  K  K  H  L  E  I  N  P  D  H  P  I  V  E  T  L  R  Q

1921    AAGGCTGAGGCCGACAAGAATGATAAGGCAGTTAAGGACCTGGTGGTGCTGCTGTTTGAA
641          K  A  E  A  D  K  N  D  K  A  V  K  D  L  V  V  L  L  F  E

1981    ACCGCCCTGCTATCTTCTGGCTTTTCCCTTGAGGATCCCCAGACCCACTCCAACCGCATC
661          T  A  L  L  S  S  G  F  S  L  E  D  P  Q  T  H  S  N  R  I

2041    TATCGCATGATCAAGCTAGGTCTAGGTATTGATGAAGATGAAGTGGCAGCAGAGGAACCC
681          Y  R  M  I  K  L  G  L  G  I  D  E  D  E  V  A  A  E  E  P

2101    AATGCTGCAGTTCCTGATGAGATCCCCCCTCTCGAGGGCGATGAGGATGCGTCTCGCATG
701          N  A  A  V  P  D  E  I  P  P  L  E  G  D  E  D  A  S  R  M

2161    GAAGAAGTCGATTAG
721          E  E  V  D  *
```

***P. falciparum* Hsp90** (*Pf*Hsp90*;* PlasmoDB reference number PF3D7_0708400).

Sequence codon-optimised for human expression by Genscript (Hong Kong). The sequence of the C-domain is highlighted.

745 amino acids(2235 bases), MW=86051

```
1         ATGTCCACTGAGACTTTTGCTTTCAACGCAGATATTCGGCAGCTGATGTCACTGATTATT
1          M  S  T  E  T  F  A  F  N  A  D  I  R  Q  L  M  S  L  I  I

61        AACACTTTCTATTCCAACAAGGAGATTTTCCTGCGGGAGCTGATCTCAAATGCCAGCGAC
21         N  T  F  Y  S  N  K  E  I  F  L  R  E  L  I  S  N  A  S  D

121       GCTCTGGATAAGATCAGATACGAGTCTATTACTGACACCCAGAAACTGAGTGCCGAGCCC
41         A  L  D  K  I  R  Y  E  S  I  T  D  T  Q  K  L  S  A  E  P

181       GAATTCTTTATTCGCATCATTCCTGATAAGACCAACAATACACTGACTATCGAGGACTCT
61         E  F  F  I  R  I  I  P  D  K  T  N  N  T  L  T  I  E  D  S

241       GGAATTGGCATGACAAAAAACGATCTGATCAACAATCTGGGGACTATTGCCCGAAGTGGA
81         G  I  G  M  T  K  N  D  L  I  N  N  L  G  T  I  A  R  S  G

301       ACCAAGGCTTTCATGGAGGCAATCCAGGCCAGCGGCGACATCTCCATGATTGGGCAGTTC
101        T  K  A  F  M  E  A  I  Q  A  S  G  D  I  S  M  I  G  Q  F

361       GGGGTGGGATTTTACTCCGCTTATCTGGTCGCAGATCACGTGGTCGTGATCTCTAAGAAC
121        G  V  G  F  Y  S  A  Y  L  V  A  D  H  V  V  V  I  S  K  N

421       AATGACGATGAACAGTATGTGTGGGAGAGTGCAGCTGGAGGCAGCTTCACCGTCACAAAG
141        N  D  D  E  Q  Y  V  W  E  S  A  A  G  G  S  F  T  V  T  K

481       GACGAGACAAATGAAAAACTGGGCAGGGGGACTAAGATCATTCTGCACCTGAAAGAAGAC
161        D  E  T  N  E  K  L  G  R  G  T  K  I  I  L  H  L  K  E  D

541       CAGCTGGAGTACCTGGAGGAAAAACGCATCAAGGATCTGGTGAAGAAACATTCTGAATTC
181        Q  L  E  Y  L  E  E  K  R  I  K  D  L  V  K  K  H  S  E  F

601       ATCAGTTTCCCAATTAAGCTGTACTGCGAGCGACAGAACGAGAAAGAAATTACCGCATCT
201        I  S  F  P  I  K  L  Y  C  E  R  Q  N  E  K  E  I  T  A  S

661       GAGGAAGAGGAAGGAGAGGGCGAAGGAGAGCGAGAAGGAGAGGAAGAGGAAGAGAAGAAA
221        E  E  E  E  G  E  G  E  G  E  R  E  G  E  E  E  E  E  K  K

721       AAGAAAACAGGAGAAGACAAGAACGCTGATGAGAGCAAAGAAGAGAATGAAGACGAAGAG
241        K  K  T  G  E  D  K  N  A  D  E  S  K  E  E  N  E  D  E  E

781       AAGAAAGAGGATAACGAAGAGGACGATAATAAGACTGACCACCCCAAAGTGGAGGATGTC
261        K  K  E  D  N  E  E  D  D  N  K  T  D  H  P  K  V  E  D  V

841       ACCGAAGAGCTGGAGAATGCCGAAAAGAAAAAGAAAGAAAAAAGAAAGAAAAAGATCCAC
281        T  E  E  L  E  N  A  E  K  K  K  K  E  K  R  K  K  K  I  H

901       ACCGTGGAGCATGAATGGGAAGAGCTGAACAAACAGAAGCCTCTGTGGATGAGGAAGCCA
301        T  V  E  H  E  W  E  E  L  N  K  Q  K  P  L  W  M  R  K  P

961       GAAGAGGTGACAAATGAAGAGTACGCTTCATTCTATAAGAGCCTGACTAACGACTGGGAG
321        E  E  V  T  N  E  E  Y  A  S  F  Y  K  S  L  T  N  D  W  E

1021      GATCACCTGGCAGTGAAACATTTTTCCGTCGAAGGCCAGCTGGAGTTCAAGGCTCTGCTG
```

```
341          D  H  L  A  V  K  H  F  S  V  E  G  Q  L  E  F  K  A  L  L

1081    TTTATCCCAAAAAGGGCACCCTTCGACATGTTTGAGAATAGGAAAAAGCGCAACAATATC
361          F  I  P  K  R  A  P  F  D  M  F  E  N  R  K  K  R  N  N  I

1141    AAGCTGTACGTGCGGAGAGTCTTCATTATGGACGATTGCGAAGAGATCATTCCAGAGTGG
381          K  L  Y  V  R  R  V  F  I  M  D  D  C  E  E  I  I  P  E  W

1201    CTGAACTTTGTGAAGGGGGTCGTGGACAGCGAAGATCTGCCCCTGAACATCTCCCGCGAG
401          L  N  F  V  K  G  V  V  D  S  E  D  L  P  L  N  I  S  R  E

1261    TCTCTGCAGCAGAACAAGATCCTGAAAGTGATCAAGAAGAACCTGATCAAGAAGTGTCTG
421          S  L  Q  Q  N  K  I  L  K  V  I  K  K  N  L  I  K  K  C  L

1321    GACATGTTCAGCGAGCTGGCCGAAAACAAGGAGAACTACAAGAAGTTCTACGAGCAGTTT
441          D  M  F  S  E  L  A  E  N  K  E  N  Y  K  K  F  Y  E  Q  F

1381    TCCAAGAATCTGAAGCTGGGCATCCACGAAGACAACGCTAATAGAACTAAGATTACCGAG
461          S  K  N  L  K  L  G  I  H  E  D  N  A  N  R  T  K  I  T  E

1441    CTGCTGAGGTTTCAGACCAGCAAGTCCGGAGATGAAATGATCGGCCTGAAAGAGTACGTG
481          L  L  R  F  Q  T  S  K  S  G  D  E  M  I  G  L  K  E  Y  V

1501    GACCGGATGAAGGAAAACCAGAAGGATATCTACTACATCACTGGAGAGTCTATTAACGCC
501          D  R  M  K  E  N  Q  K  D  I  Y  Y  I  T  G  E  S  I  N  A

1561    GTGTCTAATAGTCCTTTCCTGGAAGCTCTGACCAAAAAGGGCTTTGAAGTGATCTACATG
521          V  S  N  S  P  F  L  E  A  L  T  K  K  G  F  E  V  I  Y  M

1621    GTCGACCCAATTGATGAGTATGCCGTGCAGCAGCTGAAGGACTTCGATGGAAAAAAGCTG
541          V  D  P  I  D  E  Y  A  V  Q  Q  L  K  D  F  D  G  K  K  L

1681    AAGTGCTGTACAAAAGAGGGCCTGGACATCGACGATAGCGAAGAGGCAAAAAAGGATTTT
561          K  C  C  T  K  E  G  L  D  I  D  D  S  E  E  A  K  K  D  F

1741    GAGACTCTGAAGGCCGAGTACGAAGGCCTGTGCAAAGTGATCAAGGACGTCCTGCATGAA
581          E  T  L  K  A  E  Y  E  G  L  C  K  V  I  K  D  V  L  H  E

1801    AAAGTGGAGAAGGTCGTGGTCGGCCAGCGGATTACCGATAGCCCTTGTGTGCTGGTCACA
601          K  V  E  K  V  V  V  G  Q  R  I  T  D  S  P  C  V  L  V  T

1861    AGCGAATTCGGGTGGTCCGCCAATATGGAGCGCATCATGAAGGCACAGGCCCTGCGAGAC
621          S  E  F  G  W  S  A  N  M  E  R  I  M  K  A  Q  A  L  R  D

1921    AACAGTATGACCTCATATATGCTGTCCAAAAAGATCATGGAGATTAACGCAAGACACCCC
641          N  S  M  T  S  Y  M  L  S  K  K  I  M  E  I  N  A  R  H  P

1981    ATCATTTCAGCCCTGAAACAGAAGGCTGACGCAGATAAAAGCGACAAGACAGTGAAAGAT
661          I  I  S  A  L  K  Q  K  A  D  A  D  K  S  D  K  T  V  K  D

2041    CTGATCTGGCTGCTGTTTGATACATCCCTGCTGACTTCTGGGTTCGCCCTGGAAGAGCCT
681          L  I  W  L  L  F  D  T  S  L  L  T  S  G  F  A  L  E  E  P

2101    ACCACCTTCAGCAAGCGAATCCATCGGATGATCAAGCTGGGACTGTCAATCGACGAAGAG
701          T  T  F  S  K  R  I  H  R  M  I  K  L  G  L  S  I  D  E  E

2161    GAAAACAATGACATTGATCTGCCCCCTCTGGAGGAAACCGTGGACGCTACAGATAGCAAG
721          E  N  N  D  I  D  L  P  P  L  E  E  T  V  D  A  T  D  S  K

2221    ATGGAGGAAGTCGATTGA
741          M  E  E  V  D  *
```

Murine Hop (*Mus musculus* stress-induced phosphoprotein 1; NCBI reference sequence NM_016737.2), The sequence of the TPR2A-domain is highlighted. The sequence of the TPR peptide used by Horibe *et al*. (2011) to inhibit human Hsp90-Hop interaction is underlined.

543 amino acids(1629 bases), MW=62493

```
1          ATGGAGCAGGTGAATGAGCTAAAGGAGAAGGGCAATAAGGCCCTGAGTGCTGGGAACATT
1           M  E  Q  V  N  E  L  K  E  K  G  N  K  A  L  S  A  G  N  I

61         GATGATGCCTTACAGTGCTACTCTGAGGCAATTAAACTAGATCCCCAGAACCATGTGCTC
21          D  D  A  L  Q  C  Y  S  E  A  I  K  L  D  P  Q  N  H  V  L

121        TACAGCAATCGCTCTGCAGCCTACGCCAAGAAAGGAGACTACCAGAAGGCCTATGAGGAC
41          Y  S  N  R  S  A  A  Y  A  K  K  G  D  Y  Q  K  A  Y  E  D

181        GGCTGCAAGACTGTTGACCTGAAGCCTGACTGGGGCAAGGGTTATTCAAGAAAAGCAGCA
61          G  C  K  T  V  D  L  K  P  D  W  G  K  G  Y  S  R  K  A  A

241        GCCCTTGAATTCCTAAACCGGTTTGAGGAAGCCAAACGAACCTATGAAGAAGGTTTAAAA
81          A  L  E  F  L  N  R  F  E  E  A  K  R  T  Y  E  E  G  L  K

301        CATGAAGCCAATAATCTCCAGCTTAAGGAGGGCTTGCAGAACATGGAGGCCAGGTTGGCA
101         H  E  A  N  N  L  Q  L  K  E  G  L  Q  N  M  E  A  R  L  A

361        GAGAGGAAATTCATGAATCCATTCAACTTGCCTAATCTATACCAAAAGTTGGAAAACGAC
121         E  R  K  F  M  N  P  F  N  L  P  N  L  Y  Q  K  L  E  N  D

421        CCCAGGACAAGGTCGCTGCTCAGTGACCCCACCTACAGGGAGCTCATAGAACAGCTGCAG
141         P  R  T  R  S  L  L  S  D  P  T  Y  R  E  L  I  E  Q  L  Q

481        AACAAGCCGTCAGACCTGGGCACGAAACTACAGGATCCCCGGGTGATGACTACTCTGAGT
161         N  K  P  S  D  L  G  T  K  L  Q  D  P  R  V  M  T  T  L  S

541        GTCCTCCTTGGGGTTGATCTGGGCAGCATGGATGAAGAGGAAGAGGCAGCAACACCCCCA
181         V  L  L  G  V  D  L  G  S  M  D  E  E  E  E  A  A  T  P  P

601        CCCCCACCTCCTCCCAAAAAGGAGCCCAAGCCAGAACCAATGGAAGAAGATCTTCCAGAG
201         P  P  P  P  P  K  K  E  P  K  P  E  P  M  E  E  D  L  P  E

661        AATAAGAAACAGGCACTGAAAGAGAAGGAGCTGGGAAATGATGCCTACAAGAAGAAAGAT
221         N  K  K  Q  A  L  K  E  K  E  L  G  N  D  A  Y  K  K  K  D

721        TTTGACAAGGCCCTGAAGCATTATGACAGAGCCAAGGAACTGGACCCTACCAACATGACC
241         F  D  K  A  L  K  H  Y  D  R  A  K  E  L  D  P  T  N  M  T

781        TACATAACTAATCAAGCAGCTGTGCACTTTGAGAAGGGCGACTATAACAAATGCCGGGAG
261         Y  I  T  N  Q  A  A  V  H  F  E  K  G  D  Y  N  K  C  R  E

841        CTCTGTGAGAAGGCCATTGAAGTGGGCAGAGAGAACCGAGAGGACTACCGGCAGATCGCC
281         L  C  E  K  A  I  E  V  G  R  E  N  R  E  D  Y  R  Q  I  A

901        AAAGCTTATGCCCGAATTGGCAATTCCTATTTCAAAGAAGAAAAGTACAAGGATGCTATA
301         K  A  Y  A  R  I  G  N  S  Y  F  K  E  E  K  Y  K  D  A  I

961        CATTTCTACAACAAGTCTCTAGCAGAGCACCGAACCCCAGATGTGCTCAAGAAGTGCCAG
321          H  F  Y  N  K  S  L  A  E  H  R  T  P  D  V  L  K  K  C  Q

1021       CAGGCAGAGAAAATTCTGAAGGAACAGGAGCGCTTGGCTTATATCAACCCTGACTTGGCT
341         Q  A  E  K  I  L  K  E  Q  E  R  L  A  Y  I  N  P  D  L  A
```

```
1081      TTGGAGGAGAAGAACAAGGGCAACGAATGCTTCCAGAAAGGGGACTACCCCCAAGCCATG
361        L  E  E  K  N  K  G  N  E  C  F  Q  K  G  D  Y  P  Q  A  M

1141      AAGCACTATACAGAAGCCATTAAAAGGAACCCGAGAGATGCCAAACTGTACAGCAACCGA
381        K  H  Y  T  E  A  I  K  R  N  P  R  D  A  K  L  Y  S  N  R

1201      GCTGCCTGCTACACCAAGCTCCTGGAGTTTCAGCTGGCACTCAAGGACTGTGAGGAGTGC
401        A  A  C  Y  T  K  L  L  E  F  Q  L  A  L  K  D  C  E  E  C

1261      ATCCAGCTAGAGCCAACCTTCATCAAGGGTTATACACGGAAAGCAGCTGCTCTGGAAGCC
421        I  Q  L  E  P  T  F  I  K  G  Y  T  R  K  A  A  A  L  E  A

1321      ATGAAGGACTATACAAAAGCCATGGATGTGTACCAAAAAGCGTTAGACCTGGACTCCAGC
441        M  K  D  Y  T  K  A  M  D  V  Y  Q  K  A  L  D  L  D  S  S

1381      TGTAAGGAAGCAGCAGATGGTTACCAACGCTGTATGATGGCACAGTACAACAGACATGAT
461        C  K  E  A  A  D  G  Y  Q  R  C  M  M  A  Q  Y  N  R  H  D

1441      AGCCCTGAGGATGTGAAGCGGCGGGCCATGGCTGACCCTGAGGTGCAGCAGATAATGAGT
481        S  P  E  D  V  K  R  R  A  M  A  D  P  E  V  Q  Q  I  M  S

1501      GACCCAGCCATGAGACTCATCCTGGAGCAGATGCAAAAGGACCCCCAGGCTCTGAGCGAA
501        D  P  A  M  R  L  I  L  E  Q  M  Q  K  D  P  Q  A  L  S  E

1561      CACTTAAAGAATCCTGTAATAGCGCAGAAGATCCAGAAGCTGATGGATGTGGGTCTCATC
521        H  L  K  N  P  V  I  A  Q  K  I  Q  K  L  M  D  V  G  L  I

1621      GCAATTCGGTGA
541        A  I  R  *
```

***P. falciparum* Hop** (*Pf*Hop; PlasmoDB reference number PF3D7_1434300). Sequence codon-optimised for human expression by Genscript (Hong Kong). The sequence of the *Pf*TPR2A-domain is highlighted. The sequence of the TPR peptide used in this study to inhibit *Pf*Cdom-*Pf*TPR2A interaction is underlined.

```
564 amino acids (1692 bases), MW=65964

1         ATGGTCAACAAGGAGGAGGCACAGAGGCTGAAGGAACTGGGCAACAAATGCTTTCAGGAG
1          M  V  N  K  E  E  A  Q  R  L  K  E  L  G  N  K  C  F  Q  E

61        GGCAAATACGAAGAGGCCGTCAAATACTTCTCTGACGCCATCACTAATGACCCCCTGGAT
21         G  K  Y  E  E  A  V  K  Y  F  S  D  A  I  T  N  D  P  L  D

121       CACGTGCTGTACTCAAACCTGAGCGGAGCTTTCGCAAGTCTGGGCCGGTTTTATGAGGCT
41         H  V  L  Y  S  N  L  S  G  A  F  A  S  L  G  R  F  Y  E  A

181       CTGGAAAGTGCAAATAAGTGCATCTCAATTAAGAAAGATTGGCCCAAGGGATACATCCGG
61         L  E  S  A  N  K  C  I  S  I  K  K  D  W  P  K  G  Y  I  R

241       AAAGGCTGTGCTGAGCATGGGCTGAGACAGCTGAGCAACGCAGAGAAGACATATCTGGAA
81         K  G  C  A  E  H  G  L  R  Q  L  S  N  A  E  K  T  Y  L  E

301       GGCCTGAAGATTGACCCTAACAACAAGAGCCTGCAGGATGCCCTGTCCAAGGTGAGAAAC
101        G  L  K  I  D  P  N  N  K  S  L  Q  D  A  L  S  K  V  R  N

361       GAGAATATGCTGGAAAATGCCCAGCTGATCGCTCACCTGAACAATATCATTGAGAACGAC
```

```
121         E  N  M  L  E  N  A  Q  L  I  A  H  L  N  N  I  I  E  N  D

421       CCCCAGCTGAAGTCTTACAAGGAGGAAAACAGTAACTACCCTCATGAACTGCTGAATACC
141         P  Q  L  K  S  Y  K  E  E  N  S  N  Y  P  H  E  L  L  N  T

481       ATCAAGTCCATTAACTCTAATCCTATGAACATCCGCATCATTCTGTCAACATGCCACCCA
161         I  K  S  I  N  S  N  P  M  N  I  R  I  I  L  S  T  C  H  P

541       AAGATTAGCGAGGGGGTGGAAAAGTTCTTTGGCTTCAAGTTCACCGGCGAGGGGAATGAT
181         K  I  S  E  G  V  E  K  F  F  G  F  K  F  T  G  E  G  N  D

601       GCCGAGGAAAGACAGAGGCAGCAGCGAGAGGAAGAGGAAAGAAGAAAGAAAAAGGAGGAA
201         A  E  E  R  Q  R  Q  Q  R  E  E  E  E  E  R  R  K  K  K  E  E

661       GAGGAAAGGAAAAAGAAAGAGGAAGAGGAAATGAAGAAACAGAATCGCACTCCAGAGCAG
221         E  E  R  K  K  K  E  E  E  E  M  K  K  Q  N  R  T  P  E  Q

721       ATCCAGGGCGATGAACATAAGCTGAAAGGGAACGAGTTCTACAAGCAGAAGAAATTTGAC
241         I  Q  G  D  E  H  K  L  K  G  N  E  F  Y  K  Q  K  K  F  D

781       GAGGCCCTGAAAGAATATGAGGAAGCTATCCAGATTAACCCCAATGATATCATGTACCAC
261         E  A  L  K  E  Y  E  E  A  I  Q  I  N  P  N  D  I  M  Y  H

841       TATAATAAGGCCGCTGTGCATATTGAGATGAAGAACTACGACAAAGCAGTCGAGACCTGT
281         Y  N  K  A  A  V  H  I  E  M  K  N  Y  D  K  A  V  E  T  C

901       CTGTACGCCATCGAAAATCGATATAACTTCAAGGCTGAGTTTATTCAGGTGGCAAAACTG
301         L  Y  A  I  E  N  R  Y  N  F  K  A  E  F  I  Q  V  A  K  L

961       TACAATCGGCTGGCCATCAGCTACATCAACATGAAGAAGTACGATCTGGCCATCGAGGCT
321         Y  N  R  L  A  I  S  Y  I  N  M  K  K  Y  D  L  A  I  E  A

1021      TATCGGAAGTCCCTGGTCGAAGACAACAATCGCGCAACACGAAACGCCCTGAAAGAGCTG
341         Y  R  K  S  L  V  E  D  N  N  R  A  T  R  N  A  L  K  E  L

1081      GAAAGGCGCAAGGAGAAAGAGGAAAAGGAAGCTTACATCGACCCTGATAAAGCAGAGGAA
361         E  R  R  K  E  K  E  E  K  E  A  Y  I  D  P  D  K  A  E  E

1141      CACAAGAACAAGGGCAACGAGTACTTCAAGAACAATGACTTTCCAAATGCCAAGAAAGAG
381         H  K  N  K  G  N  E  Y  F  K  N  N  D  F  P  N  A  K  K  E

1201      TATGATGAAGCTATTCGACGGAACCCCAATGACGCTAAGCTGTACAGTAACAGAGCAGCC
401         Y  D  E  A  I  R  R  N  P  N  D  A  K  L  Y  S  N  R  A  A

1261      GCTCTGACTAAACTGATCGAGTATCCTTCAGCACTGGAAGACGTGATGAAGGCCATTGAG
421         A  L  T  K  L  I  E  Y  P  S  A  L  E  D  V  M  K  A  I  E

1321      CTGGACCCCACCTTTGTCAAGGCCTATTCCAGGAAAGGGAATCTGCATTTCTTTATGAAG
441         L  D  P  T  F  V  K  A  Y  S  R  K  G  N  L  H  F  F  M  K

1381      GATTACTACAAGGCACTGCAGGCCTACAACAAGGGGCTGGAGCTGGACCCAAACAACAAG
461         D  Y  Y  K  A  L  Q  A  Y  N  K  G  L  E  L  D  P  N  N  K

1441      GAGTGCCTGGAAGGATATCAGAGGTGTGCTTTCAAGATCGATGAGATGAGCAAGTCCGAA
481         E  C  L  E  G  Y  Q  R  C  A  F  K  I  D  E  M  S  K  S  E

1501      AAAGTGGACGAGGAACAGTTTAAGAAATCCATGGCCGATCCCGAGATTCAGCAGATCATT
501         K  V  D  E  E  Q  F  K  K  S  M  A  D  P  E  I  Q  Q  I  I

1561      TCTGACCCTCAGTTCCAGATCATTCTGCAGAAGCTGAACGAGAATCCAAACTCTATCAGT
521         S  D  P  Q  F  Q  I  I  L  Q  K  L  N  E  N  P  N  S  I  S
```

```
1621      GAATACATTAAGGACCCCAAAATCTTTAACGGACTGCAGAAGCTGATCGCAGCCGGCATT
541        E  Y  I  K  D  P  K  I  F  N  G  L  Q  K  L  I  A  A  G  I

1681      CTGAAAGTCCGCTGA
561        L  K  V  R  *
```